Latest results from T2K

Ciro Riccio

Seminar IRFU/DPhP

April, 8th 2022

Stony Brook University

Neutrino oscillations

Neutrino mixing described by the PMNS matrix: 3 mixing angles and 1 complex CPV phase

$$\begin{pmatrix} \nu_e \\ \nu_\mu \\ \nu_\tau \end{pmatrix} = \begin{pmatrix} 1 & 0 & 0 \\ 0 & c_{23} & s_{23} \\ 0 & -s_{23} & c_{23} \end{pmatrix} \begin{pmatrix} c_{13} & 0 & s_{13}e^{-i\delta_{CP}} \\ 0 & 1 & 0 \\ -s_{13}e^{i\delta_{CP}} & 0 & c_{13} \end{pmatrix} \begin{pmatrix} c_{12} & s_{12} & 0 \\ -s_{12} & c_{12} & 0 \\ 0 & 0 & 1 \end{pmatrix} \begin{pmatrix} \nu_1 \\ \nu_2 \\ \nu_3 \end{pmatrix}$$

$\Delta m^2_{ji} = m^2_j - m^2_i \quad c_{ij} = \cos\theta_{ij} \quad s_{ij} = \sin\theta_{ij}$

Neutrino oscillations

Neutrino mixing described by the PMNS matrix: 3 mixing angles and 1 complex CPV phase

$$\begin{pmatrix} \nu_e \\ \nu_\mu \\ \nu_\tau \end{pmatrix} = \begin{pmatrix} 1 & 0 & 0 \\ 0 & c_{23} & s_{23} \\ 0 & -s_{23} & c_{23} \end{pmatrix} \begin{pmatrix} c_{13} & 0 & s_{13}e^{-i\delta_{CP}} \\ 0 & 1 & 0 \\ -s_{13}e^{i\delta_{CP}} & 0 & c_{13} \end{pmatrix} \begin{pmatrix} c_{12} & s_{12} & 0 \\ -s_{12} & c_{12} & 0 \\ 0 & 0 & 1 \end{pmatrix} \begin{pmatrix} \nu_1 \\ \nu_2 \\ \nu_3 \end{pmatrix}$$

Atmospheric and accelerator
$\theta_{23} \sim 50°$
$\Delta m^2_{32} \sim 2.4 \times 10^{-3}$ eV^2

$\Delta m^2_{ji} = m^2_j - m^2_i \quad c_{ij} = \cos\theta_{ij} \quad s_{ij} = \sin\theta_{ij}$

Neutrino oscillations

Neutrino mixing described by the PMNS matrix: 3 mixing angles and 1 complex CPV phase

$$\begin{pmatrix} \nu_e \\ \nu_\mu \\ \nu_\tau \end{pmatrix} = \begin{pmatrix} 1 & 0 & 0 \\ 0 & c_{23} & s_{23} \\ 0 & -s_{23} & c_{23} \end{pmatrix} \begin{pmatrix} c_{13} & 0 & s_{13}e^{-i\delta_{CP}} \\ 0 & 1 & 0 \\ -s_{13}e^{i\delta_{CP}} & 0 & c_{13} \end{pmatrix} \begin{pmatrix} c_{12} & s_{12} & 0 \\ -s_{12} & c_{12} & 0 \\ 0 & 0 & 1 \end{pmatrix} \begin{pmatrix} \nu_1 \\ \nu_2 \\ \nu_3 \end{pmatrix}$$

Atmospheric and accelerator
$\theta_{23} \sim 50°$
$\Delta m^2_{32} \sim 2.4 \times 10^{-3}$ eV^2

Reactor and accelerator
$\theta_{13} \sim 8°$
Accelerator only δ_{CP} = ??

$\Delta m^2_{ji} = m^2_j - m^2_i \quad c_{ij} = \cos\theta_{ij} \quad s_{ij} = \sin\theta_{ij}$

Neutrino oscillations

Neutrino mixing described by the PMNS matrix: 3 mixing angles and 1 complex CPV phase

$$\begin{pmatrix} \nu_e \\ \nu_\mu \\ \nu_\tau \end{pmatrix} = \begin{pmatrix} 1 & 0 & 0 \\ 0 & c_{23} & s_{23} \\ 0 & -s_{23} & c_{23} \end{pmatrix} \begin{pmatrix} c_{13} & 0 & s_{13}e^{-i\delta_{CP}} \\ 0 & 1 & 0 \\ -s_{13}e^{i\delta_{CP}} & 0 & c_{13} \end{pmatrix} \begin{pmatrix} c_{12} & s_{12} & 0 \\ -s_{12} & c_{12} & 0 \\ 0 & 0 & 1 \end{pmatrix} \begin{pmatrix} \nu_1 \\ \nu_2 \\ \nu_3 \end{pmatrix}$$

Atmospheric and accelerator
$\theta_{23} \sim 50°$
$\Delta m^2_{32} \sim 2.4 \times 10^{-3}$ eV^2

Reactor and accelerator
$\theta_{13} \sim 8°$
Accelerator only δ_{CP} = ??

Solar and reactor
$\theta_{12} \sim 34°$
$\Delta m^2_{12} \sim 7.4 \times 10^{-5}$ eV^2

$\Delta m^2_{ji} = m^2_j - m^2_i \quad c_{ij} = \cos\theta_{ij} \quad s_{ij} = \sin\theta_{ij}$

Neutrino oscillations

Neutrino mixing described by the PMNS matrix: 3 mixing angles and 1 complex CPV phase

$$\begin{pmatrix} \nu_e \\ \nu_\mu \\ \nu_\tau \end{pmatrix} = \begin{pmatrix} 1 & 0 & 0 \\ 0 & c_{23} & s_{23} \\ 0 & -s_{23} & c_{23} \end{pmatrix} \begin{pmatrix} c_{13} & 0 & s_{13}e^{-i\delta_{CP}} \\ 0 & 1 & 0 \\ -s_{13}e^{i\delta_{CP}} & 0 & c_{13} \end{pmatrix} \begin{pmatrix} c_{12} & s_{12} & 0 \\ -s_{12} & c_{12} & 0 \\ 0 & 0 & 1 \end{pmatrix} \begin{pmatrix} \nu_1 \\ \nu_2 \\ \nu_3 \end{pmatrix}$$

Atmospheric and accelerator
$\theta_{23} \sim 50°$
$\Delta m^2_{32} \sim 2.4 \times 10^{-3}$ eV^2

Reactor and accelerator
$\theta_{13} \sim 8°$
Accelerator only δ_{CP} = ??

Solar and reactor
$\theta_{12} \sim 34°$
$\Delta m^2_{12} \sim 7.4 \times 10^{-5}$ eV^2

Inferred from $P(\nu_\alpha \rightarrow \nu_\beta) = P(E, L, \Delta m^2, \theta)$

$\Delta m^2_{ji} = m^2_j - m^2_i \quad c_{ij} = \cos\theta_{ij} \quad s_{ij} = \sin\theta_{ij}$

Neutrino oscillations

Neutrino mixing described by the PMNS matrix: 3 mixing angles and 1 complex CPV phase

$$\begin{pmatrix} \nu_e \\ \nu_\mu \\ \nu_\tau \end{pmatrix} = \begin{pmatrix} 1 & 0 & 0 \\ 0 & c_{23} & s_{23} \\ 0 & -s_{23} & c_{23} \end{pmatrix} \begin{pmatrix} c_{13} & 0 & s_{13}e^{-i\delta_{CP}} \\ 0 & 1 & 0 \\ -s_{13}e^{i\delta_{CP}} & 0 & c_{13} \end{pmatrix} \begin{pmatrix} c_{12} & s_{12} & 0 \\ -s_{12} & c_{12} & 0 \\ 0 & 0 & 1 \end{pmatrix} \begin{pmatrix} \nu_1 \\ \nu_2 \\ \nu_3 \end{pmatrix}$$

Atmospheric and accelerator
$\theta_{23} \sim 50°$
$\Delta m^2_{32} \sim 2.4\times10^{-3}$ eV^2

Reactor and accelerator
$\theta_{13} \sim 8°$
Accelerator only δ_{CP} = ??

Solar and reactor
$\theta_{12} \sim 34°$
$\Delta m^2_{12} \sim 7.4\times10^{-5}$ eV^2

Inferred from $P(\nu_\alpha \rightarrow \nu_\beta) = P(E, L, \Delta m^2, \theta)$

Open questions:
δ_{CP}, θ_{23} octant and mass ordering

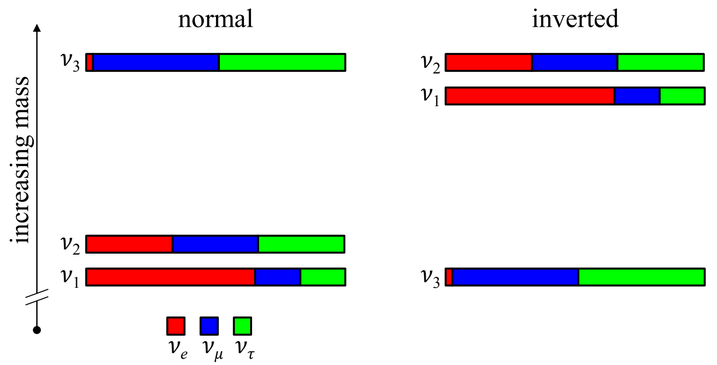

$\Delta m^2_{ji} = m^2_j - m^2_i \quad c_{ij} = \cos\theta_{ij} \quad s_{ij} = \sin\theta_{ij}$

Oscillations measurements

Long baseline accelerator-based experiments are sensitive to:

- Atmospheric parameters (θ_{23}, Δm^2_{32}) through ν_μ disappearance

$$P(\overset{(-)}{\nu}_\mu \to \overset{(-)}{\nu}_\mu) \approx 1 - \sin^2 2\theta_{23} \sin^2\left(\frac{\Delta m^2_{32} L}{4E}\right)$$

- (θ_{13}, δ_{CP}) depends on the $\nu_e/\bar{\nu}_e$ appearance

$$P(\overset{(-)}{\nu}_\mu \to \overset{(-)}{\nu}_e) \approx \sin^2 2\theta_{13} \sin^2\theta_{23} \sin^2\left(\frac{\Delta m^2_{32} L}{4E}\right) \mp O(\delta_{CP})$$

In the case of T2K δ_{CP} change the appearance probability by ±30% while the mass ordering by ~10%

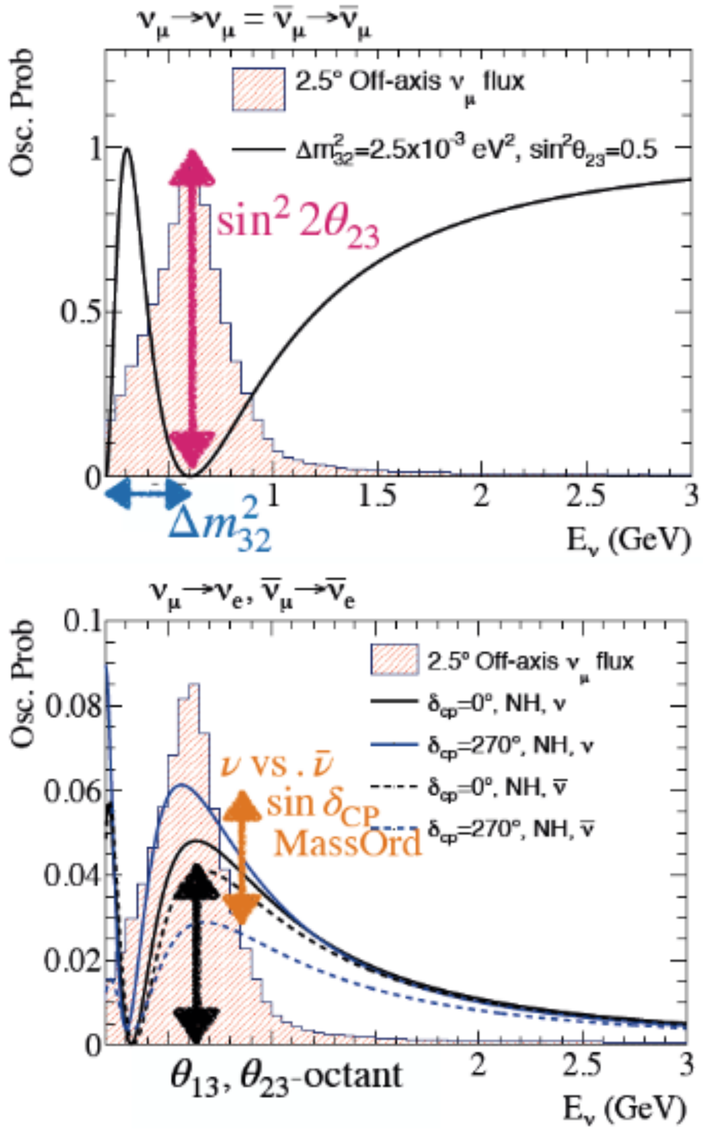

The T2K experiment

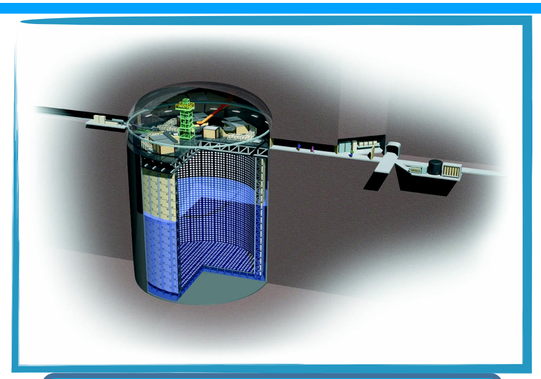

Super-Kamiokande

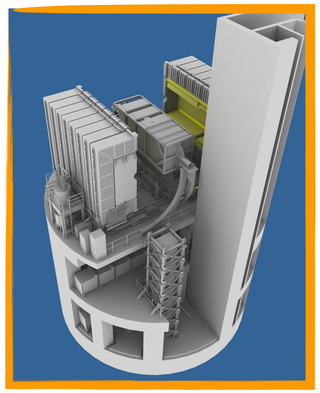

Near Detectors

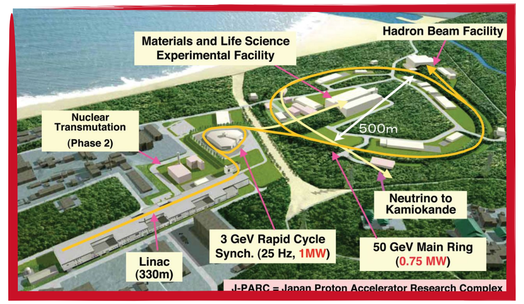

J-PARC

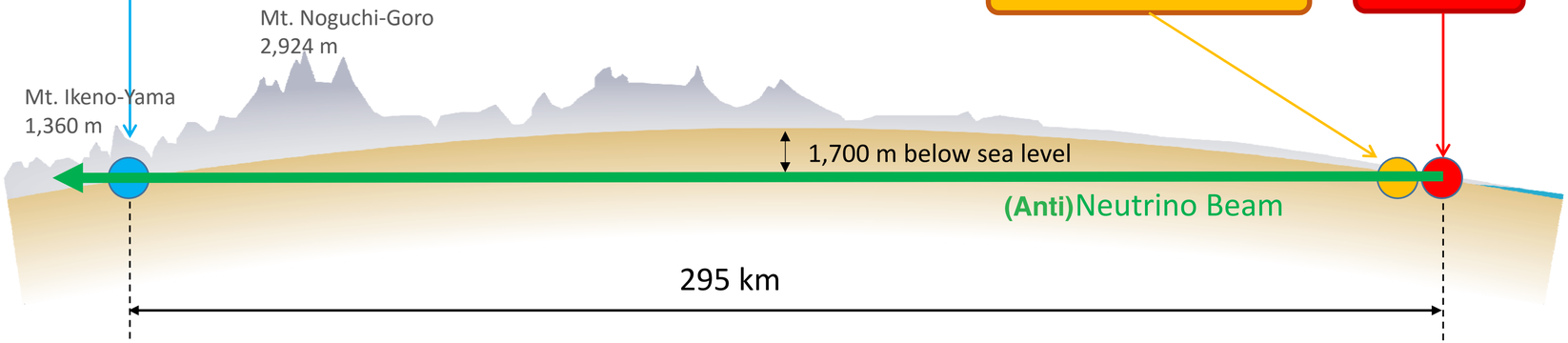

The T2K experiment

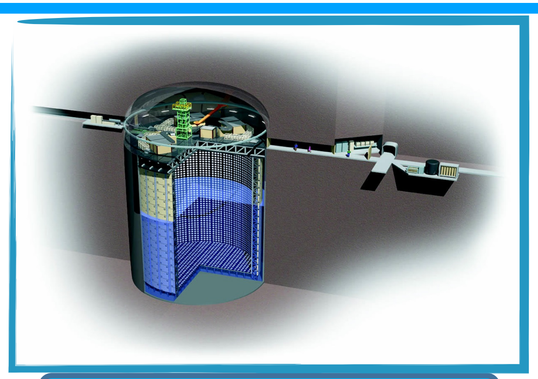

Super-Kamiokande

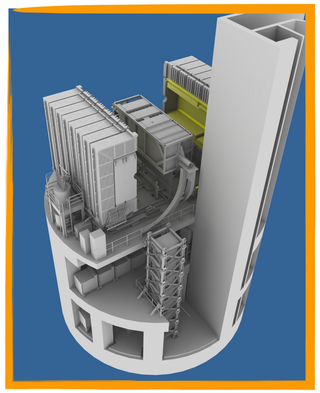

Near Detectors

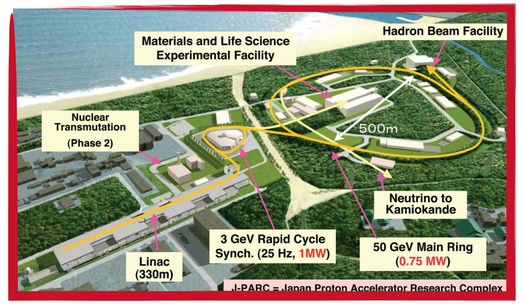

J-PARC

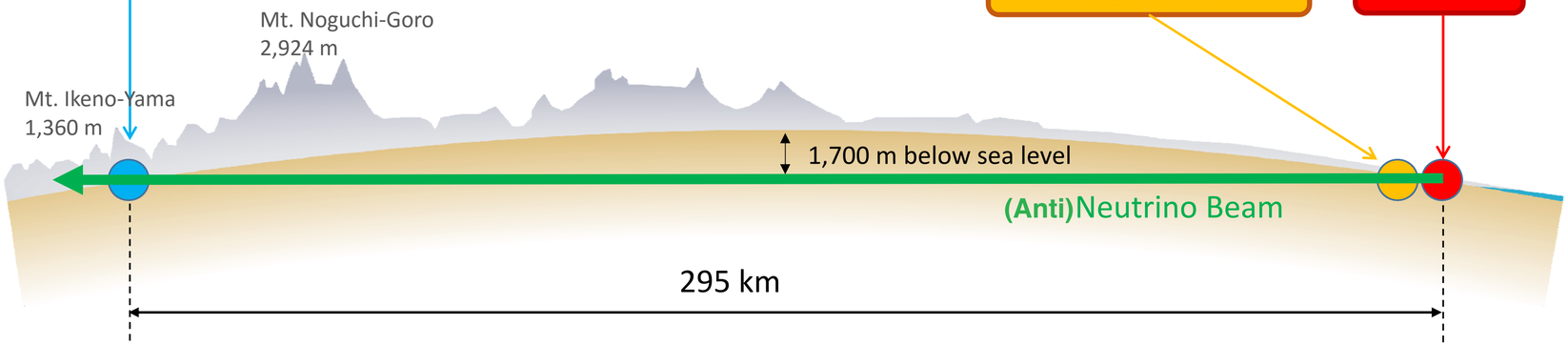

Physics goals:

The T2K experiment

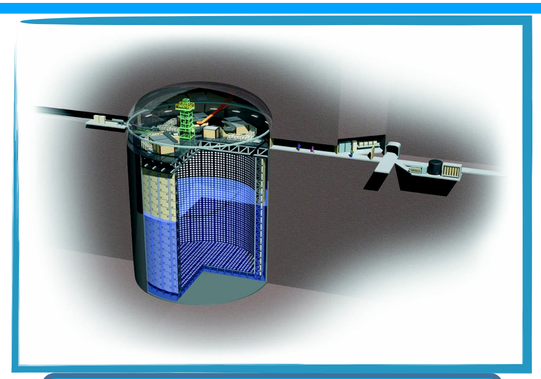

Super-Kamiokande

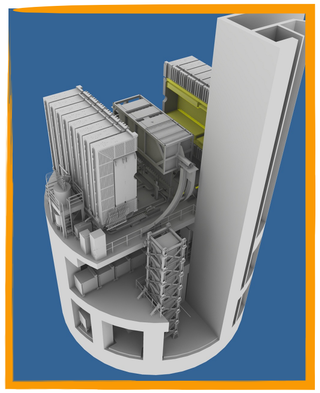

Near Detectors

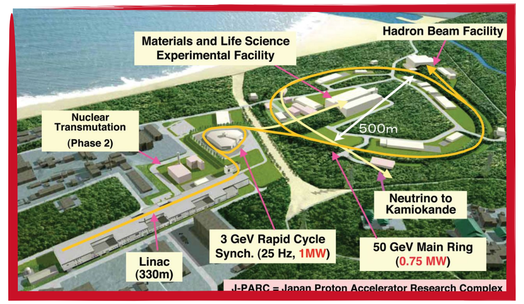

J-PARC

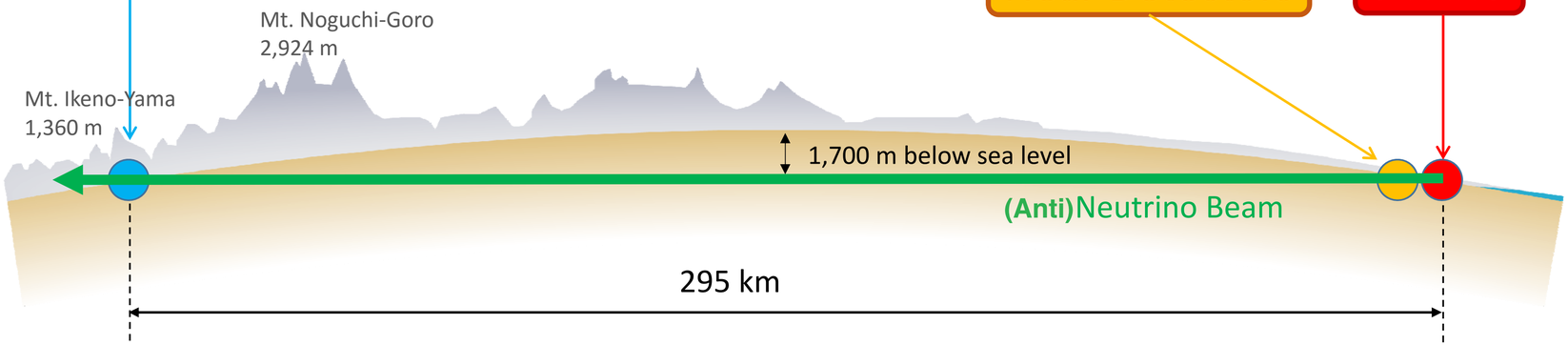

Physics goals:

- Precise measurement of θ_{23}, Δm^2_{32}

The T2K experiment

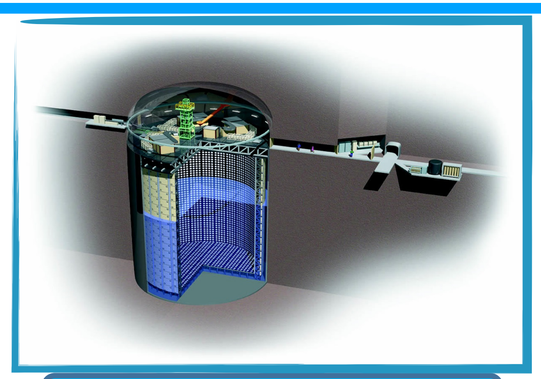

Super-Kamiokande

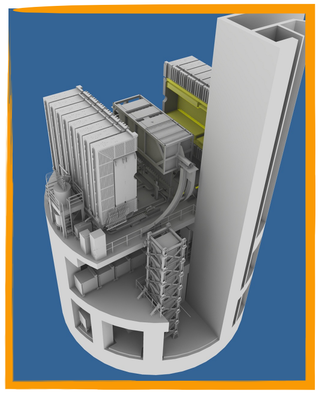

Near Detectors

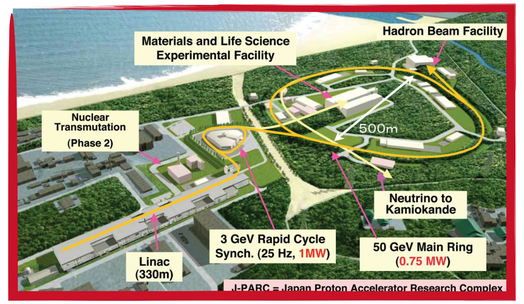

J-PARC

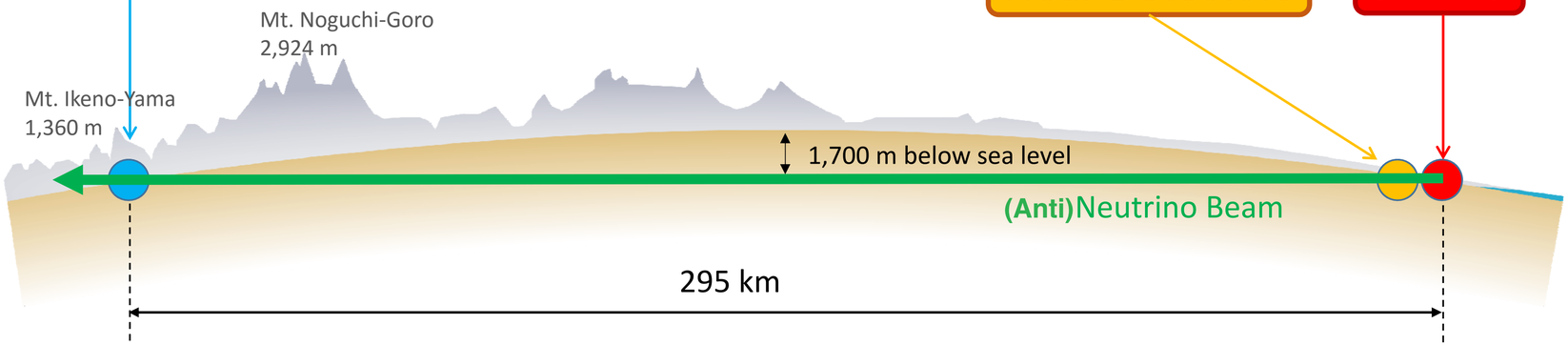

Physics goals:

- Precise measurement of θ_{23}, Δm^2_{32}
- Measurements of θ_{13} and improve limits δ_{CP}

The T2K experiment

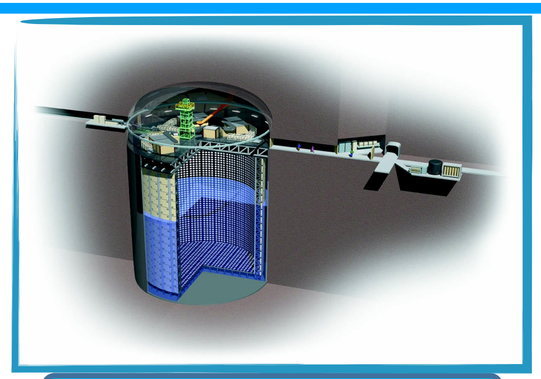

Super-Kamiokande

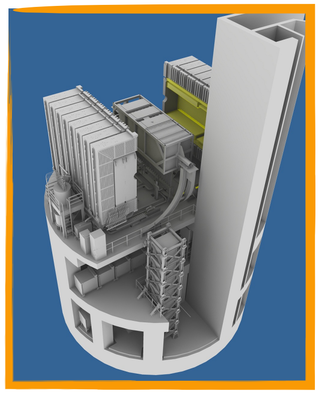

Near Detectors

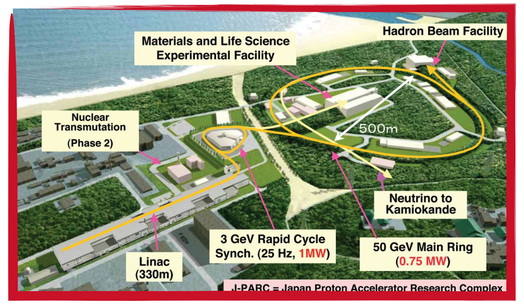

J-PARC

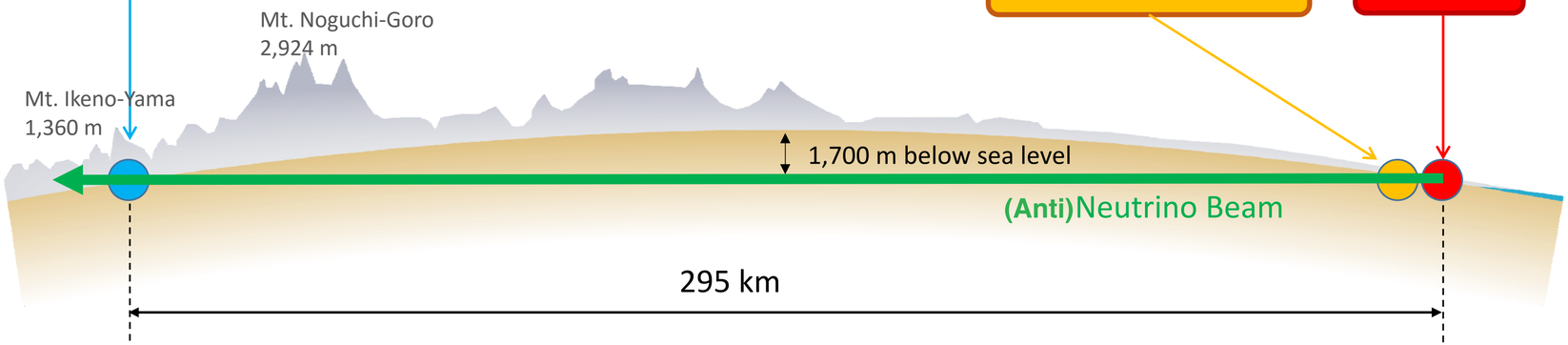

Physics goals:

- Precise measurement of θ_{23}, Δm_{32}^2
- Measurements of θ_{13} and improve limits δ_{CP}
- ν cross section measurements at the near detectors

T2K beam

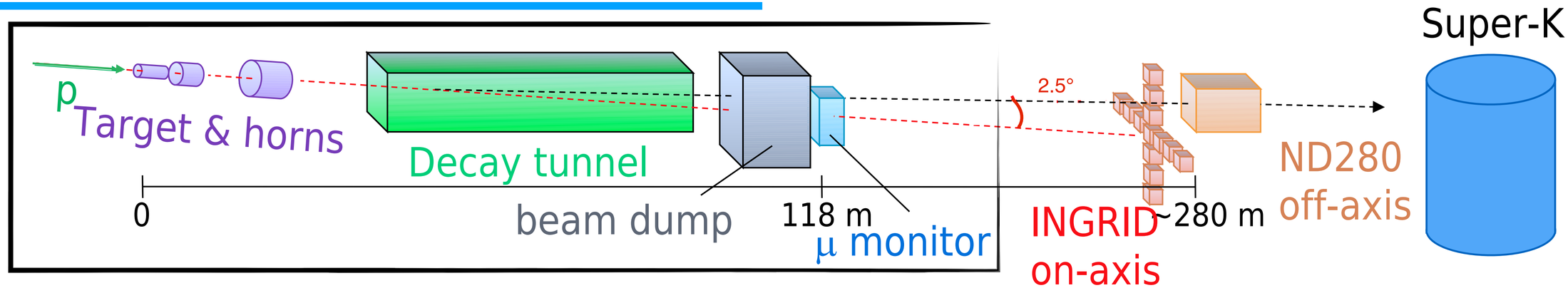
p
Target & horns
Decay tunnel
beam dump
μ monitor
0
118 m
2.5°
~280 m
INGRID
on-axis
ND280
off-axis
Super-K

T2K beam

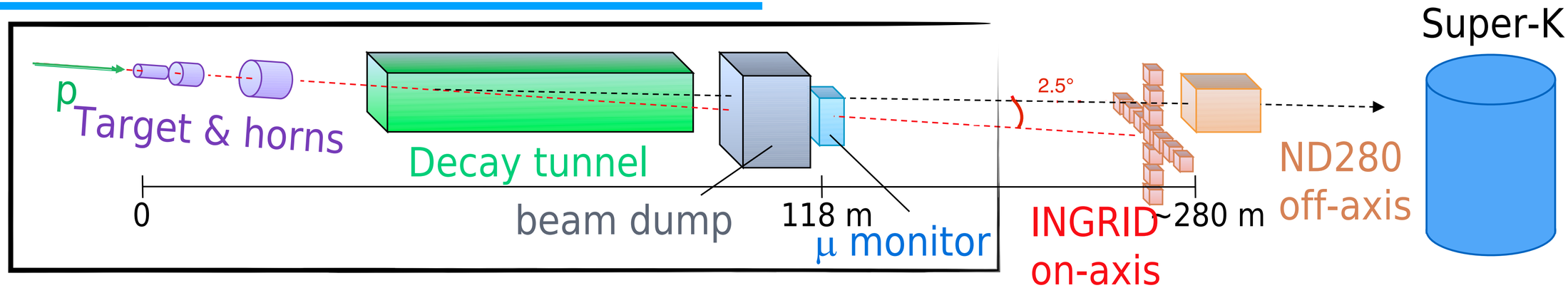

30 GeV proton beam from J-PARC Main Ring extracted onto a graphite target producing hadrons (mainly pions and kaons)

T2K beam

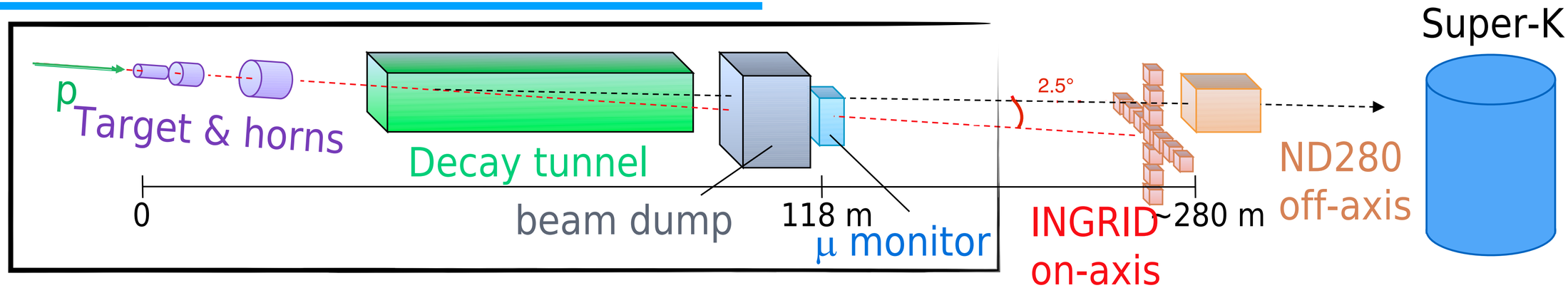

30 GeV proton beam from J-PARC Main Ring extracted onto a graphite target producing hadrons (mainly pions and kaons)

Hadrons are focused and selected in charge by 3 electromagnetic horns

ν_μ beam created by π^+ and $\overline{\nu}_\mu$ beam by π^- decay

T2K beam

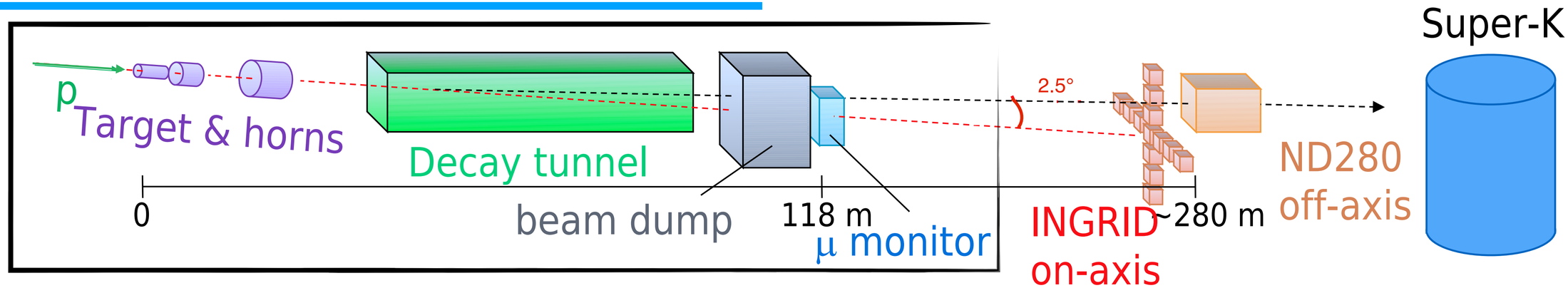

30 GeV proton beam from J-PARC Main Ring extracted onto a graphite target producing hadrons (mainly pions and kaons)

Hadrons are focused and selected in charge by 3 electromagnetic horns

ν_μ beam created by π^+ and $\overline{\nu}_\mu$ beam by π^- decay

Detectors 2.5° off the direction of the beam centered around 0.6 GeV. Off-axis method to reduce high energy tail and to maximize oscillation detection probabilities

T2K beam

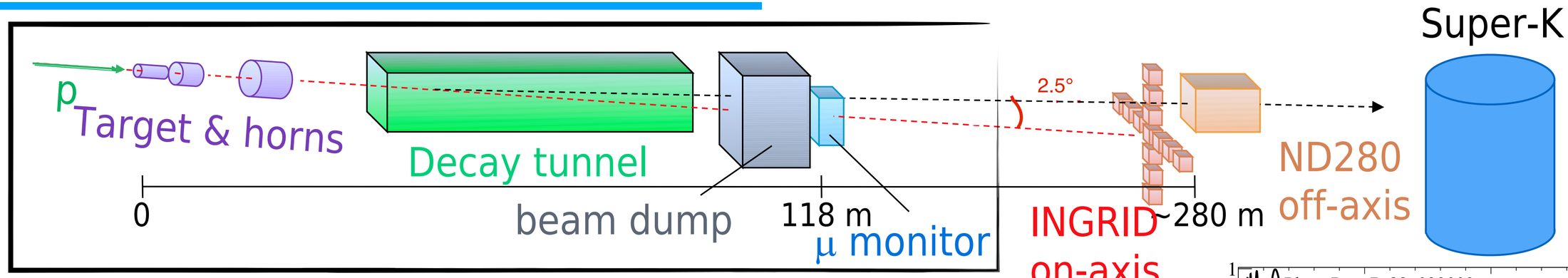

30 GeV proton beam from J-PARC Main Ring extracted onto a graphite target producing hadrons (mainly pions and kaons)

Hadrons are focused and selected in charge by 3 electromagnetic horns

ν_μ beam created by π^+ and $\overline{\nu}_\mu$ beam by π^- decay

Detectors 2.5° off the direction of the beam centered around 0.6 GeV. Off-axis method to reduce high energy tail and to maximize oscillation detection probabilities

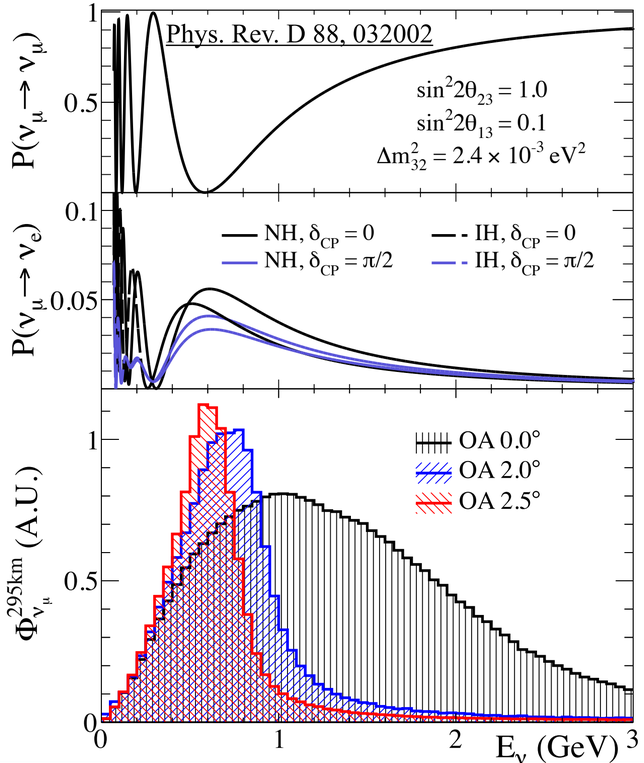

The on-axis near detector (INGRID)

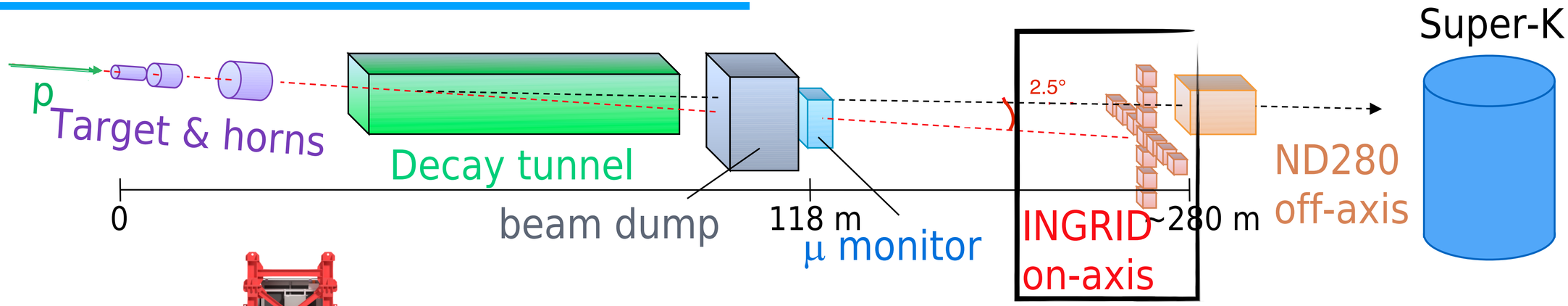

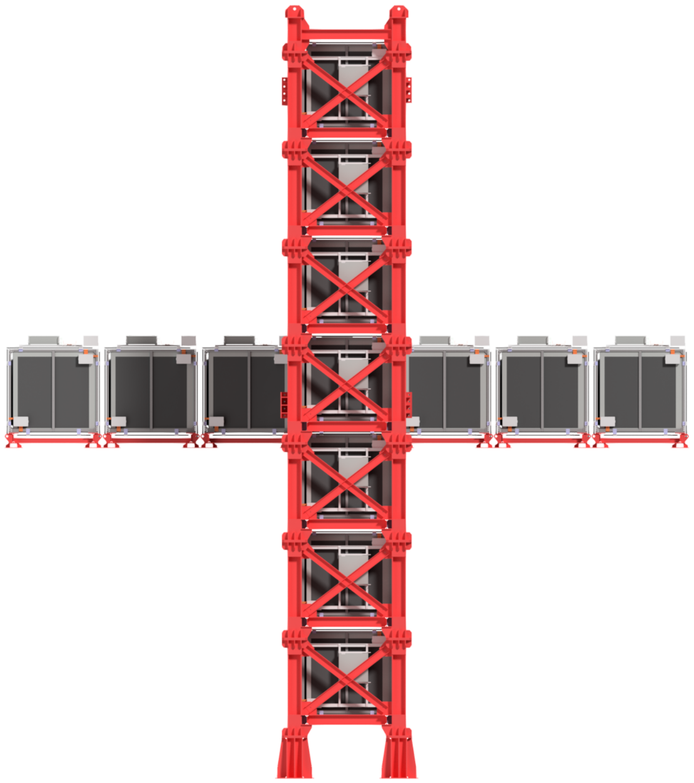

The on-axis near detector (INGRID)

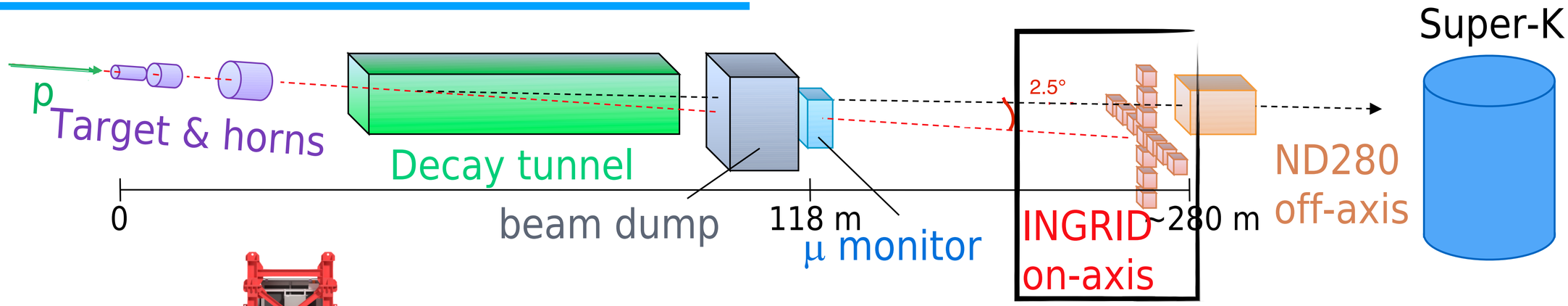

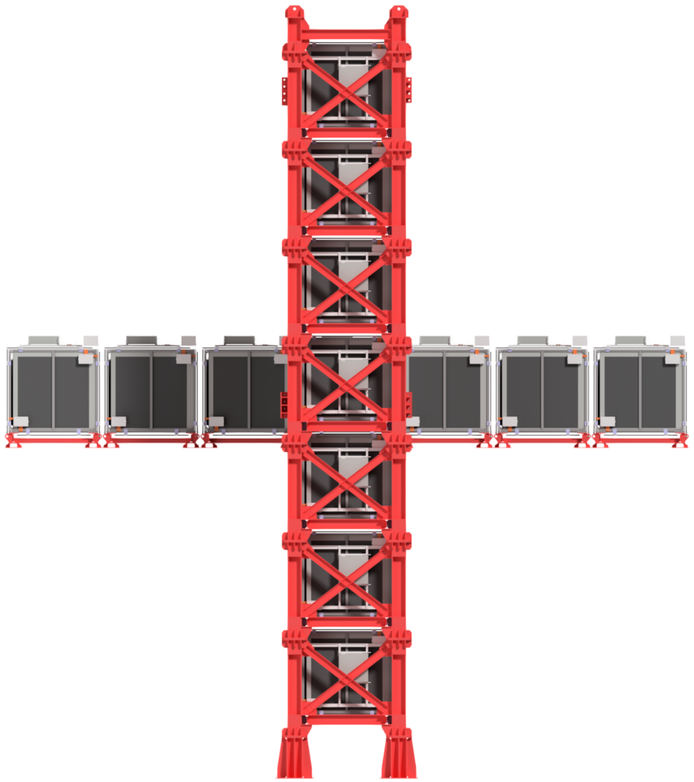

Monitor the beam stability and direction day-by-day looking at ν ($\bar{\nu}$) interactions

The on-axis near detector (INGRID)

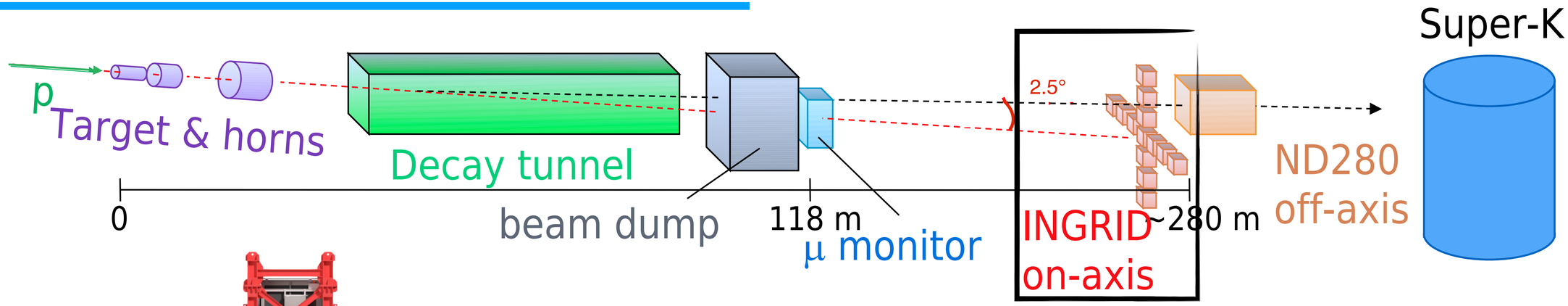

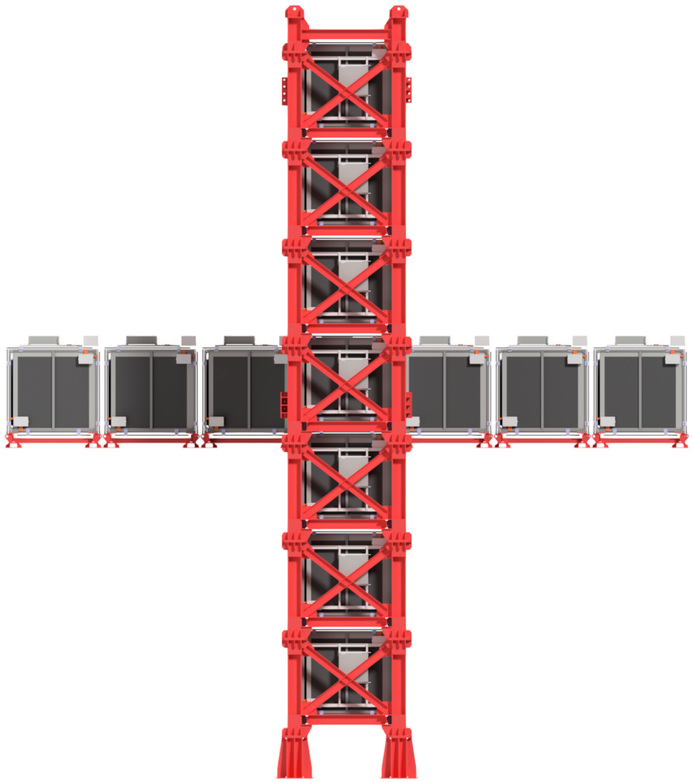

Monitor the beam stability and direction day-by-day looking at ν ($\bar{\nu}$) interactions

Also used to measure neutrino-nucleus cross-section

The off-axis near detector (ND280)

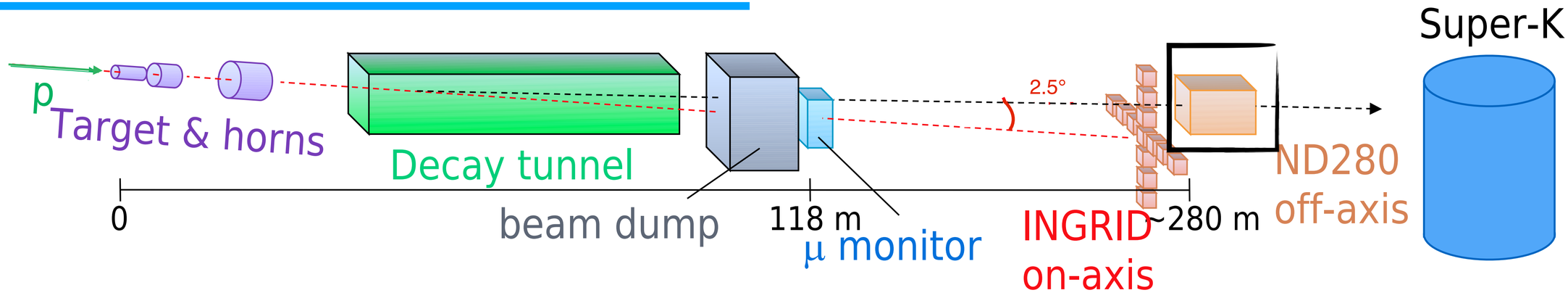

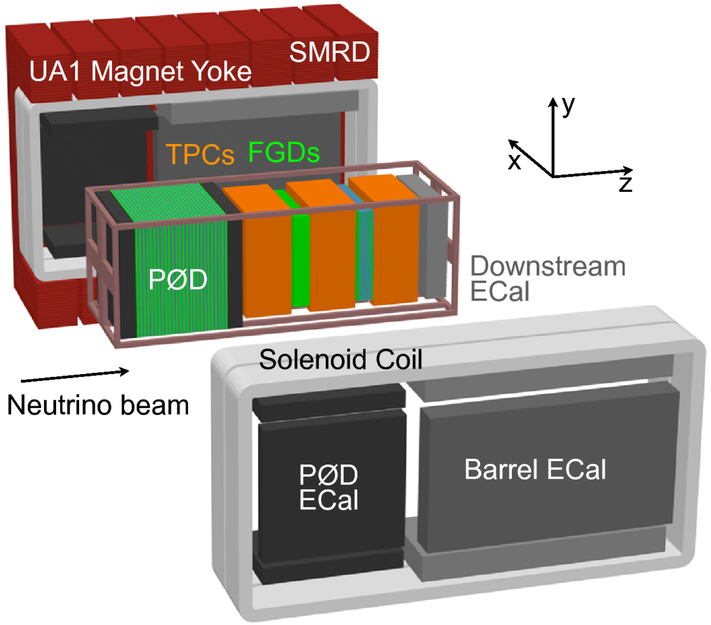

The off-axis near detector (ND280)

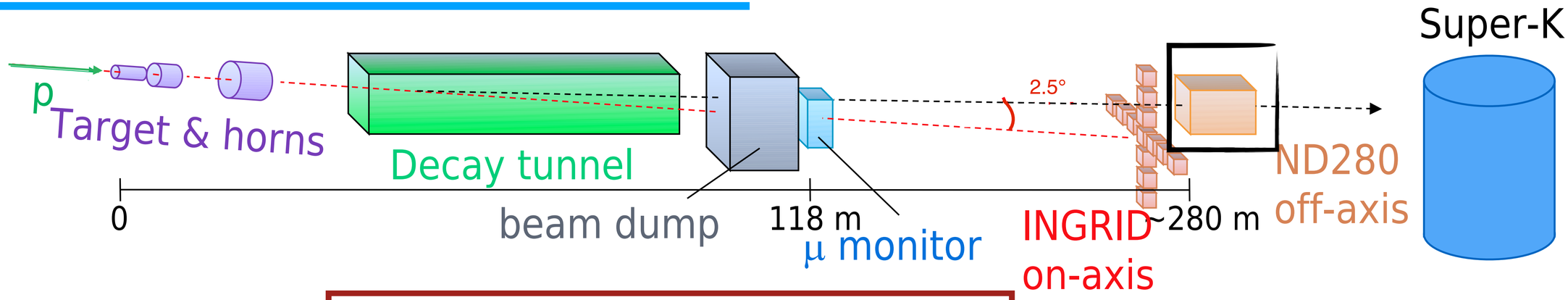

A large dipole magnet (UA1) produces 0.2 T.

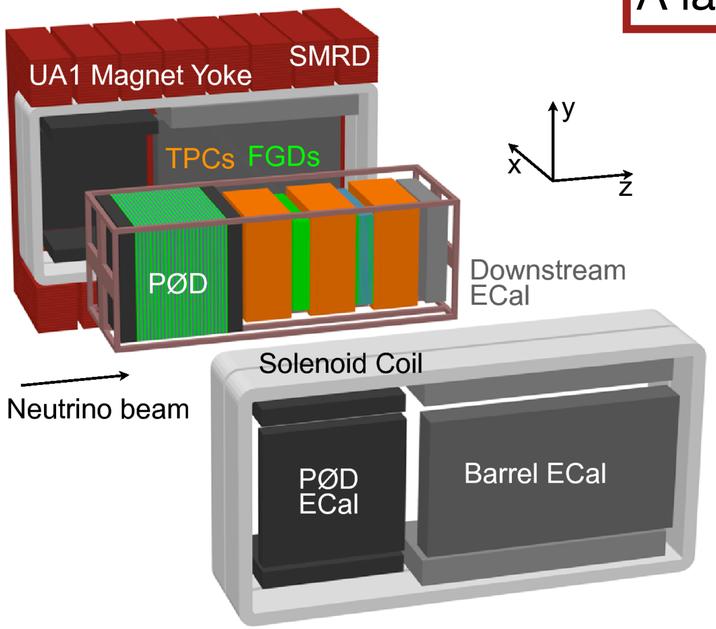

The off-axis near detector (ND280)

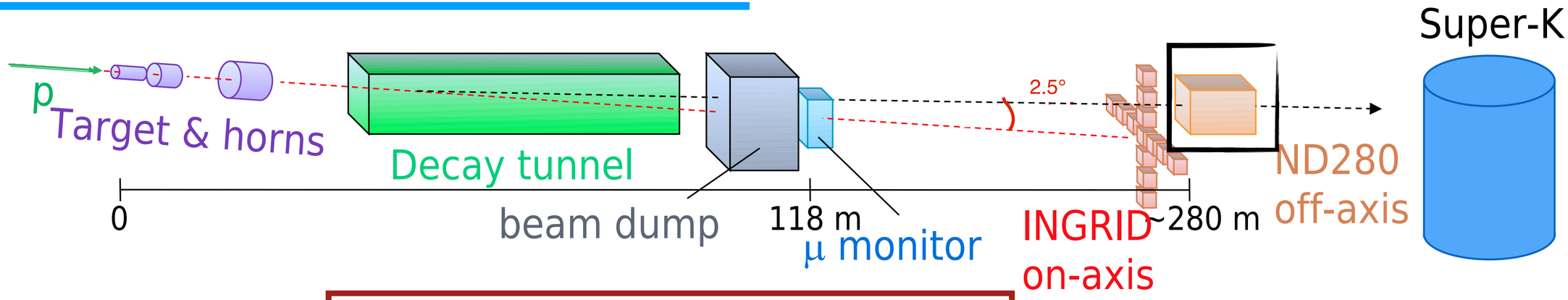

A large dipole magnet (UA1) produces 0.2 T.

Side muon range detector (SMRD): plastic scintillators instrumenting the magnet slices

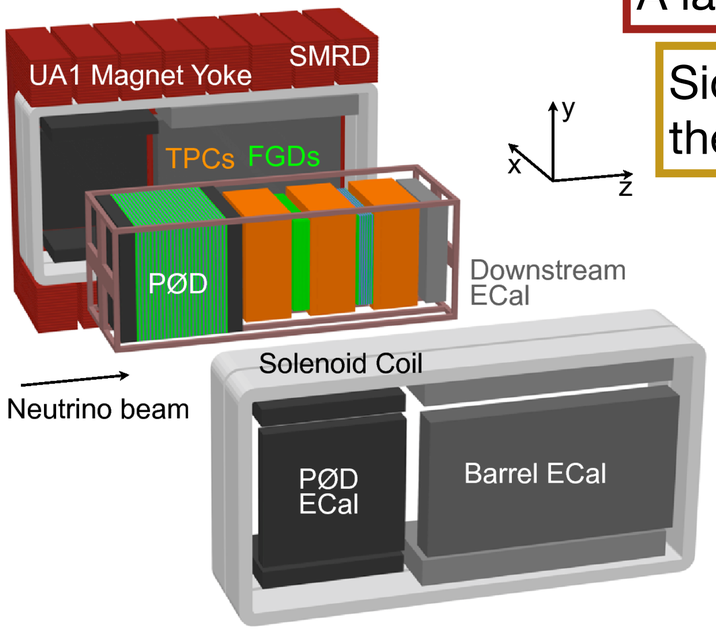

The off-axis near detector (ND280)

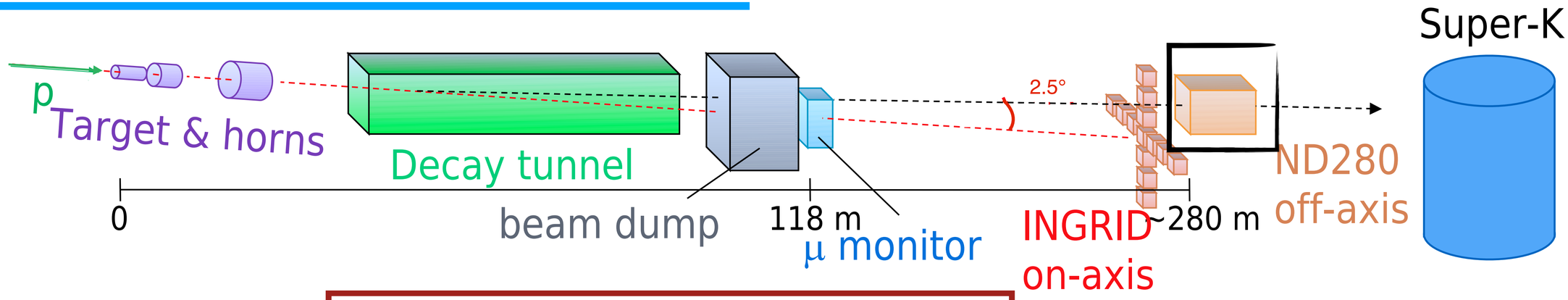

A large dipole magnet (UA1) produces 0.2 T.

Side muon range detector (SMRD): plastic scintillators instrumenting the magnet slices

π^0 detector (P0D): *xy* layers plastic scintillator alternated with water layers

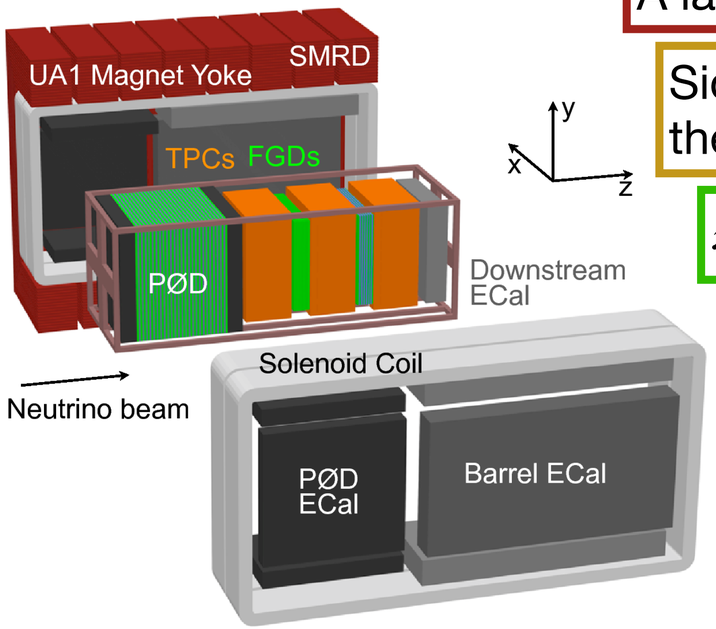

The off-axis near detector (ND280)

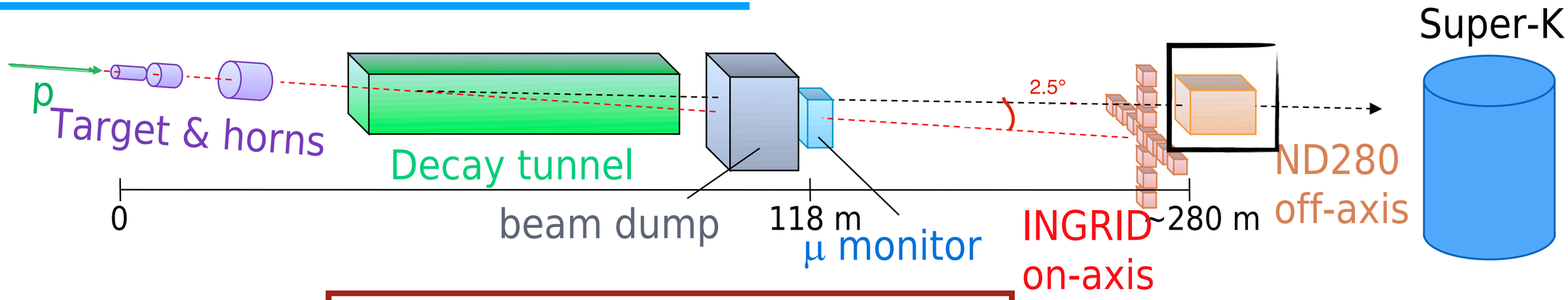

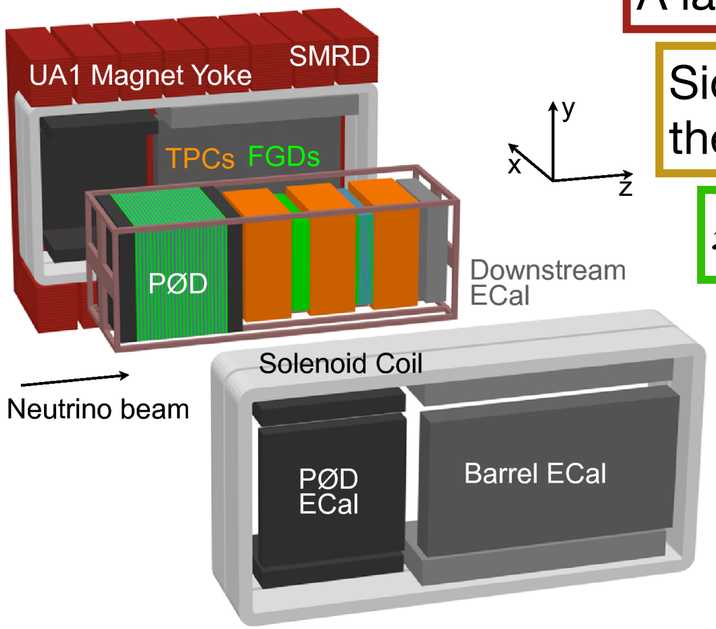

A large dipole magnet (UA1) produces 0.2 T.

Side muon range detector (SMRD): plastic scintillators instrumenting the magnet slices

π^0 detector (P0D): *xy* layers plastic scintillator alternated with water layers

3 Time projection chambers (TPC): reconstruct momentum and charge, PID based on ionization

The off-axis near detector (ND280)

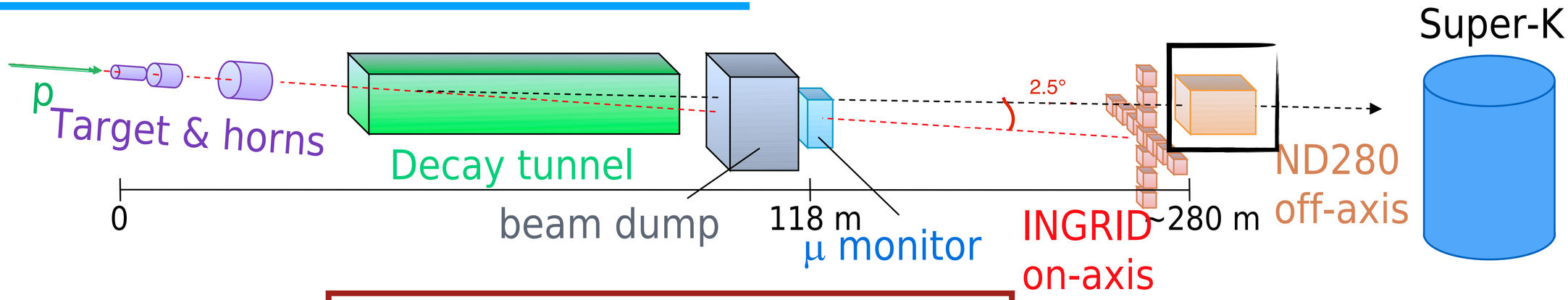

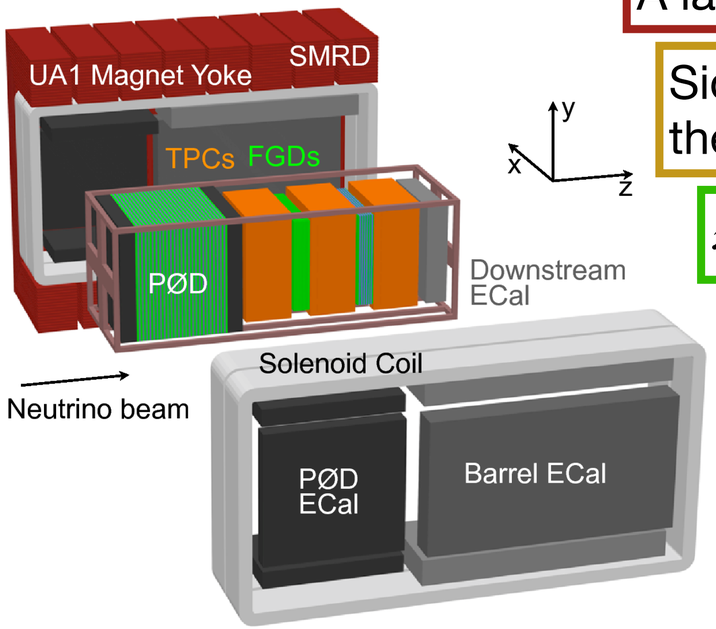

A large dipole magnet (UA1) produces 0.2 T.

Side muon range detector (SMRD): plastic scintillators instrumenting the magnet slices

π^0 detector (P0D): *xy* layers plastic scintillator alternated with water layers

3 Time projection chambers (TPC): reconstruct momentum and charge, PID based on ionization

2 Fine-grained detectors (FGD): upstream constituted of *xy* layers of plastic scintillator, the other is alternated with water layers

The off-axis near detector (ND280)

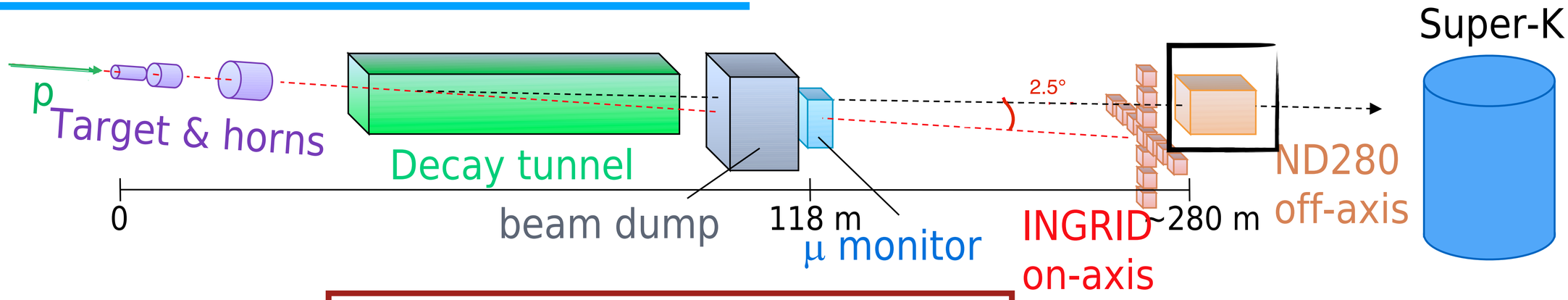

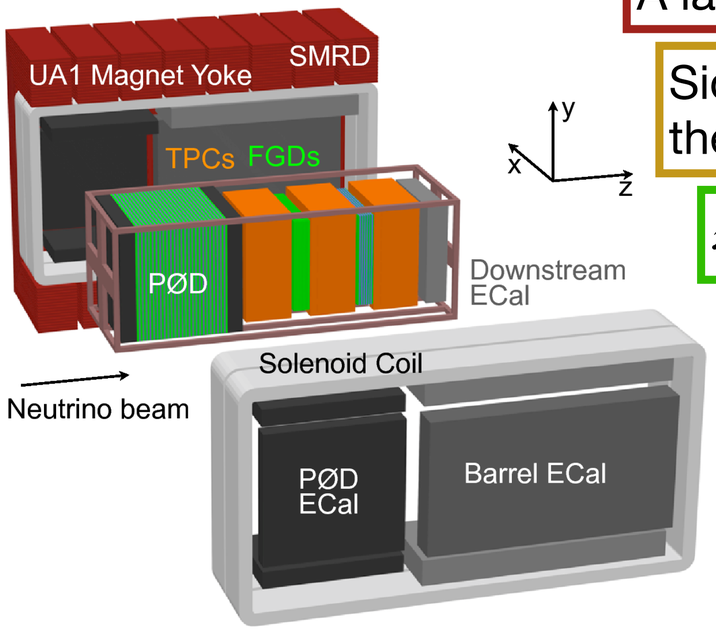

A large dipole magnet (UA1) produces 0.2 T.

Side muon range detector (SMRD): plastic scintillators instrumenting the magnet slices

π^0 detector (P0D): *xy* layers plastic scintillator alternated with water layers

3 Time projection chambers (TPC): reconstruct momentum and charge, PID based on ionization

2 Fine-grained detectors (FGD): upstream constituted of *xy* layers of plastic scintillator, the other is alternated with water layers

An electromagnetic calorimeter (ECal) is used to distinguish tracks from showers

Super-Kamiokande (SK)

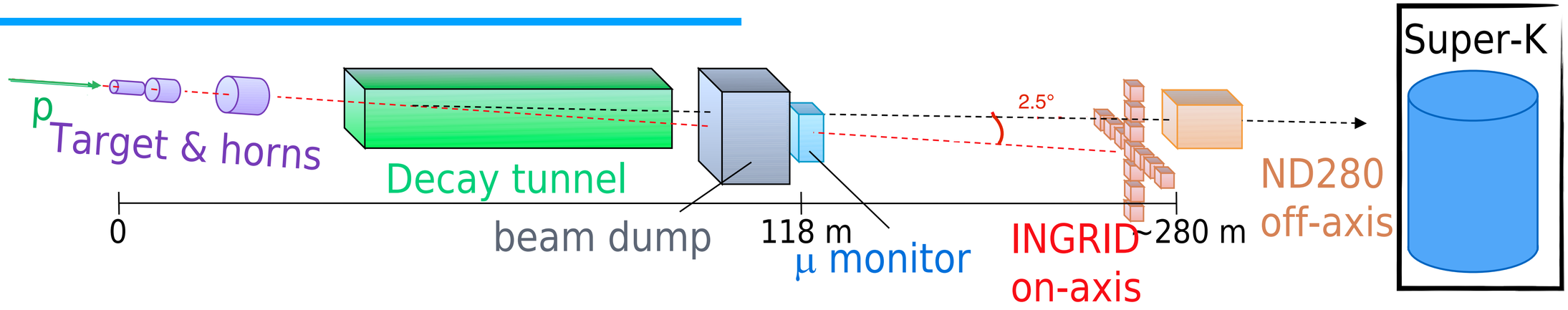

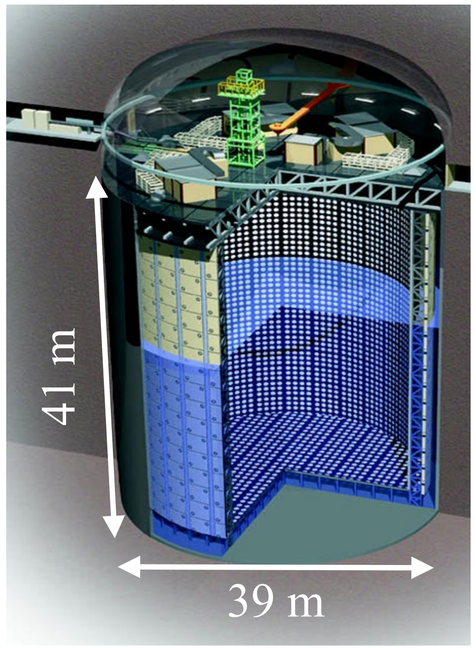

Super-Kamiokande (SK)

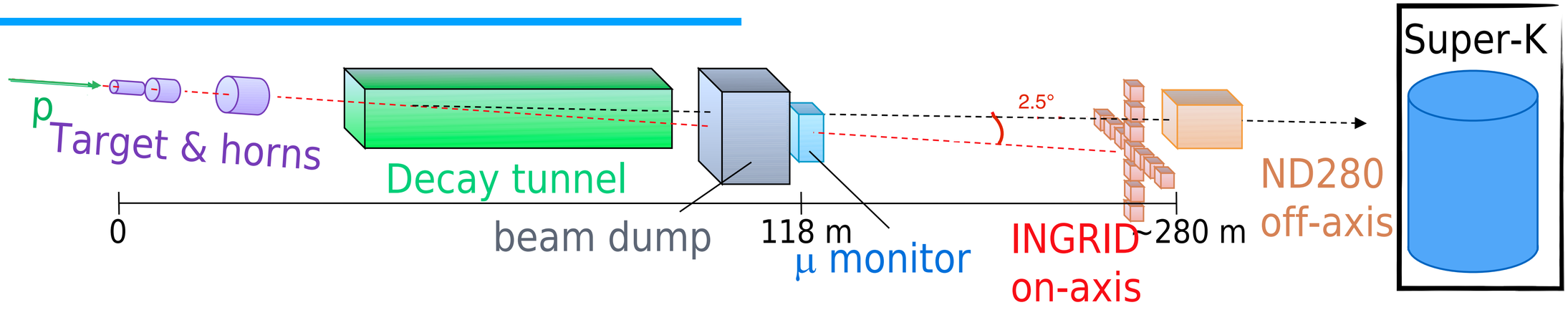

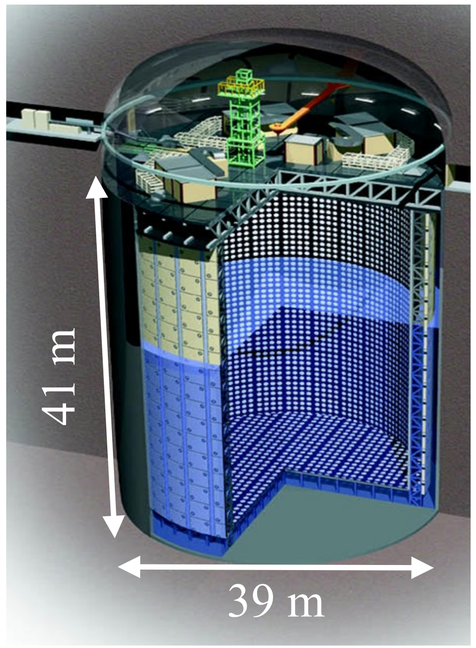

SK is a 50 kton water Cherenkov detector

Super-Kamiokande (SK)

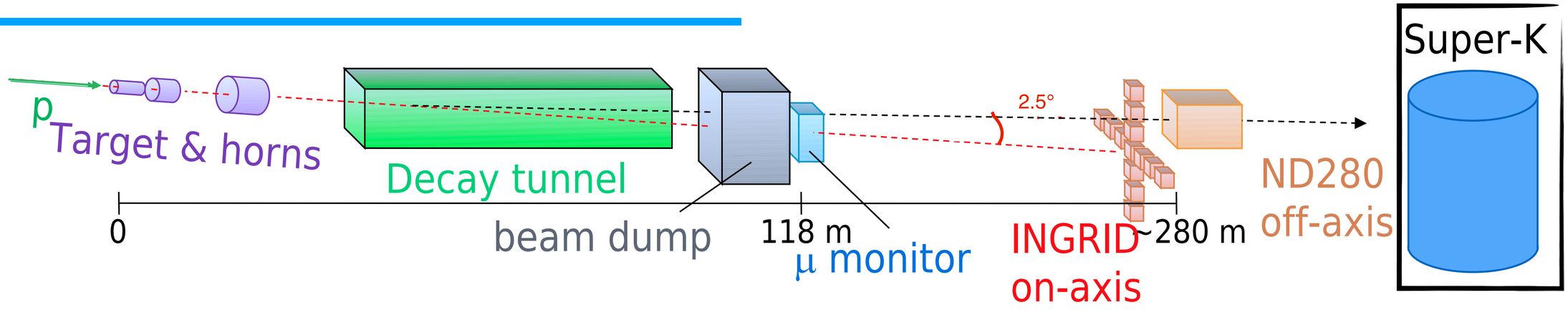

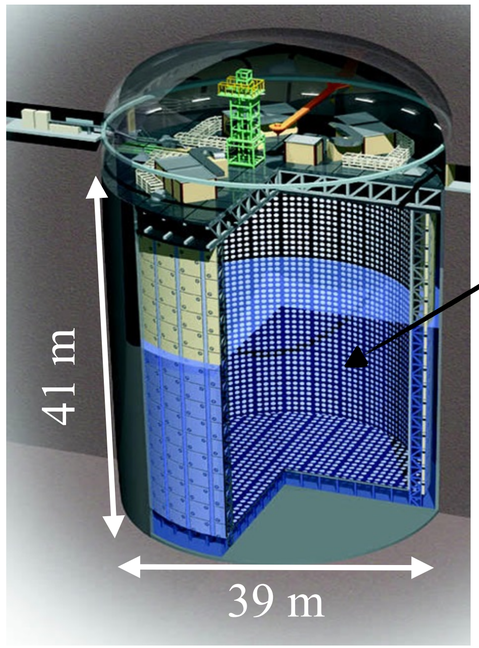

SK is a 50 kton water Cherenkov detector

Inner detector ~11000 20 inch PMTs

Super-Kamiokande (SK)

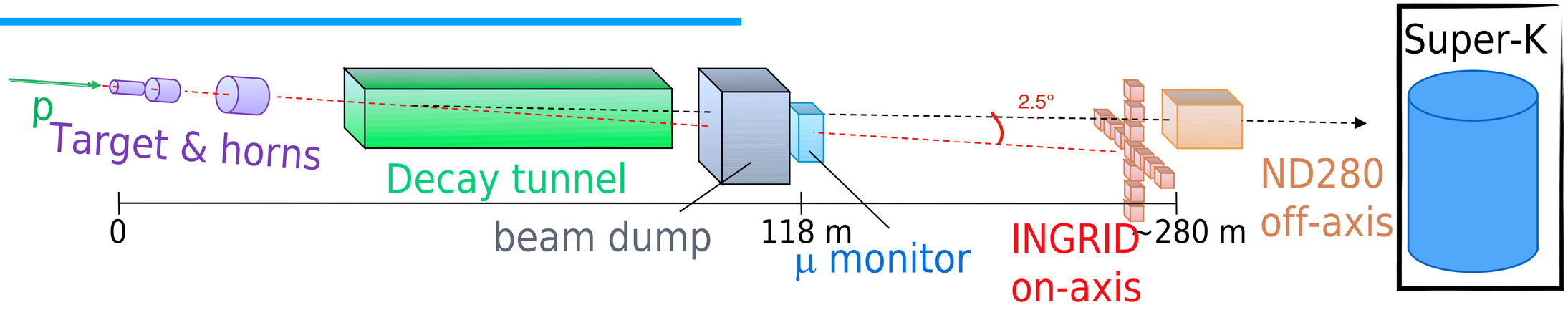

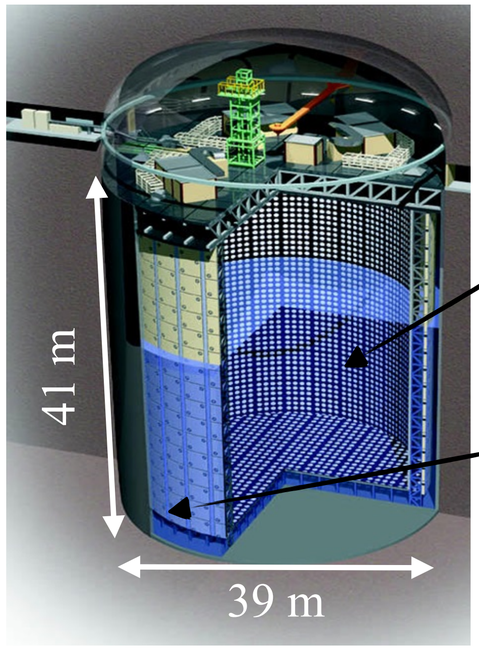

SK is a 50 kton water Cherenkov detector

Inner detector ~11000 20 inch PMTs

Outer detector ~2000 8 inch PMTs

Super-Kamiokande (SK)

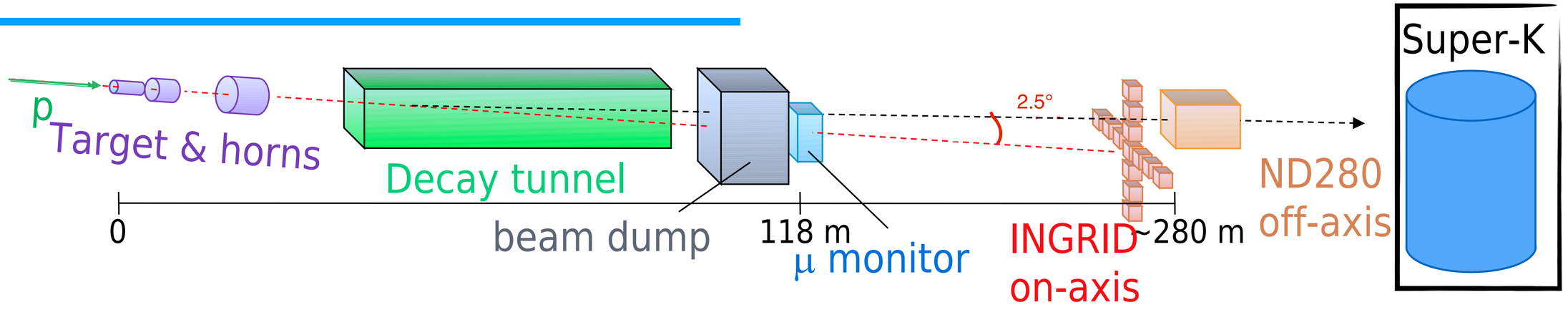

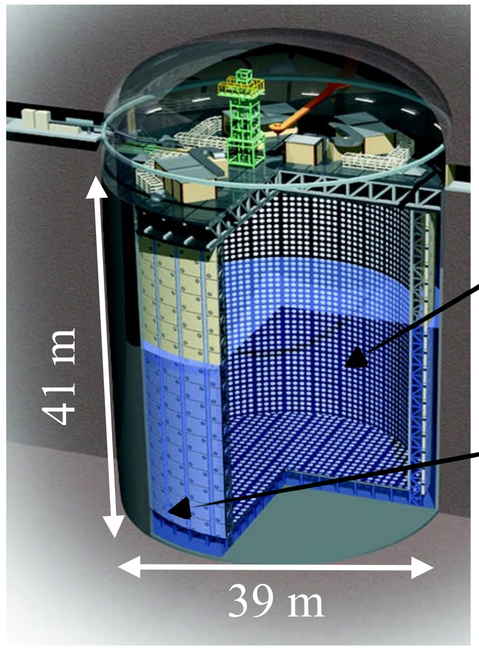

SK is a 50 kton water Cherenkov detector

Inner detector ~11000 20 inch PMTs

Outer detector ~2000 8 inch PMTs

Very good μ/e separation

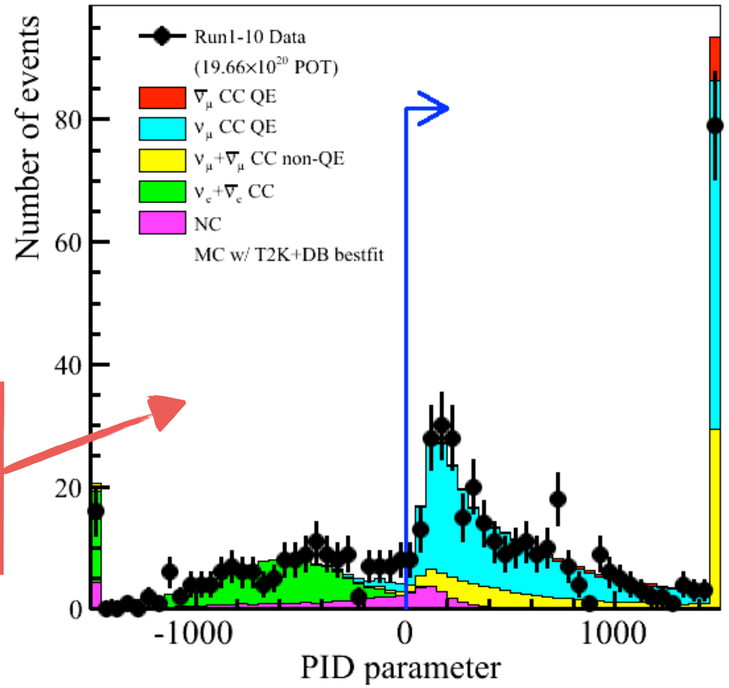

Data taking

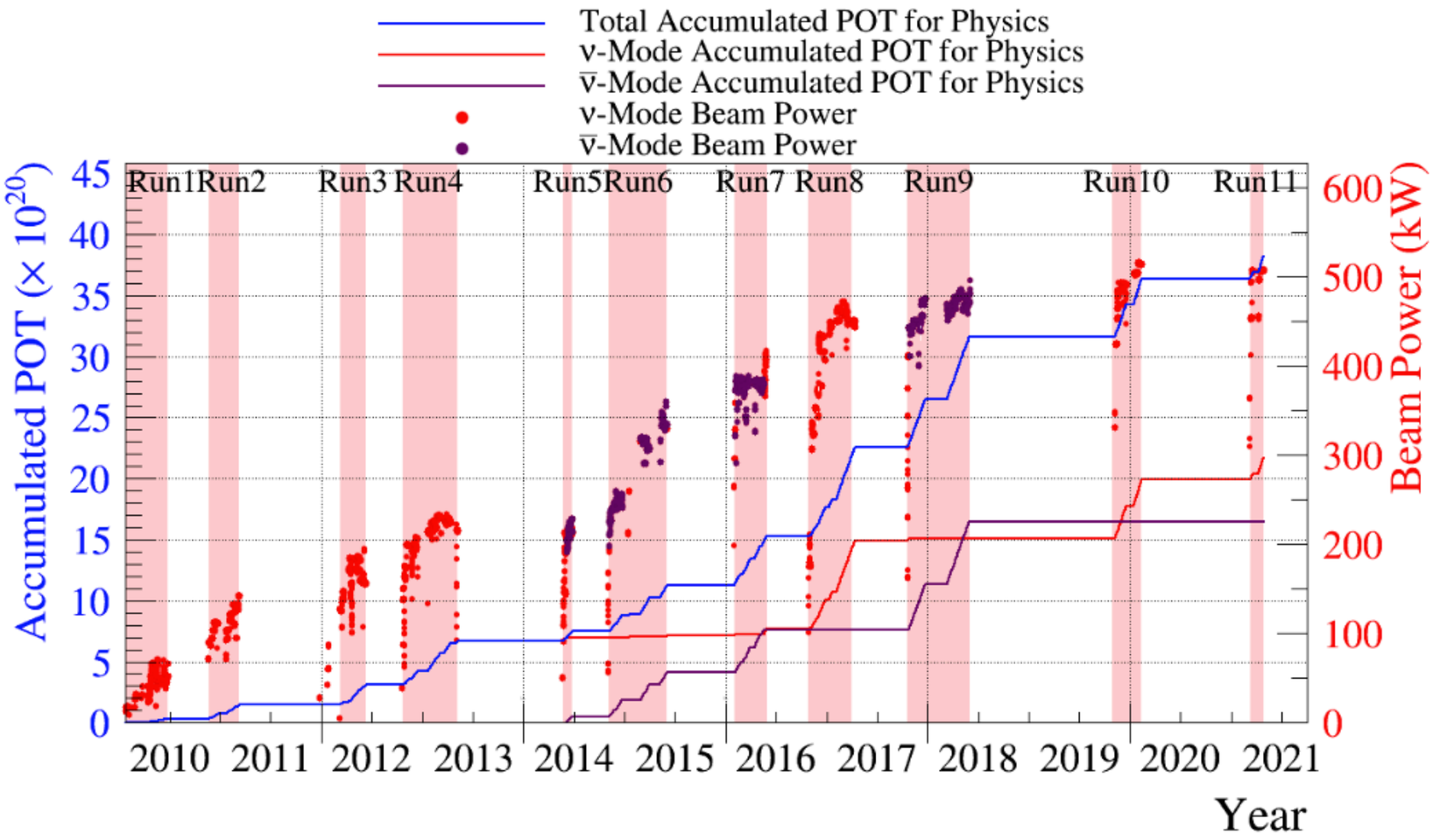

Data from 23 Jan 2010 to 27 Apr 2021

Total POT 3.8×10^{21}

ν-mode 2.2×10^{21} (56.8%)

$\bar{\nu}$-mode 1.6×10^{21} (43.2%)

Maximum Power 522 kW

Data taking

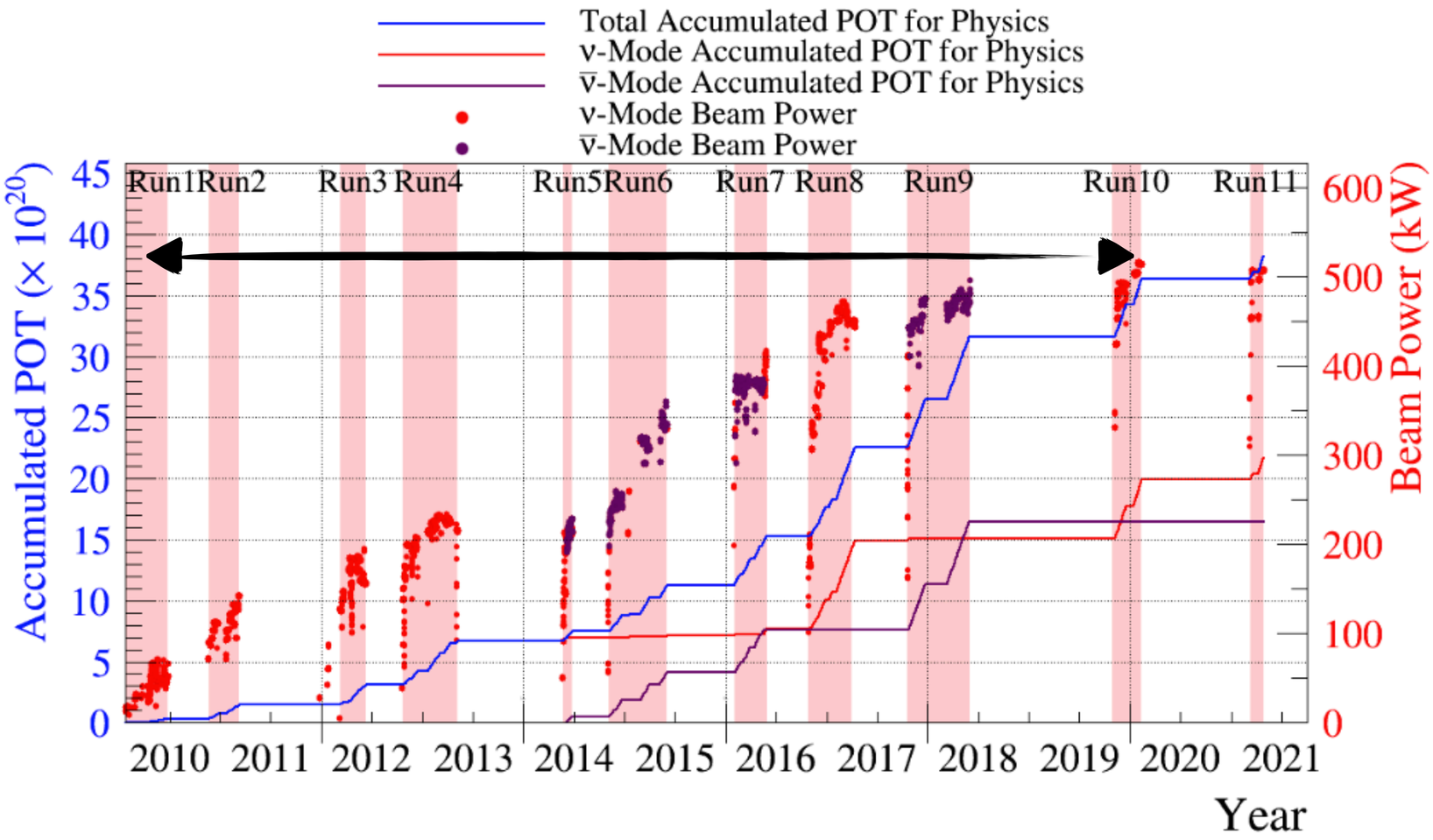

Data from 23 Jan 2010 to 27 Apr 2021

Total POT 3.8×10^{21}

ν-mode 2.2×10^{21} (56.8%)

$\bar{\nu}$-mode 1.6×10^{21} (43.2%)

Maximum Power 522 kW

Results presented here on neutrino oscillation use 3.6×10^{21} POT

T2K oscillation analysis strategy

Bayesian analysis

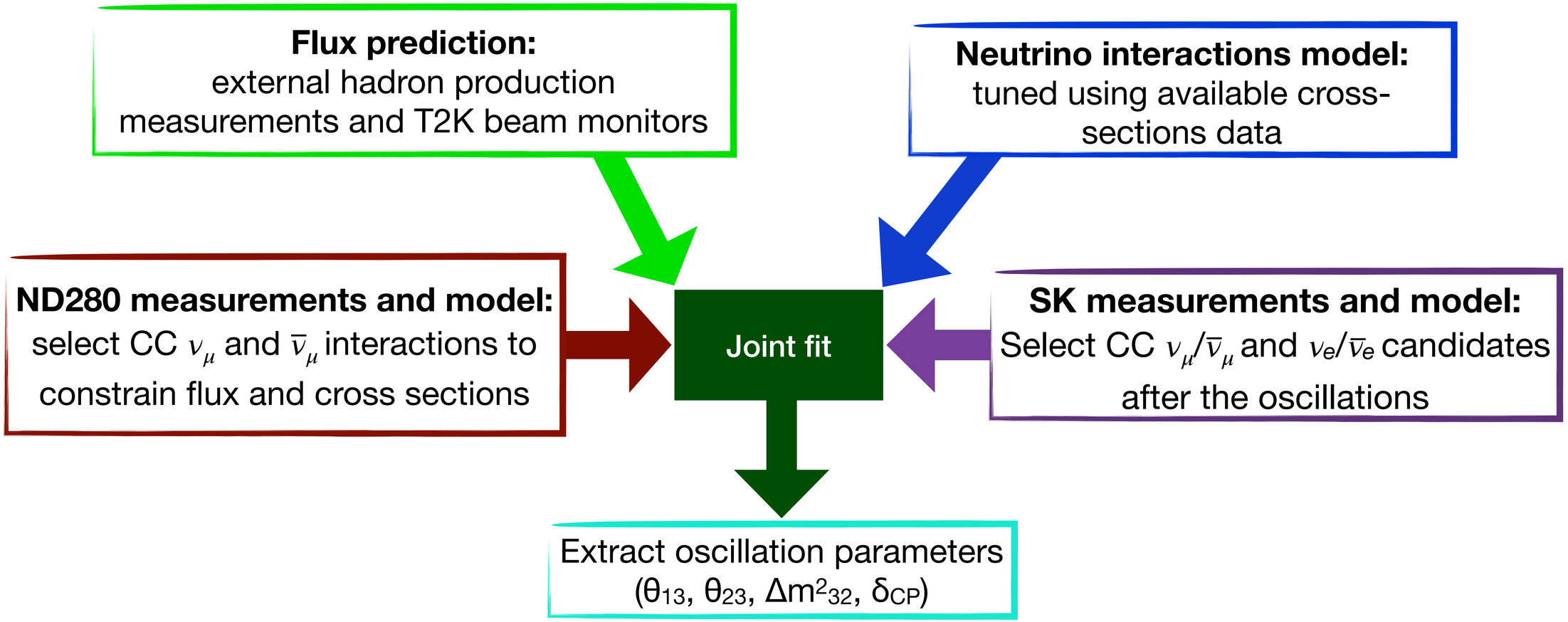

T2K oscillation analysis strategy

Hybrid-frequentist analysis

T2K oscillation analysis strategy

Hybrid-frequentist analysis

Flux prediction:
external hadron production
measurements and T2K beam monitors

T2K oscillation analysis strategy

Hybrid-frequentist analysis

Flux prediction:
external hadron production measurements and T2K beam monitors

Neutrino interactions model:
tuned using available cross-sections data

T2K oscillation analysis strategy

Hybrid-frequentist analysis

Flux prediction:
external hadron production measurements and T2K beam monitors

ND280 measurements and model:
select CC ν_μ and $\bar{\nu}_\mu$ interactions to constrain flux and cross sections

Neutrino interactions model:
tuned using available cross-sections data

T2K oscillation analysis strategy

Hybrid-frequentist analysis

Flux prediction:
external hadron production measurements and T2K beam monitors

ND280 measurements and model:
select CC ν_μ and $\bar{\nu}_\mu$ interactions to constrain flux and cross sections

Neutrino interactions model:
tuned using available cross-sections data

Prediction at the Far Detector:
ND280 measurements predict the expected events at SK

T2K oscillation analysis strategy

Hybrid-frequentist analysis

Flux prediction:
external hadron production measurements and T2K beam monitors

ND280 measurements and model:
select CC ν_μ and $\bar{\nu}_\mu$ interactions to constrain flux and cross sections

Neutrino interactions model:
tuned using available cross-sections data

Prediction at the Far Detector:
ND280 measurements predict the expected events at SK

SK measurements and model:
Select CC $\nu_\mu/\bar{\nu}_\mu$ and $\nu_e/\bar{\nu}_e$ candidates after the oscillations

T2K oscillation analysis strategy

Hybrid-frequentist analysis

Flux prediction:
external hadron production measurements and T2K beam monitors

ND280 measurements and model:
select CC ν_μ and $\bar{\nu}_\mu$ interactions to constrain flux and cross sections

Neutrino interactions model:
tuned using available cross-sections data

Prediction at the Far Detector:
ND280 measurements predict the expected events at SK

SK measurements and model:
Select CC $\nu_\mu/\bar{\nu}_\mu$ and $\nu_e/\bar{\nu}_e$ candidates after the oscillations

Extract oscillation parameters
(θ_{13}, θ_{23}, Δm^2_{32}, δ_{CP})

T2K oscillation analysis strategy

Hybrid-frequentist analysis

Flux prediction:
external hadron production measurements and T2K beam monitors

ND280 measurements and model:
select CC ν_μ and $\bar{\nu}_\mu$ interactions to constrain flux and cross sections

Neutrino interactions model:
tuned using available cross-sections data

Prediction at the Far Detector:
ND280 measurements predict the expected events at SK

SK measurements and model:
Select CC $\nu_\mu/\bar{\nu}_\mu$ and $\nu_e/\bar{\nu}_e$ candidates after the oscillations

Extract oscillation parameters
(θ_{13}, θ_{23}, Δm^2_{32}, δ_{CP})

Neutrino fluxes

Flux predictions based on NA61/SHINE measurements

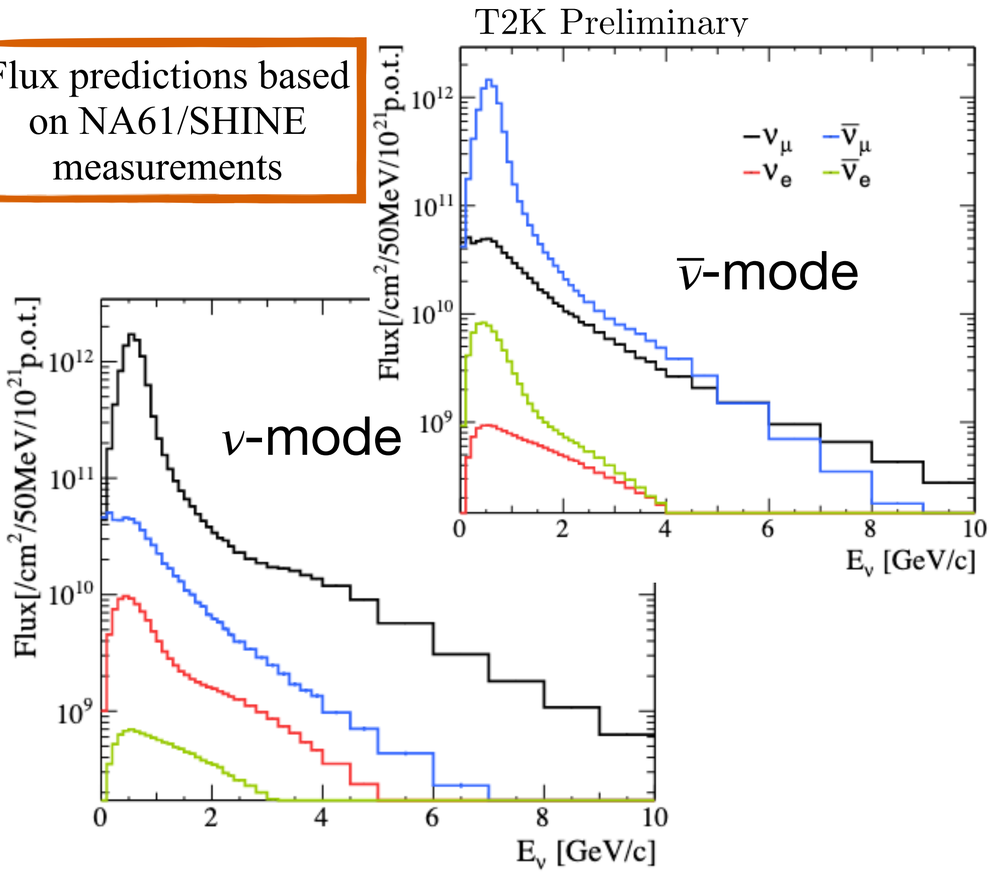

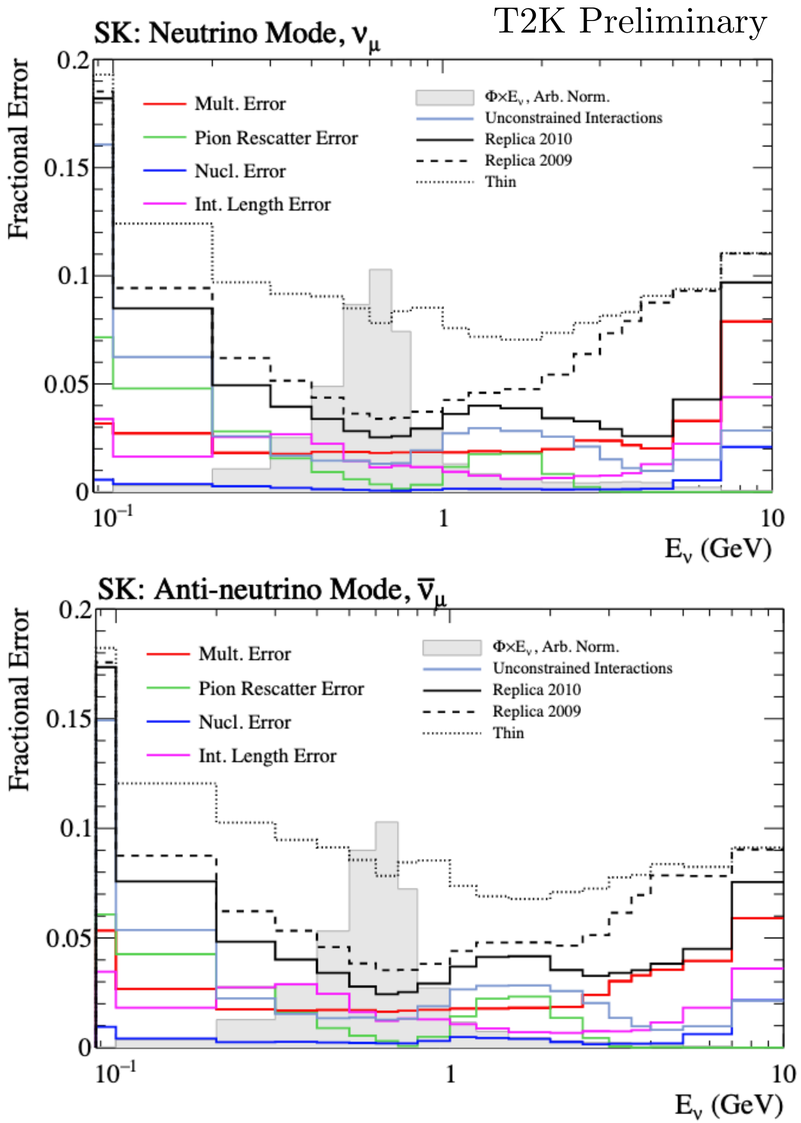

Neutrino fluxes

Flux predictions based on NA61/SHINE measurements

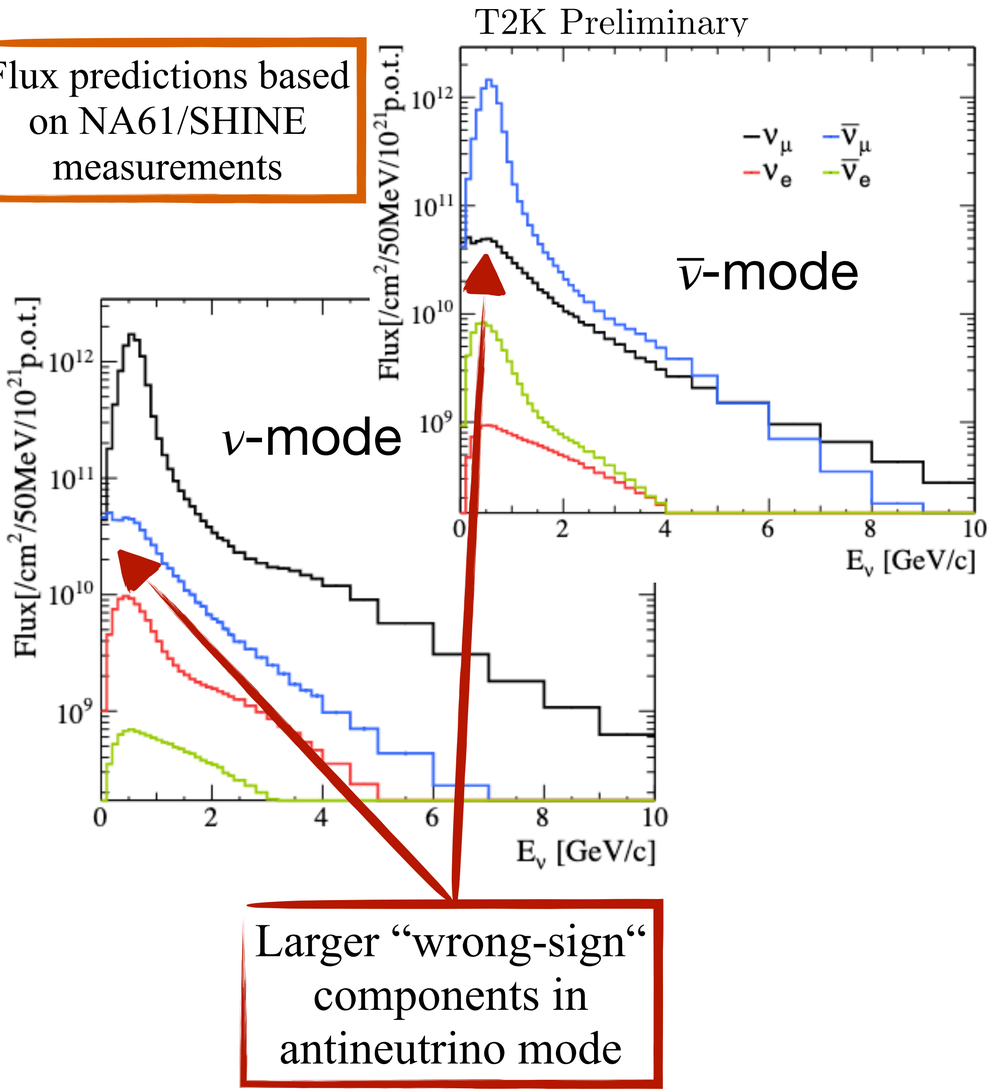

Larger "wrong-sign" components in antineutrino mode

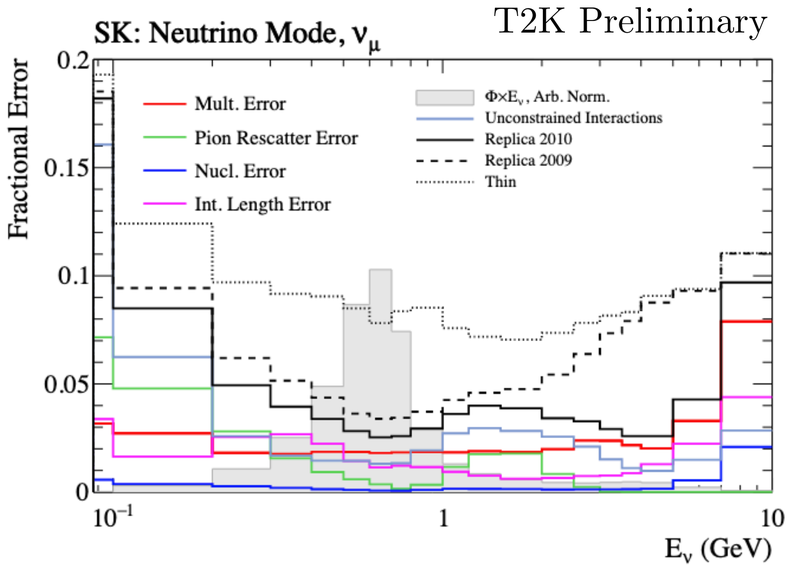

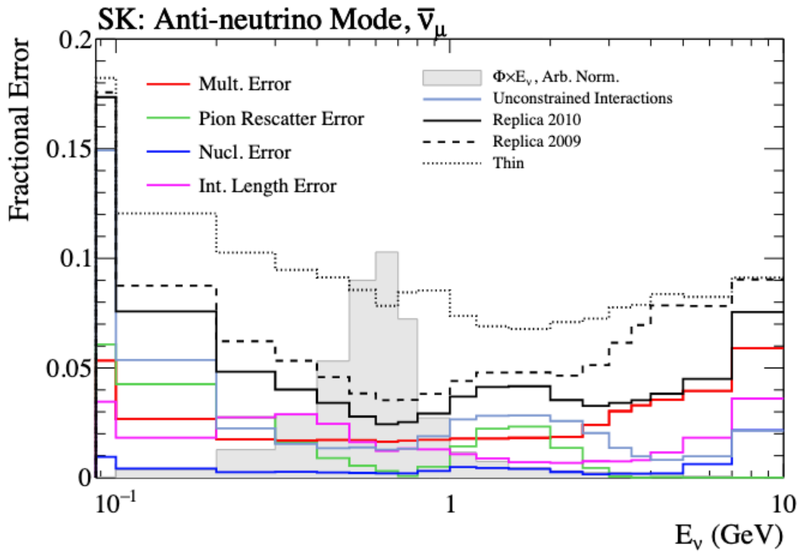

Neutrino fluxes

Flux predictions based on NA61/SHINE measurements

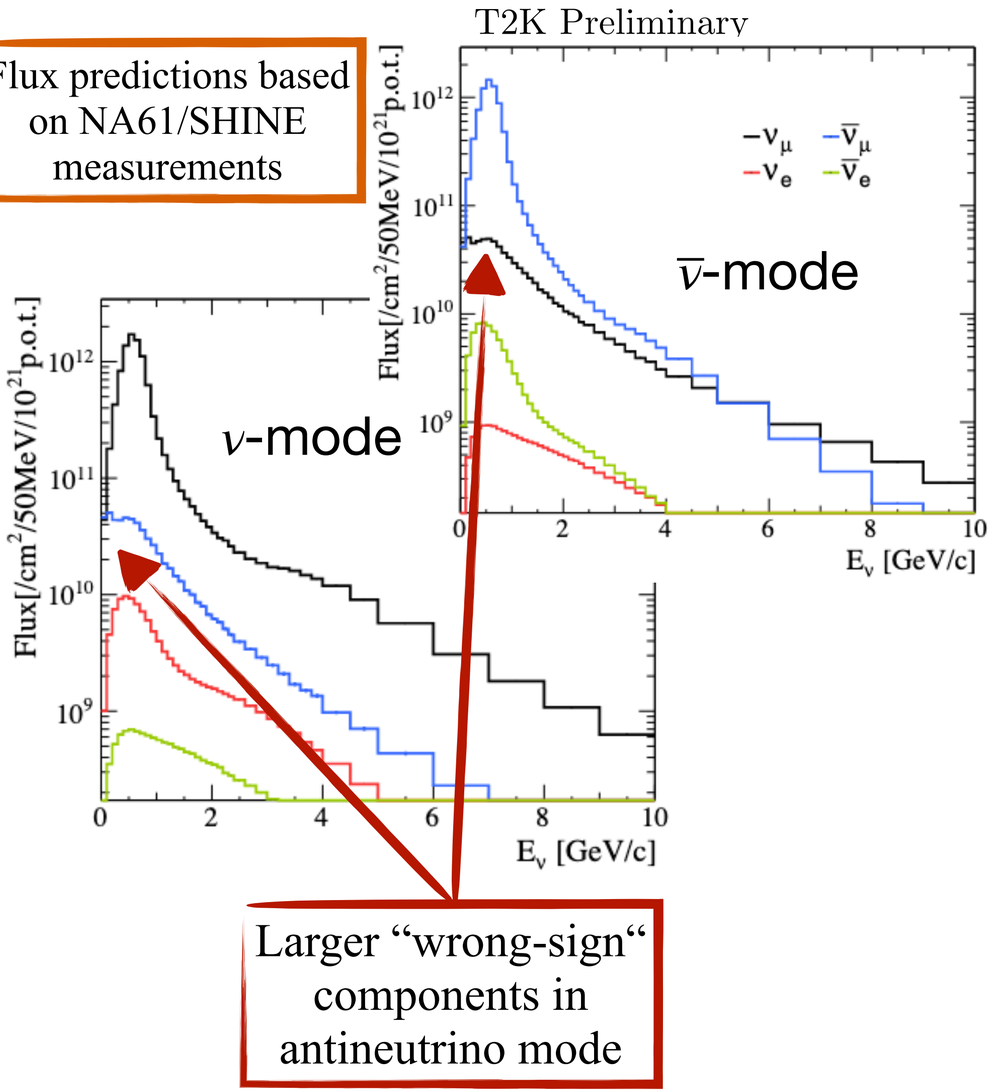

Larger "wrong-sign" components in antineutrino mode

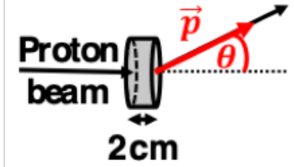

Until 2018 flux uncertainty was around 10% and was based on NA61/SHINE thin-target measurements

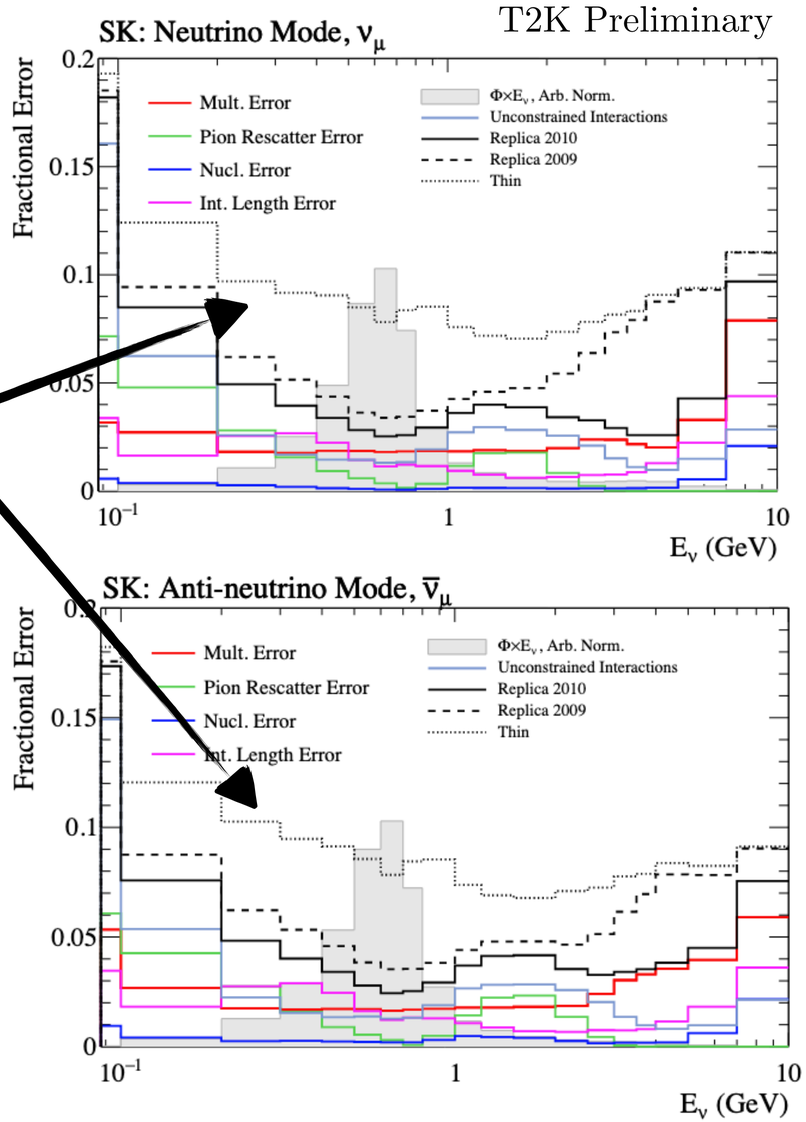

Neutrino fluxes

Flux predictions based on NA61/SHINE measurements

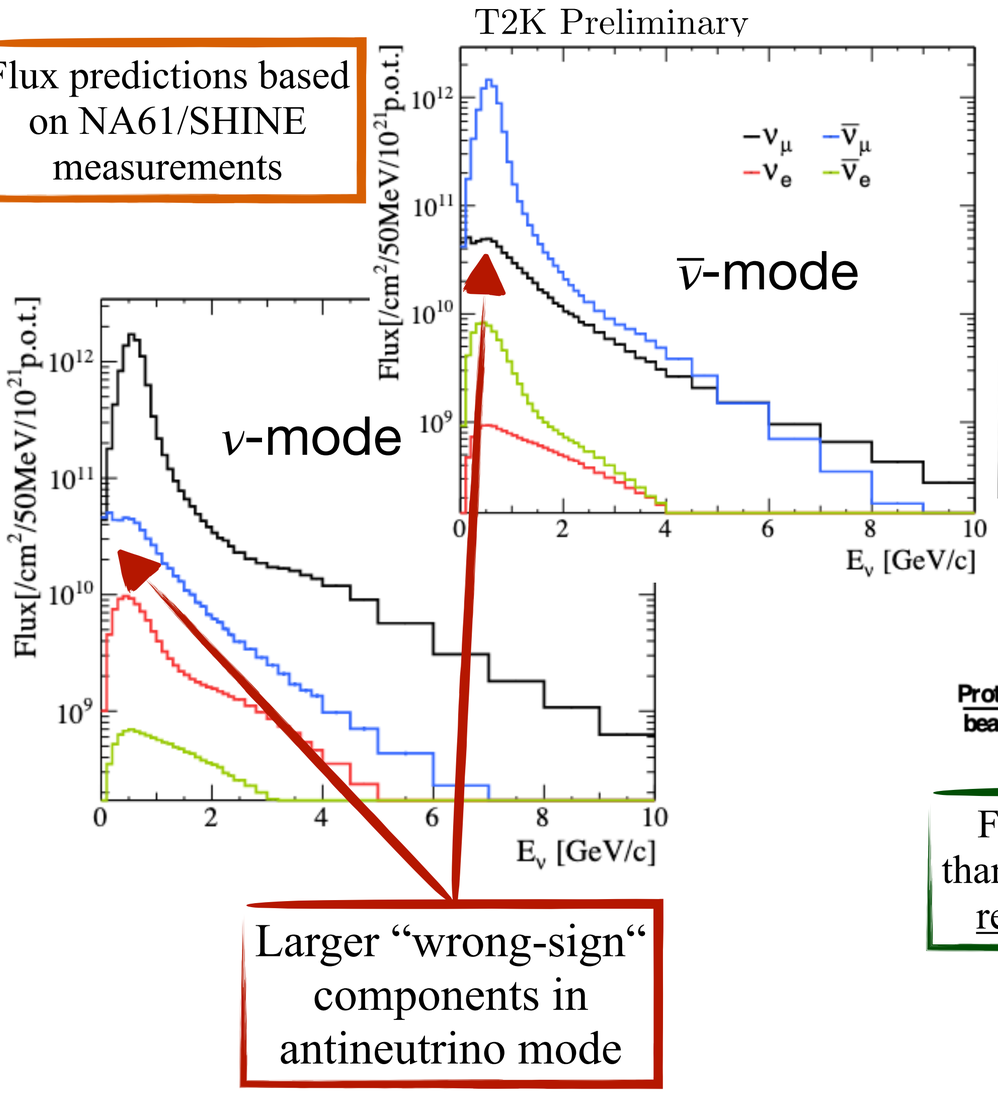

Larger "wrong-sign" components in antineutrino mode

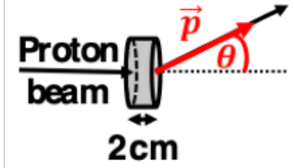

Until 2018 flux uncertainty was around 10% and was based on NA61/SHINE thin-target measurements

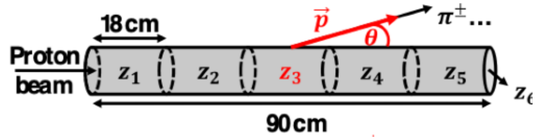

Fluxes uncertainties smaller than 5% based on NA61/SHINE replica-target measurements

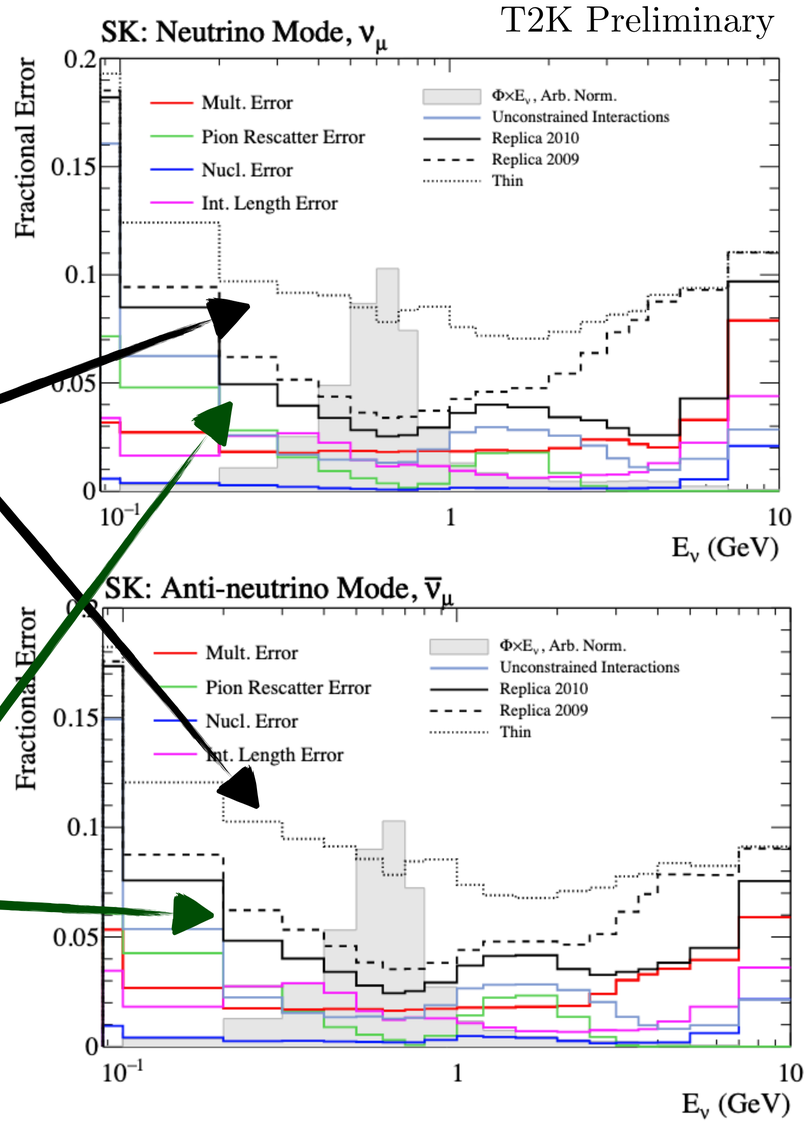

Relevant ν interactions at T2K

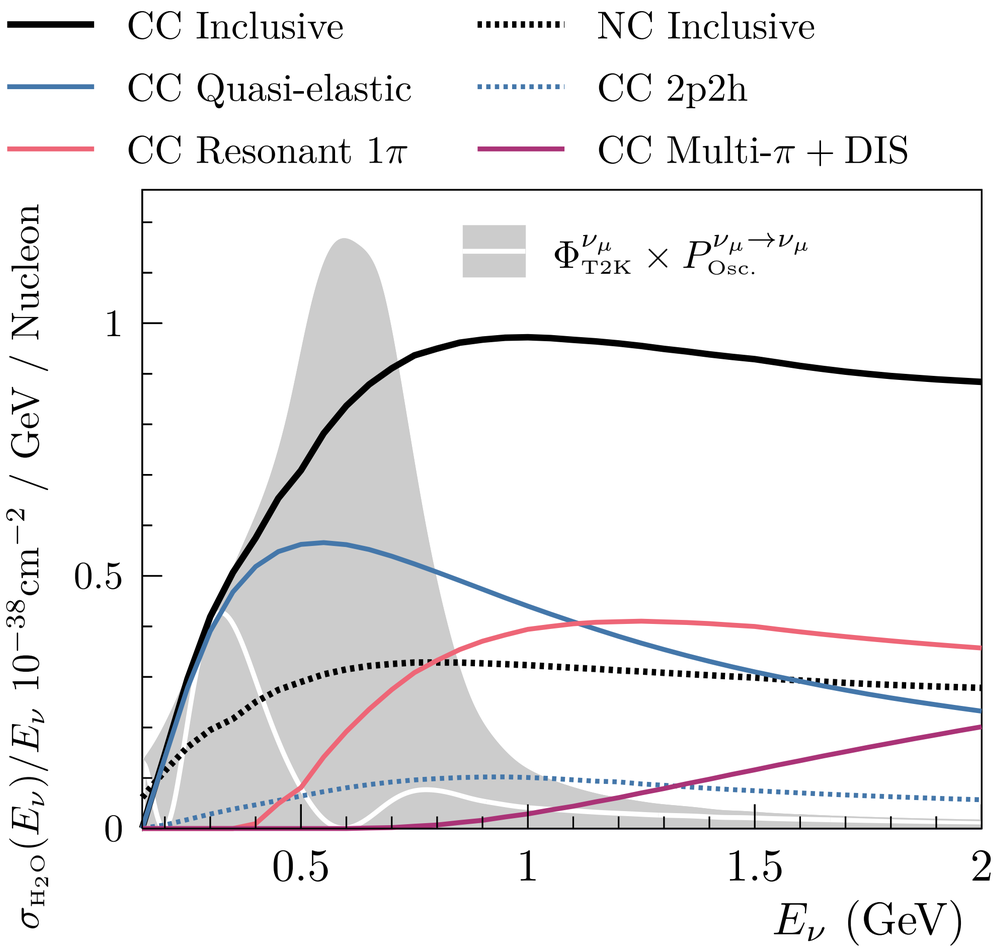

Relevant ν interactions at T2K

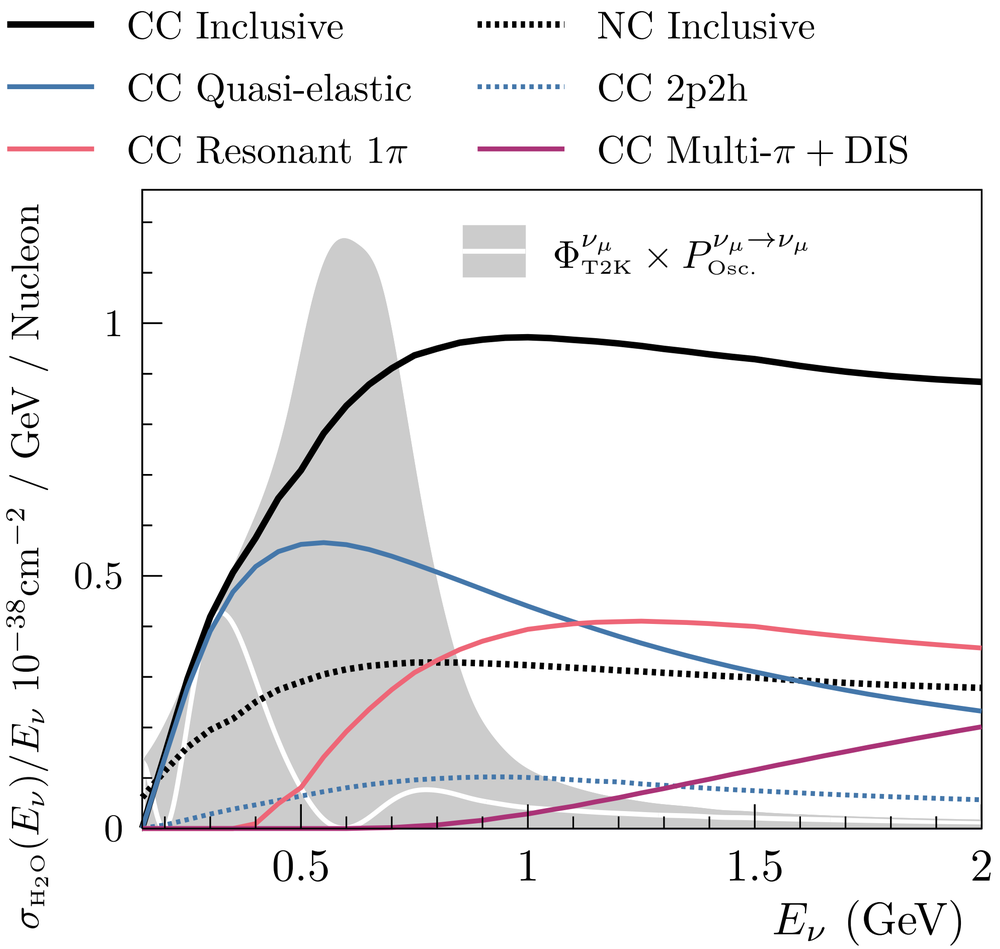

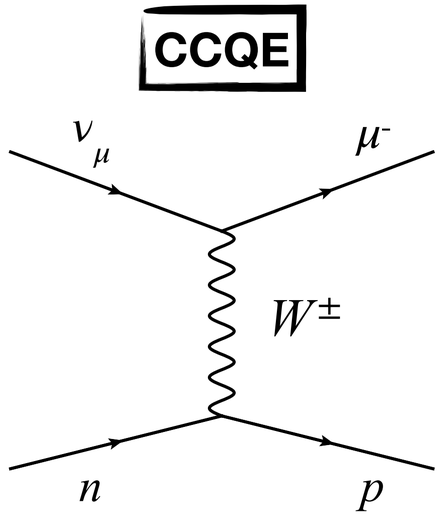

Relevant ν interactions at T2K

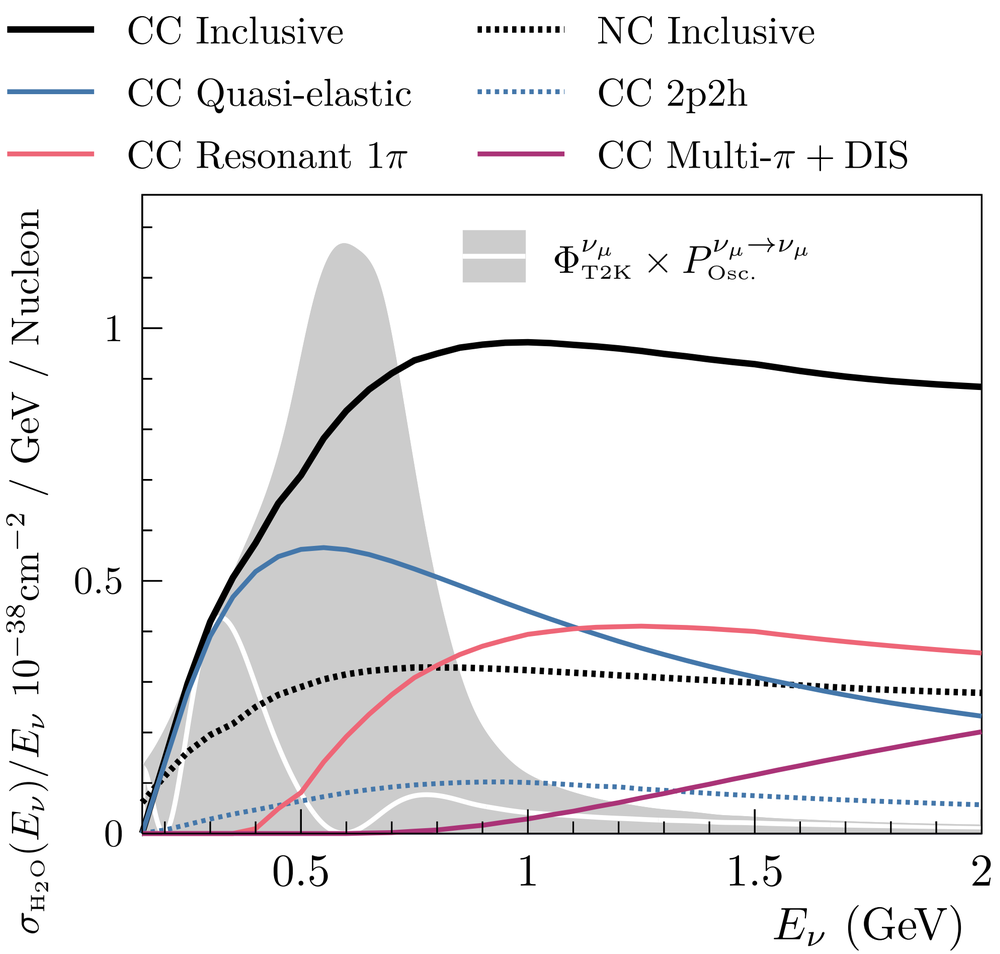

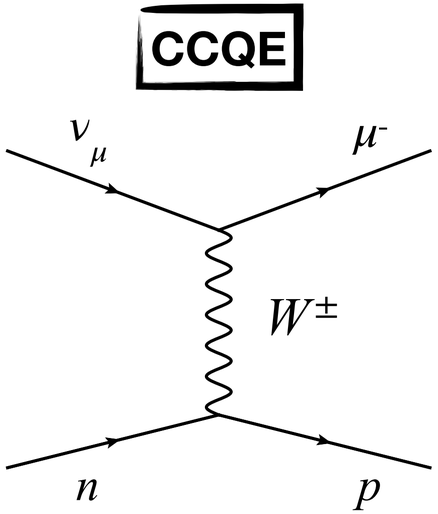

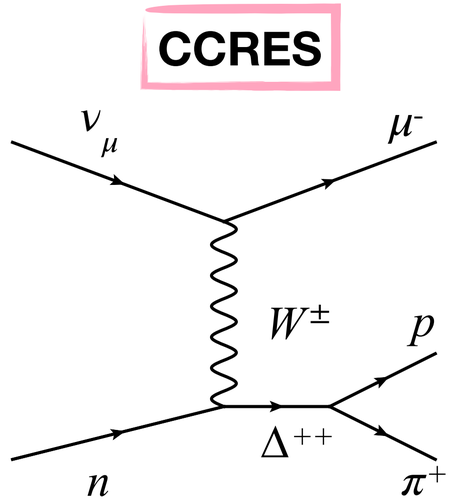

Relevant ν interactions at T2K

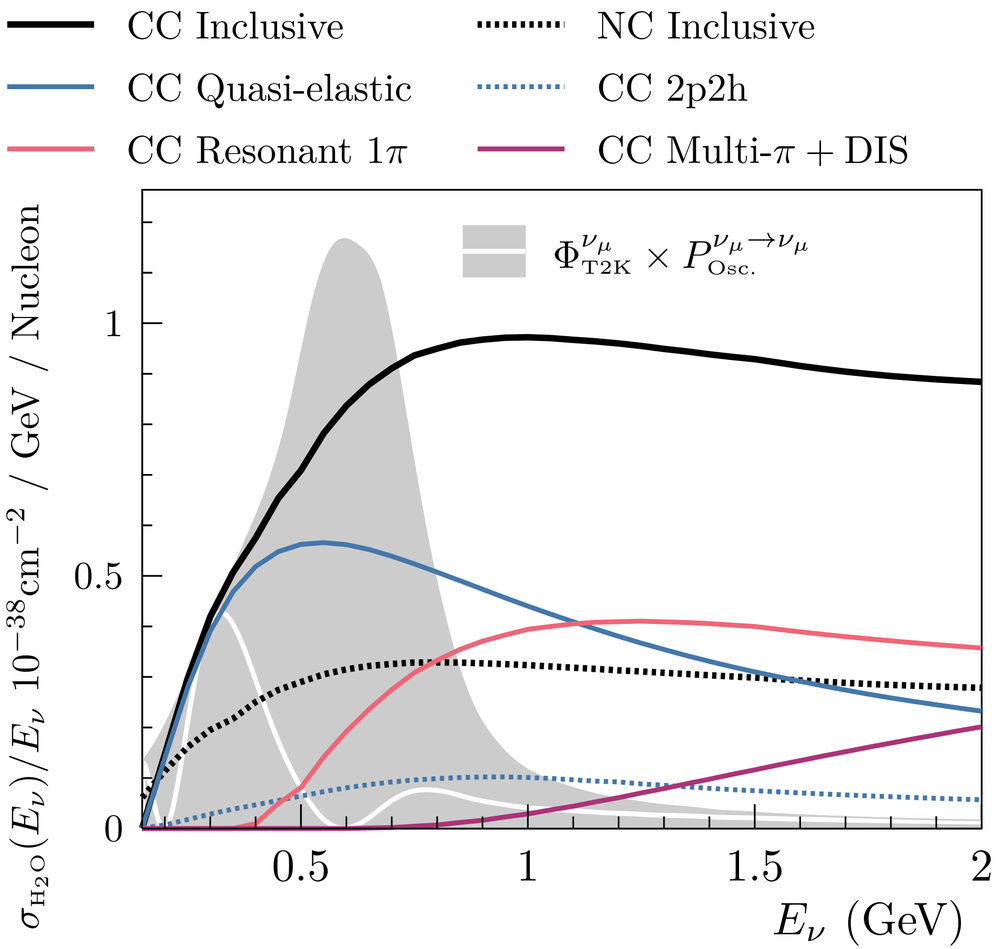

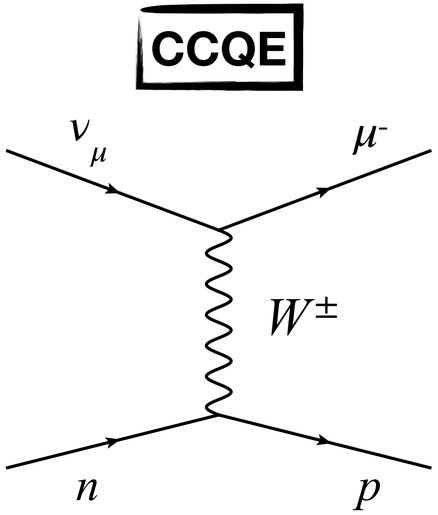

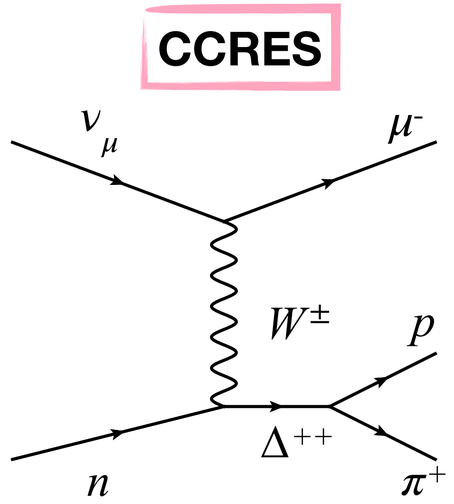

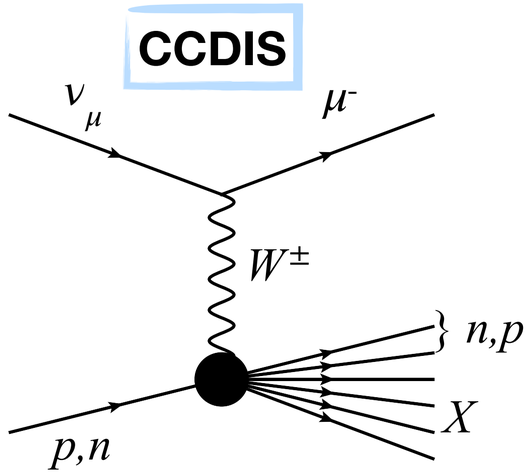

Nuclear effects

Nuclear effects

Nucleons bound in the nucleus ⇒ Nuclear effect!

Nuclear effects

Nucleons bound in the nucleus ⇒ Nuclear effect!

Fermi motion

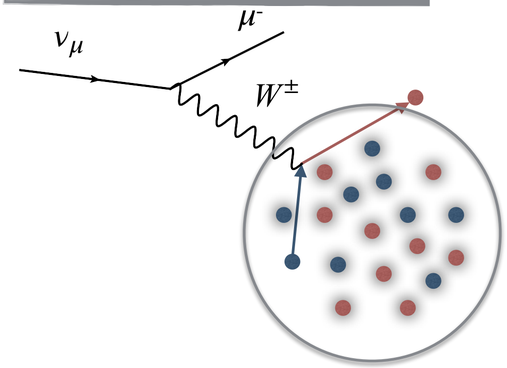

Nuclear effects

Nucleons bound in the nucleus ⇒ Nuclear effect!

Fermi motion

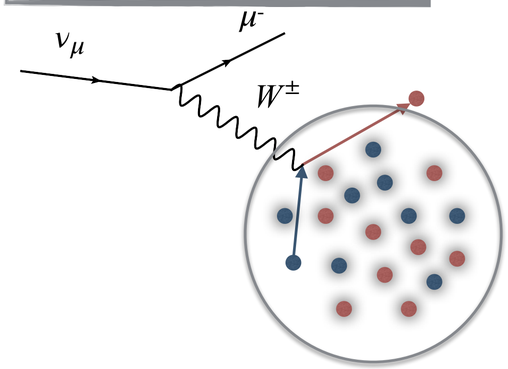

Nucleon correlations

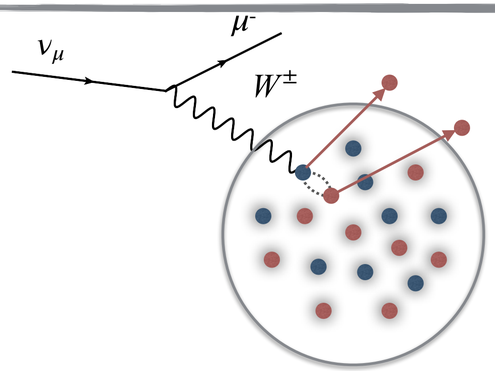

Nuclear effects

Nucleons bound in the nucleus ⇒ Nuclear effect!

Fermi motion

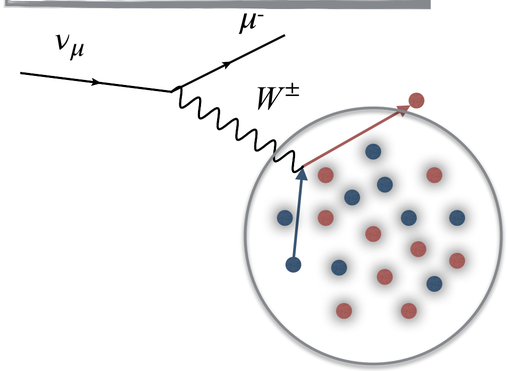

Nucleon correlations

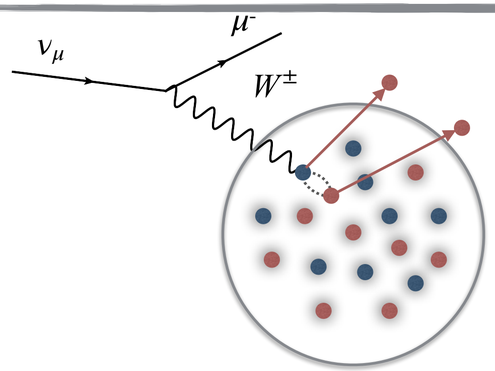

Final State Interaction (FSI)

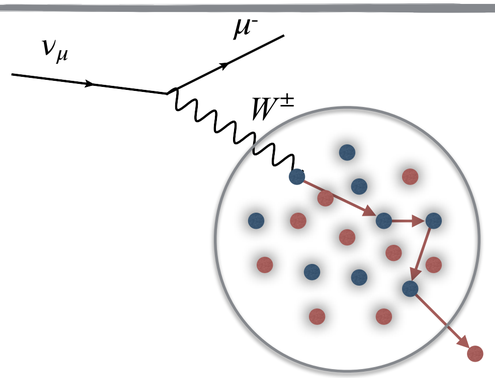

Nuclear effects

Nucleons bound in the nucleus ⇒ Nuclear effect!

Fermi motion

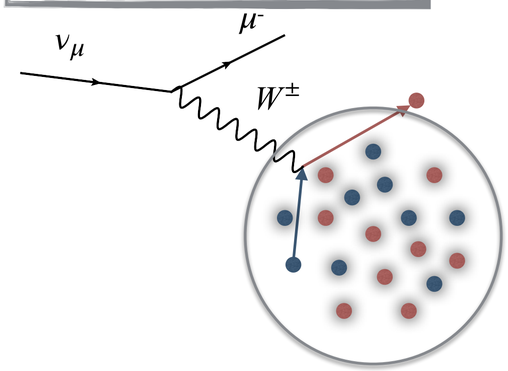

Nucleon correlations

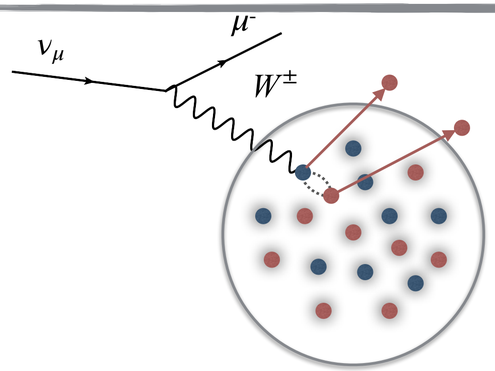

Final State Interaction (FSI)

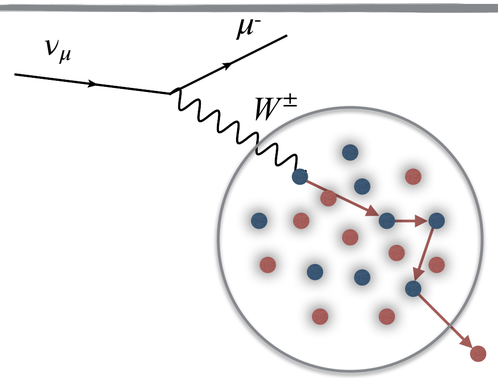

Neutrino Energy reconstructed using CCQE hypothesis at T2K

Nuclear effects

Nucleons bound in the nucleus ⇒ Nuclear effect!

Fermi motion

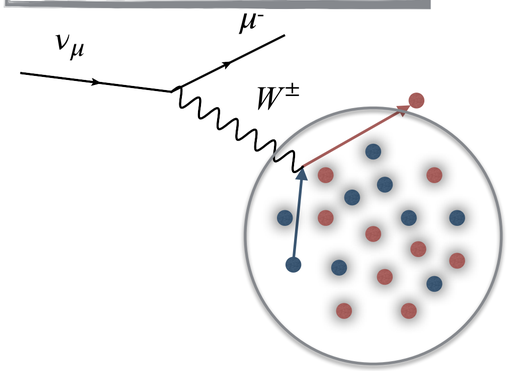

Nucleon correlations

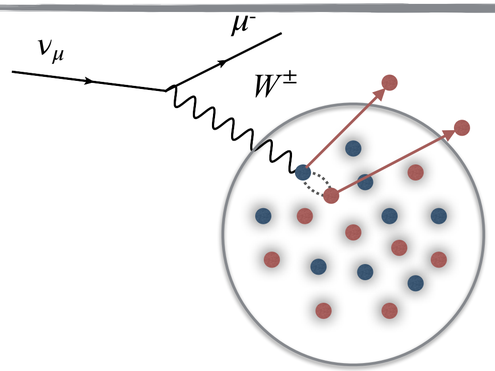

Final State Interaction (FSI)

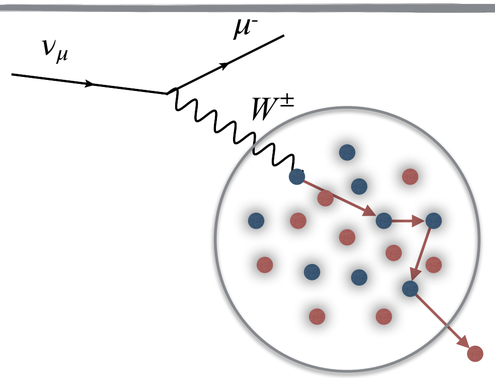

Neutrino Energy reconstructed using CCQE hypothesis at T2K

Nuclear effects introduce a bias in neutrino energy reconstruction

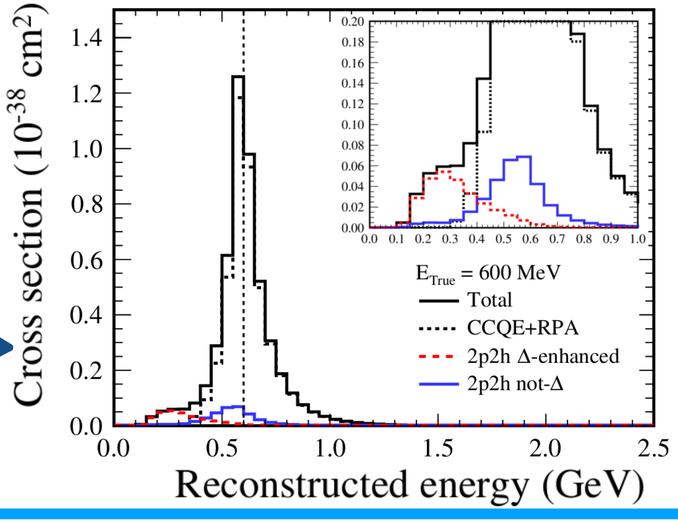

Cross-section modeling

- Significant update to interaction model and uncertainties (NEUT 5.4.1):
  - Benhar Spectral Function as nuclear initial state model for CCQE [Nuc. Phys. A 579, 493]: shell model derived from electron scattering data
  - Freedom to reduce the cross-section as function of Q^2 through theory based parameters introduced by the Benhar Spectral Function model
  - New treatment of nucleon removal energy based on electron scattering data
  - Freedom to change 2p2h shape and normalization in a different way for neutrino and antineutrino, in case the interaction is on C or O, np- or NN-pairs
  - Removal energy for RES interactions

Detector acceptance

Nucleons bound in the nucleus ⇒ Nuclear effect!

Fermi motion

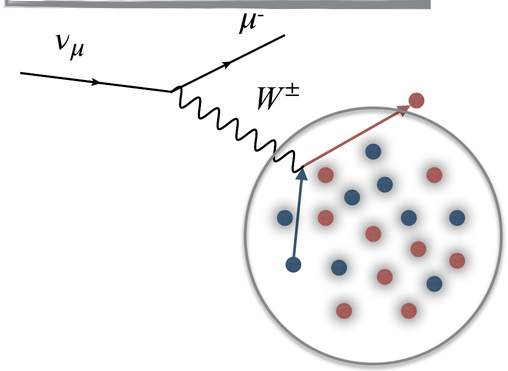

Nucleon correlations

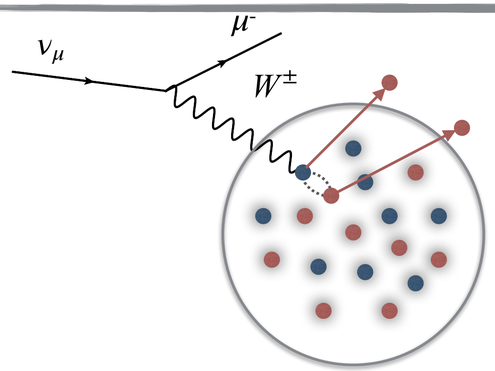

Final State Interaction (FSI)

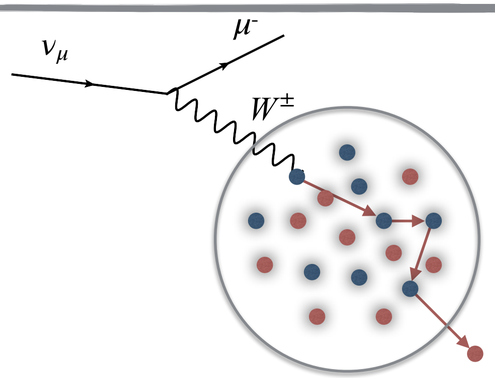

Detector acceptance

Nucleons bound in the nucleus ⇒ Nuclear effect!

Fermi motion

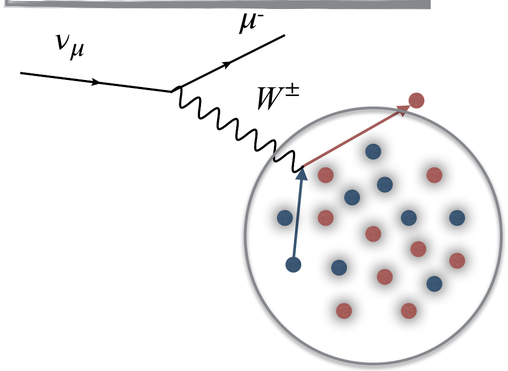

Nucleon correlations

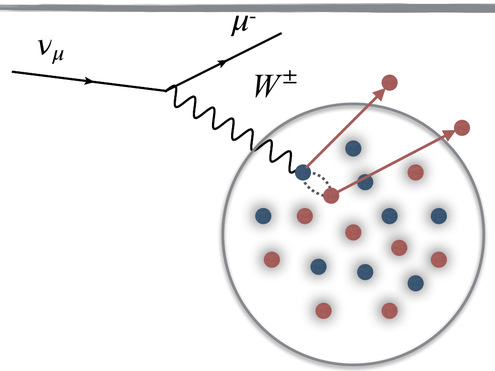

Final State Interaction (FSI)

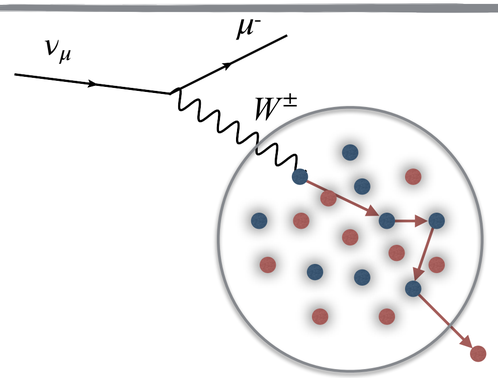

Limited detector acceptance

Detector acceptance

Nucleons bound in the nucleus ⇒ Nuclear effect!

Fermi motion

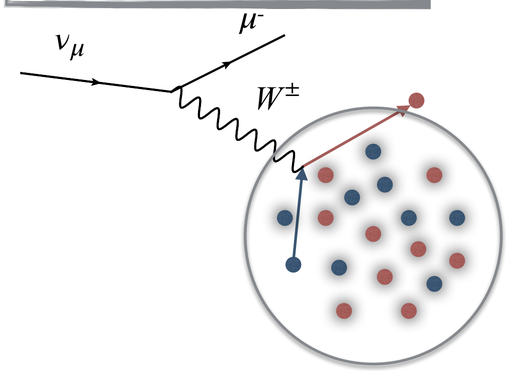

Nucleon correlations

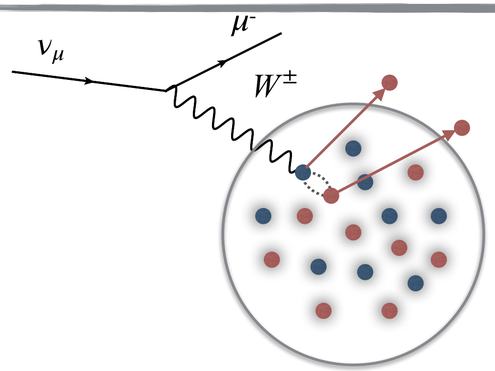

Final State Interaction (FSI)

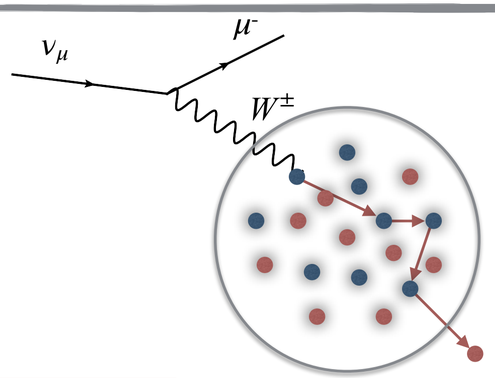

Limited detector acceptance

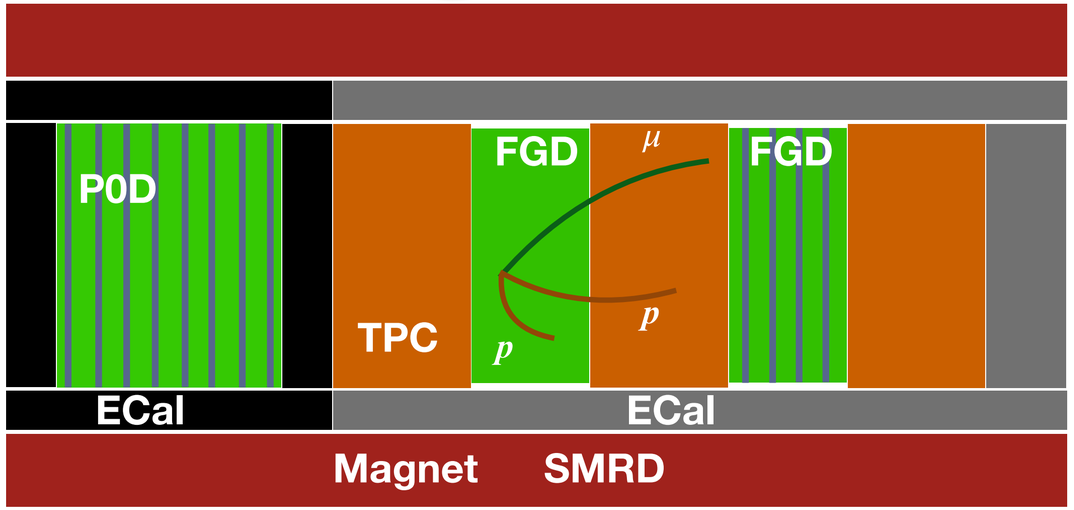

Detector acceptance

Nucleons bound in the nucleus ⇒ Nuclear effect!

Fermi motion

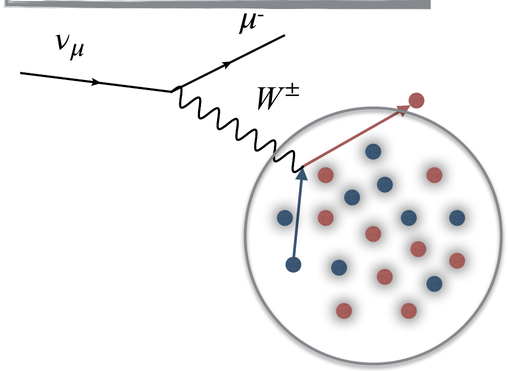

Nucleon correlations

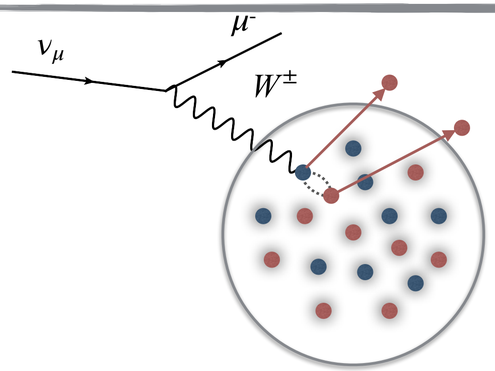

Final State Interaction (FSI)

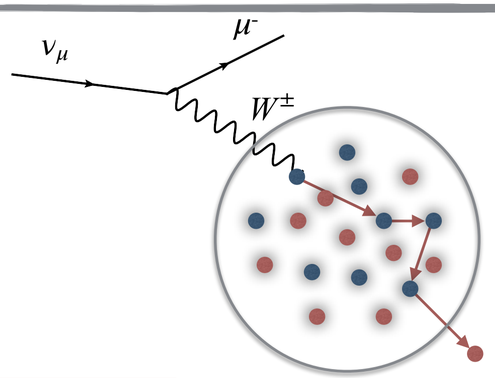

Limited detector acceptance

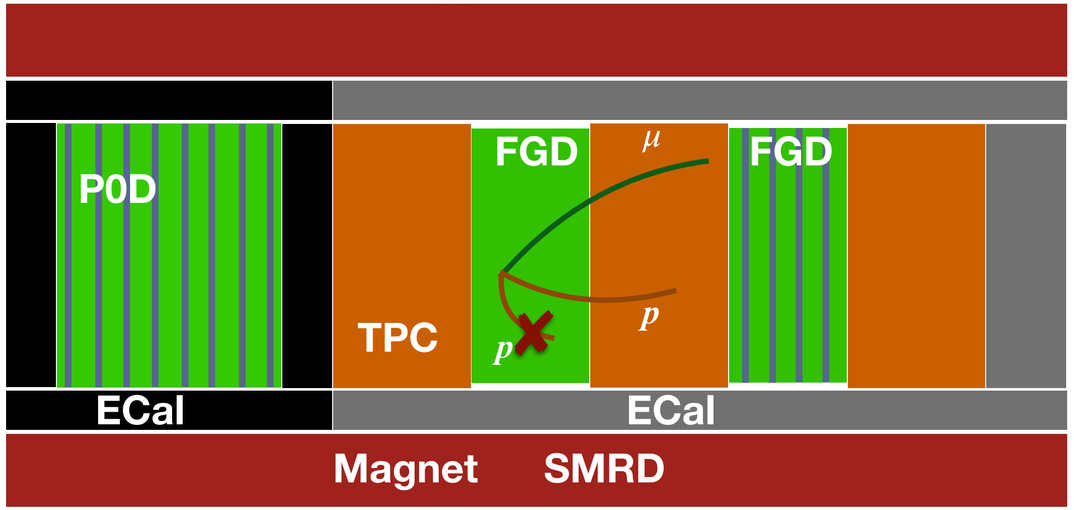

ND280 measurements: ν beam

Samples used in **last iteration** of the analysis

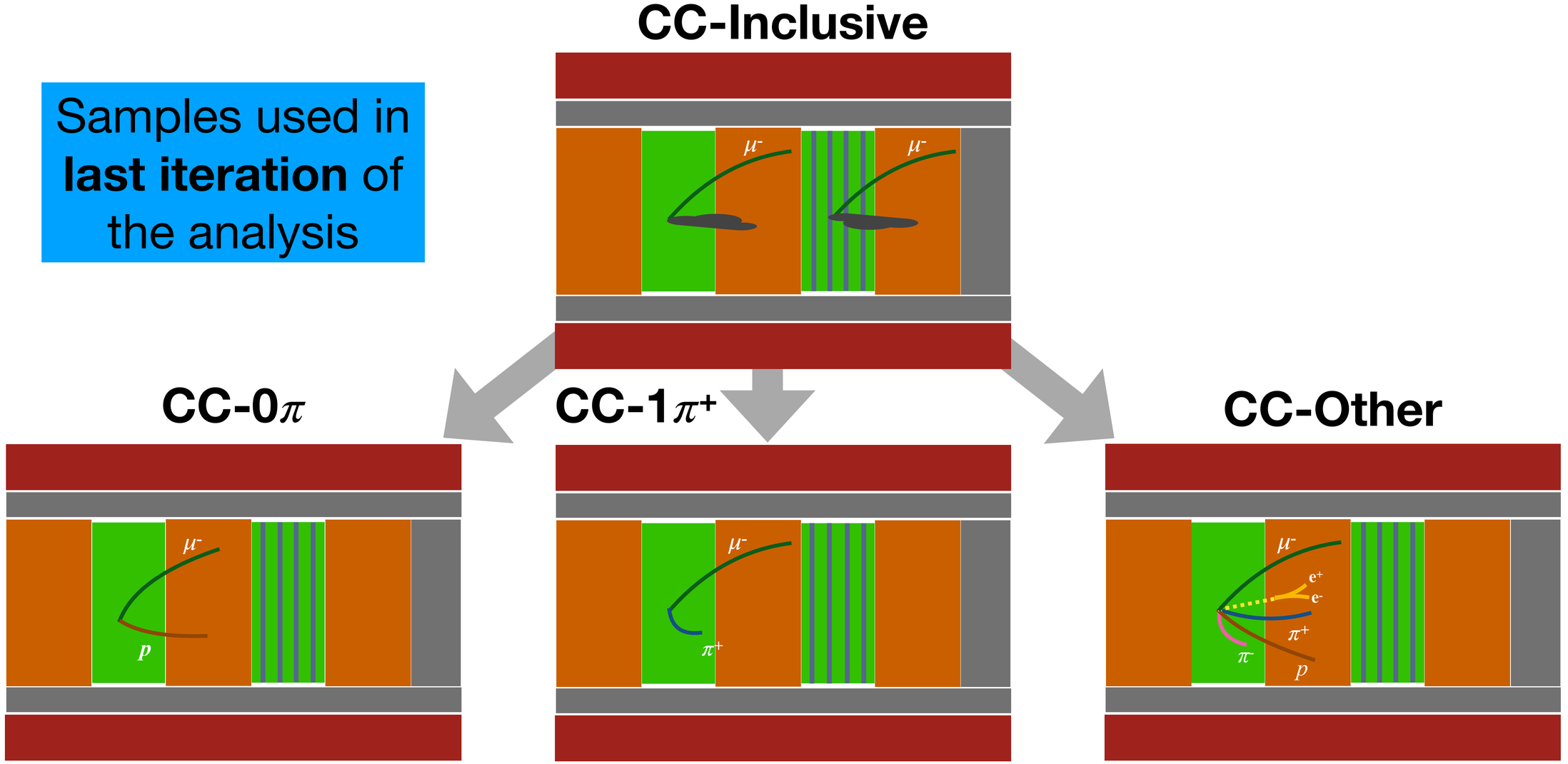

Improvements: π^0 tagging

Improved muon neutrino selection: isolate CCπ^0 interactions by looking at the photons in ECal (first time we use it!) and e^+e^- pairs in TPC

CC-Inclusive

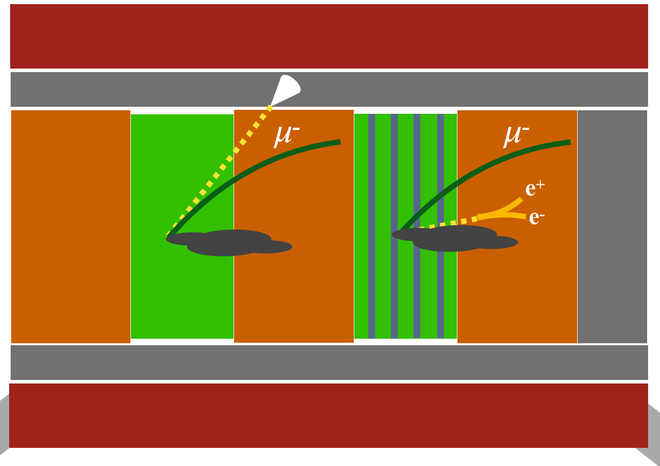

CC w/ photons

(tagged in ECal or TPC)

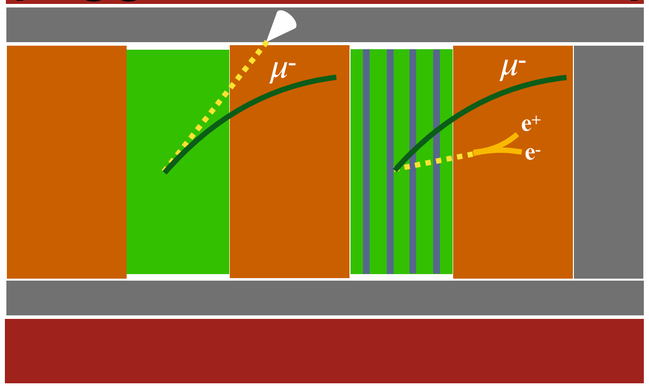

CC w/o photons

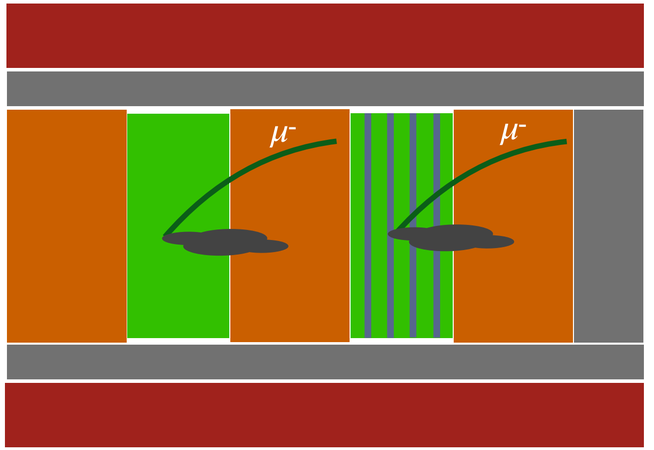

Improvements: π^0 tagging

Improved muon neutrino selection: isolate CCπ^0 interactions by looking at the photons in ECal (first time we use it!) and e^+e^- pairs in TPC

CC-Inclusive

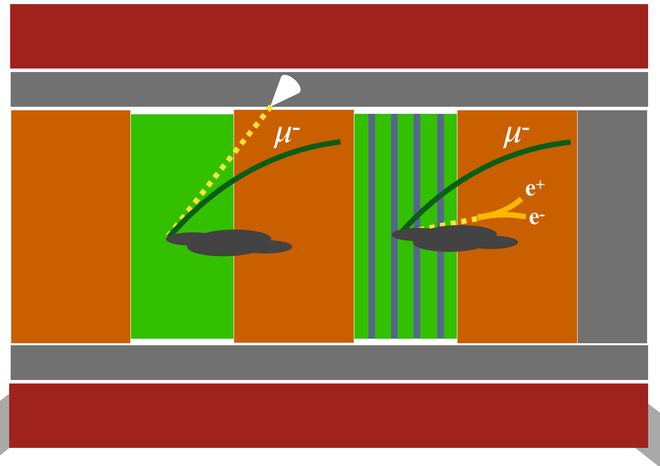

CC w/ photons

(tagged in ECal or TPC)

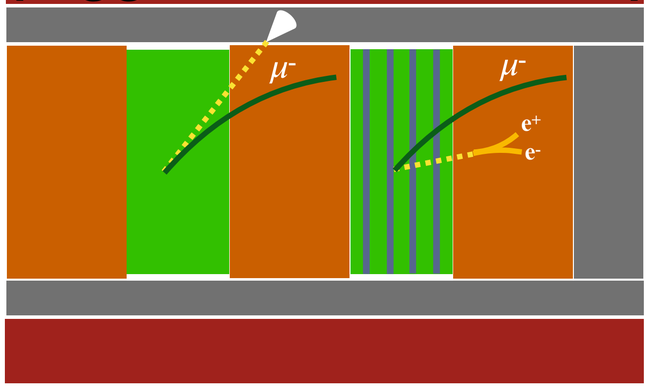

CC w/o photons

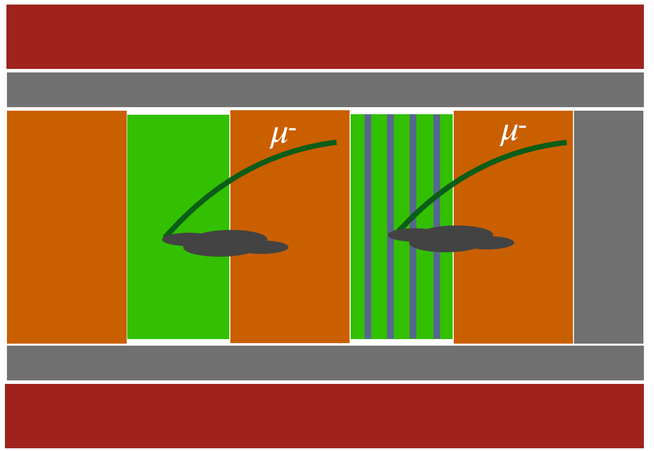

Improvements: π^0 tagging

Improved muon neutrino selection: isolate CCπ^0 interactions by looking at the photons in ECal (first time we use it!) and e^+e^- pairs in TPC

CC-Inclusive

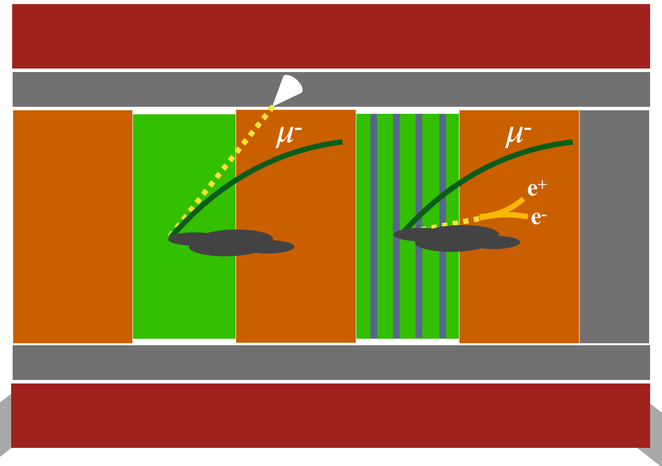

CC-0π

CC w/ photons

(tagged in ECal or TPC)

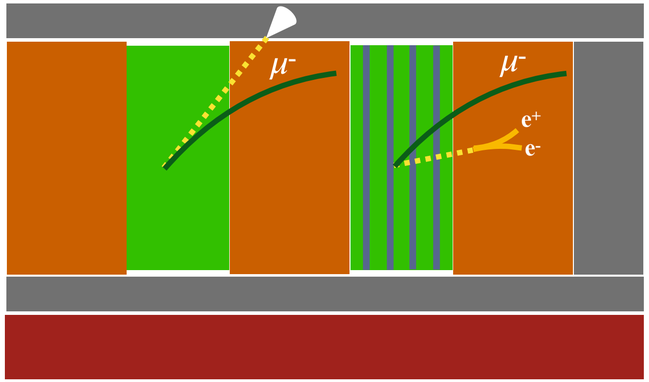

CC w/o photons

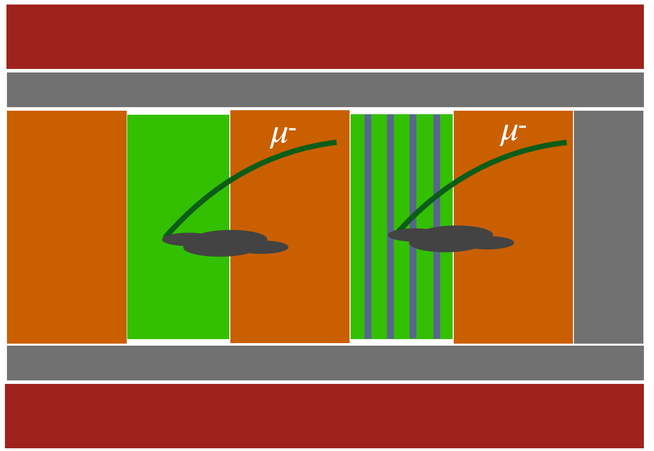

Improvements: π^0 tagging

Improved muon neutrino selection: isolate CCπ^0 interactions by looking at the photons in ECal (first time we use it!) and e^+e^- pairs in TPC

CC-Inclusive

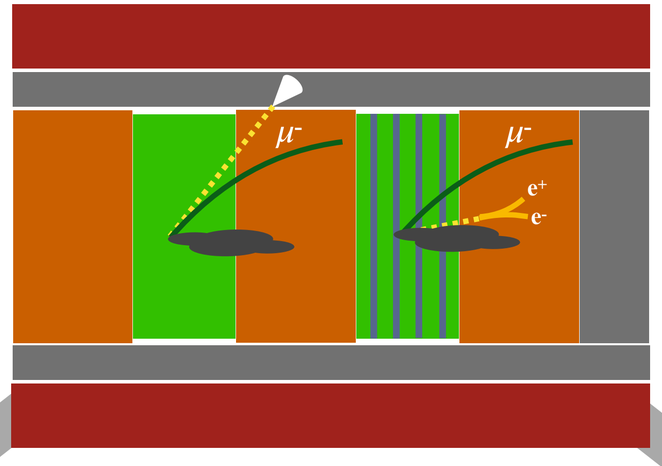

CC-0π **CC-1π^+**

CC w/ photons

(tagged in ECal or TPC)

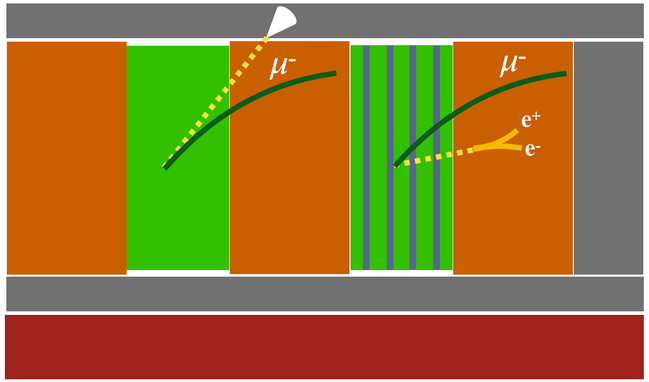

CC w/o photons

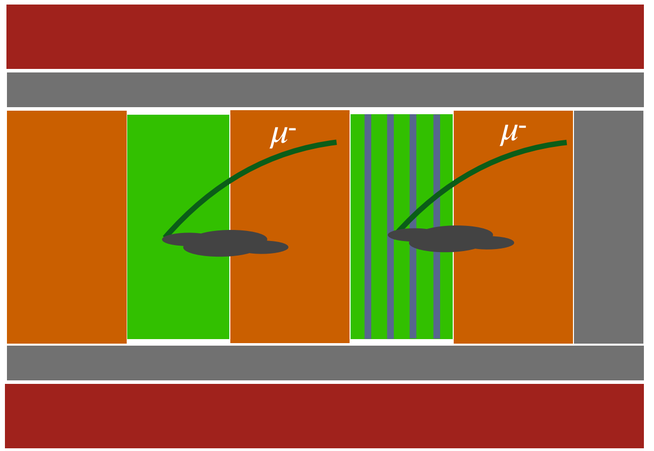

Improvements: π^0 tagging

Improved muon neutrino selection: isolate CCπ^0 interactions by looking at the photons in ECal (first time we use it!) and e^+e^- pairs in TPC

CC-Inclusive

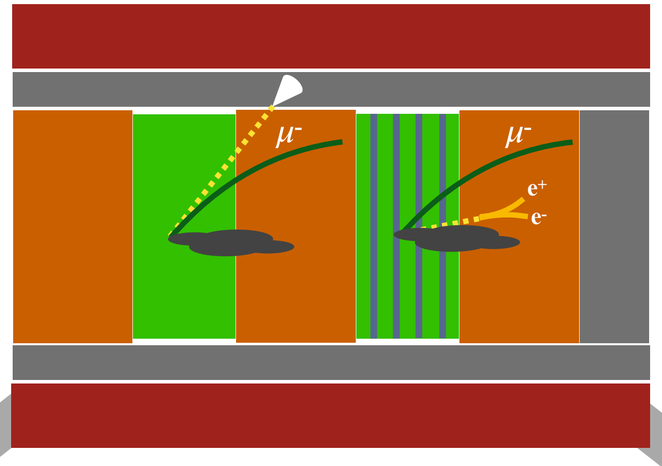

CC-0π **CC-1π^+** **CC-Nπ**

CC w/ photons

(tagged in ECal or TPC)

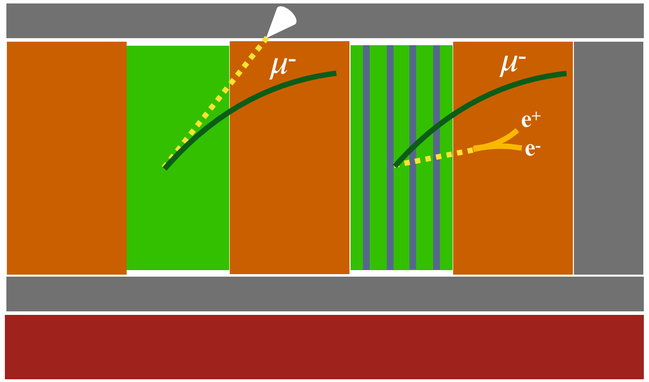

CC w/o photons

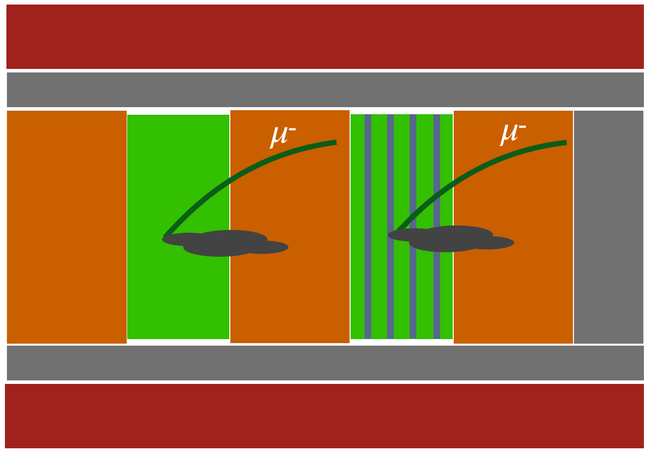

Improvements: Proton tagging

Improved sensitivity to nuclear effects by splitting CC-0π0γ sample depending on the presence or not of protons

CC-0π0γ

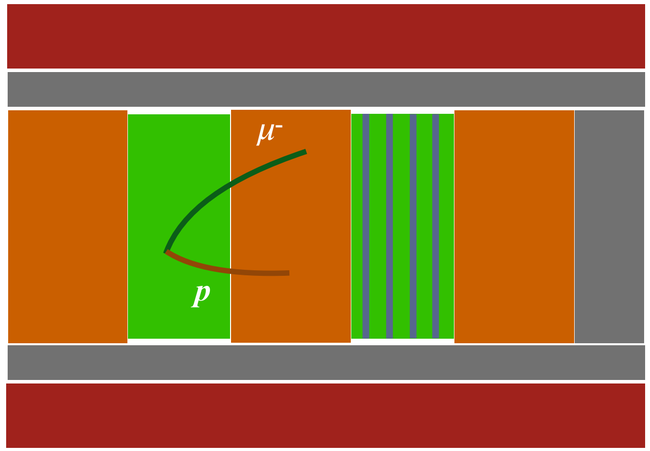

Improvements: Proton tagging

Improved sensitivity to nuclear effects by splitting CC-0π0γ sample depending on the presence or not of protons

CC-0π0γ

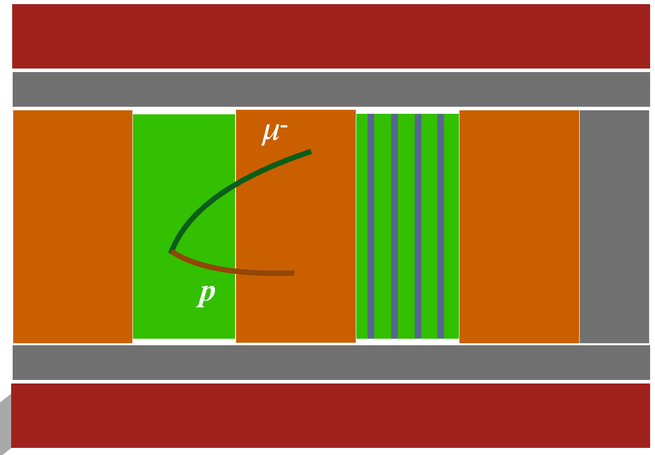

CC-0π0p0γ

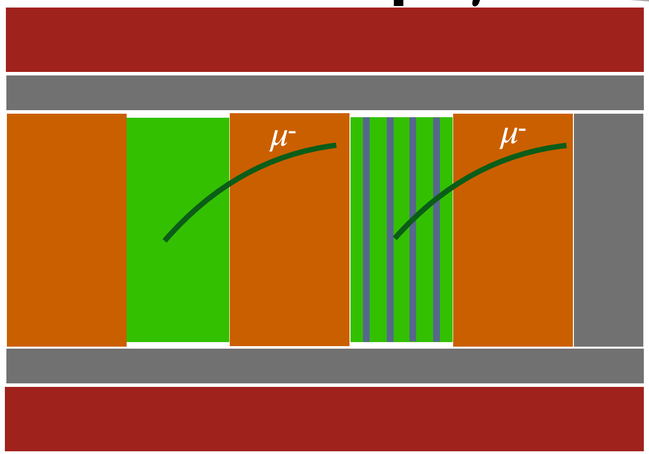

Improvements: Proton tagging

Improved sensitivity to nuclear effects by splitting CC-0π0γ sample depending on the presence or not of protons

CC-0π0γ

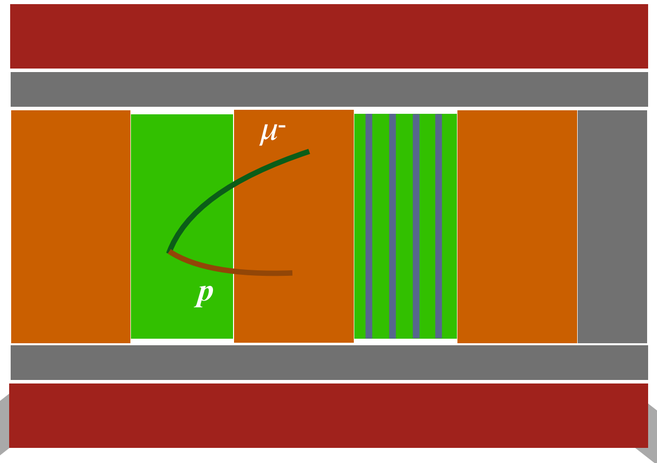

CC-0π0p0γ

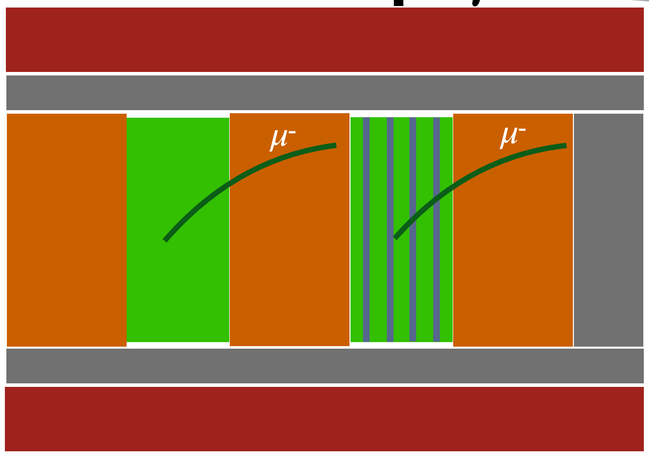

CC-0πNp0γ

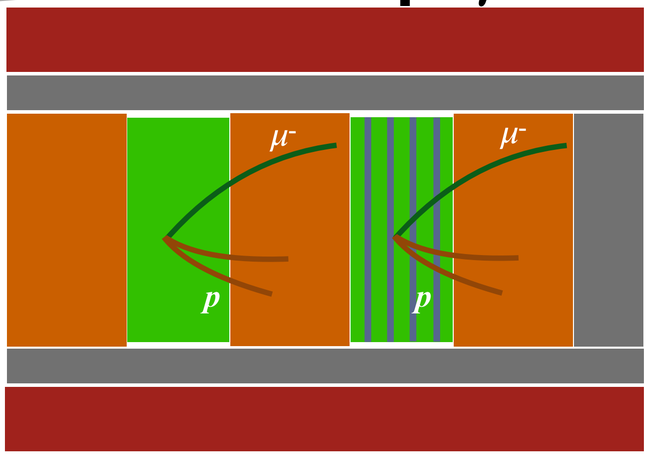

ND280 measurements: ν beam

CC-0π0p0γ | CC-0πNp0γ | CC-1π^+0γ | CC-Nπ0γ | CC-Nγ

A sample for each FGD for a total of 10. Scattering angle used in the analysis but not shown here.

ND280 measurements: $\bar{\nu}$ beam

CC-0π

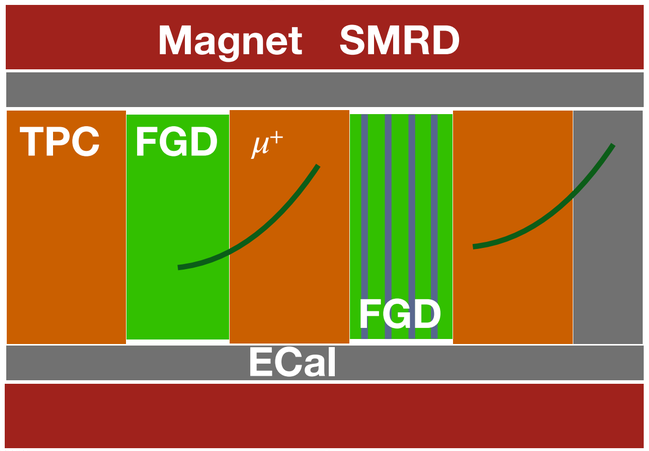

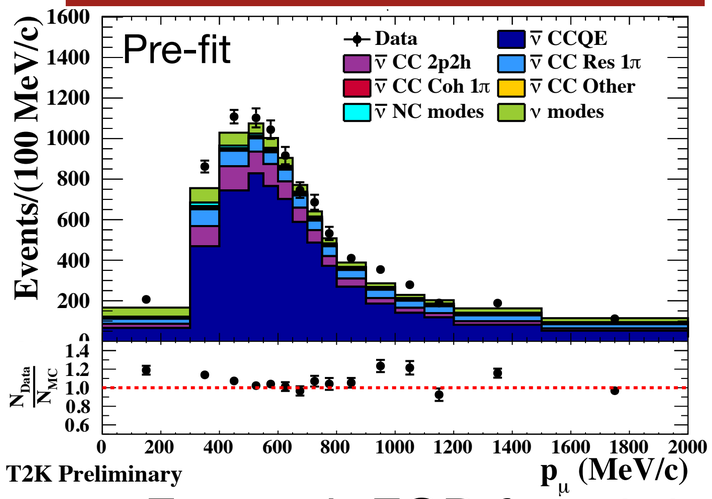

CC-1π^-

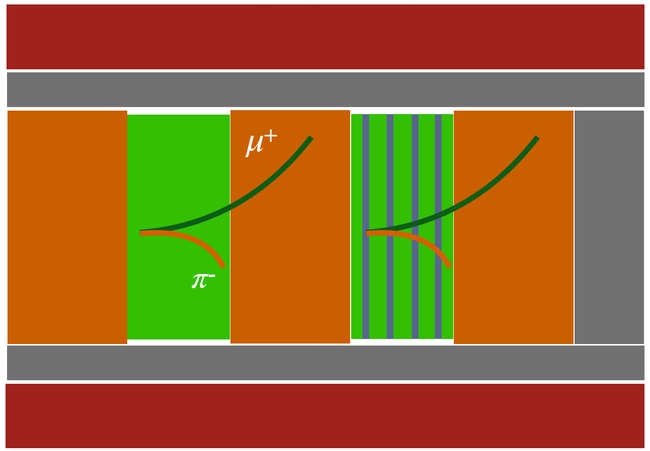

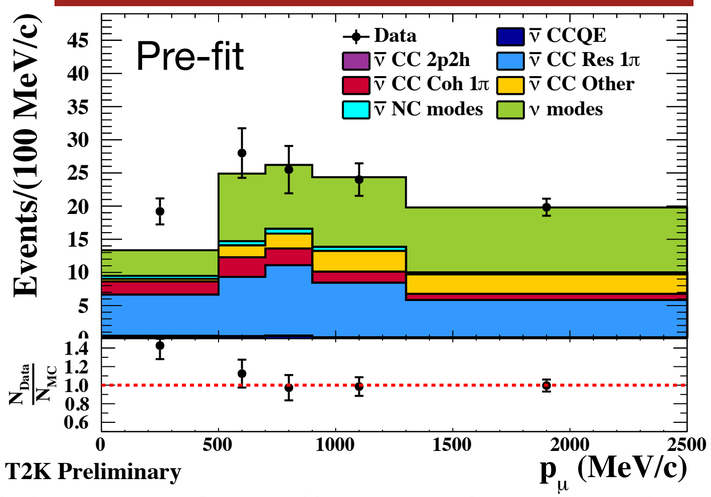

CC-Other

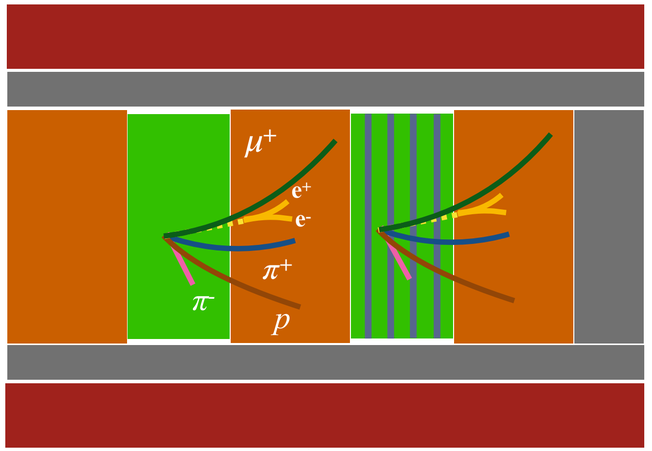

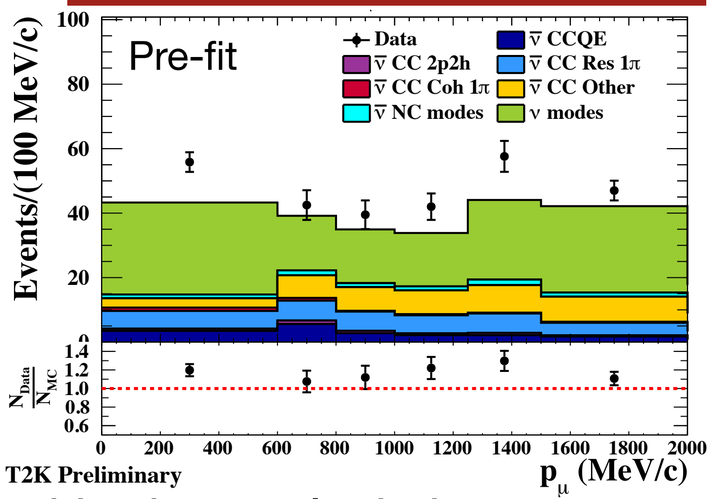

For each FGD for a total of 6 samples. Scattering angle used in the analysis but not shown here.

ND280 measurements: $\bar{\nu}$ beam

CC-0π

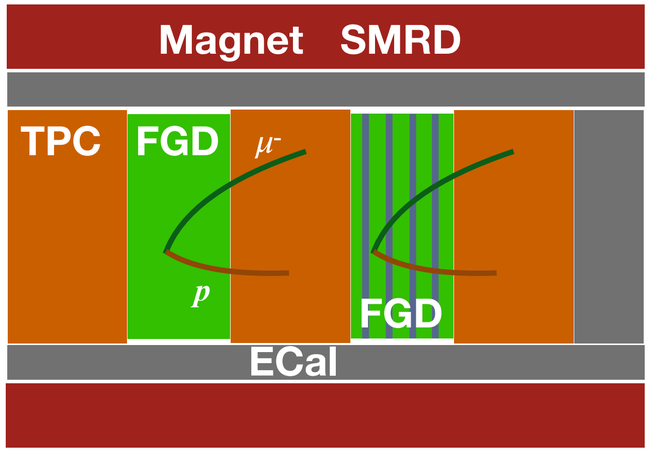

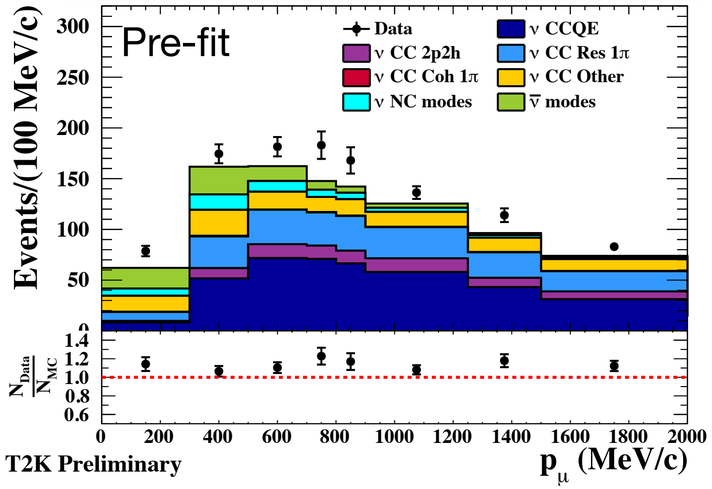

CC-1π^+

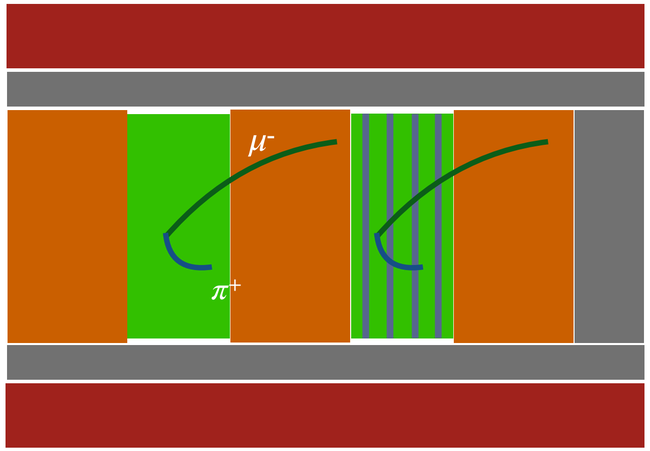

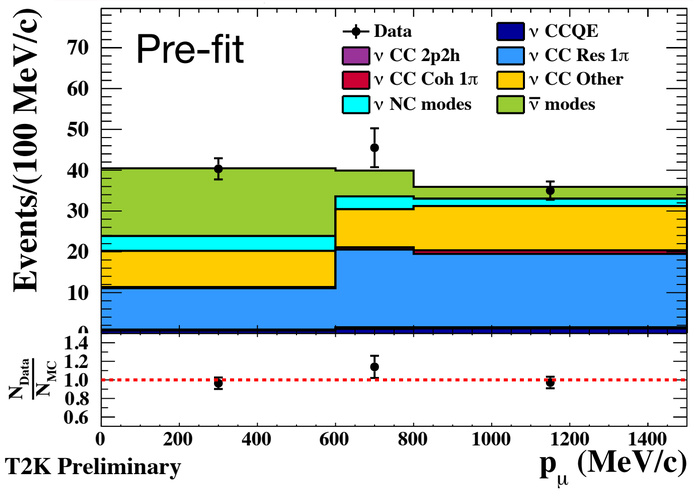

CC-Other

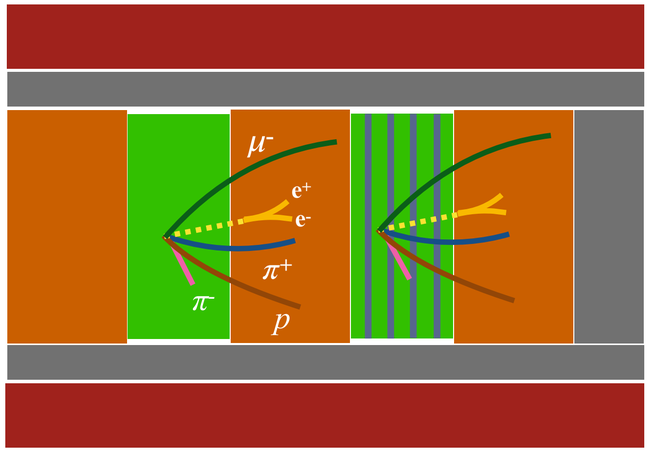

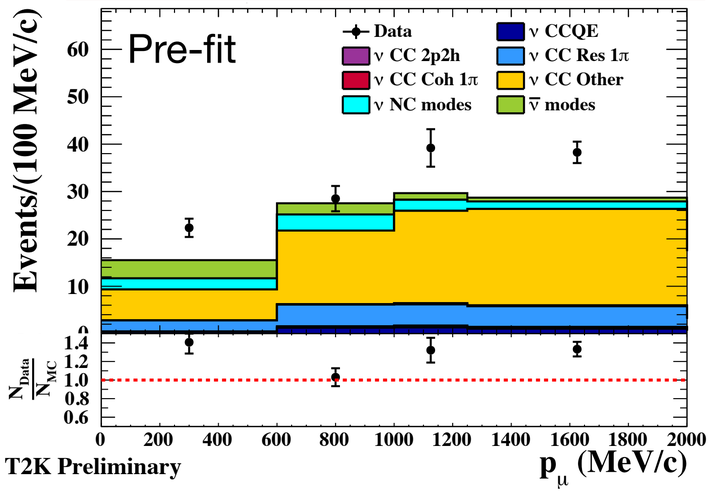

For each FGD for a total of 6 samples. Scattering angle used in the analysis but not shown here.

ND280 Fit

Flux prediction:
external hadron production measurements and T2K beam monitors

ND280 measurements and model:
select CC ν_μ and $\bar{\nu}_\mu$ interactions to constrain flux and cross sections

Neutrino interactions model:
tuned using available cross-sections data

Perform an extended binned likelihood fit to the number of selected events in all the 22 sample as a function of muon kinematics. Our model is a good fit to data (p-value of 11%)

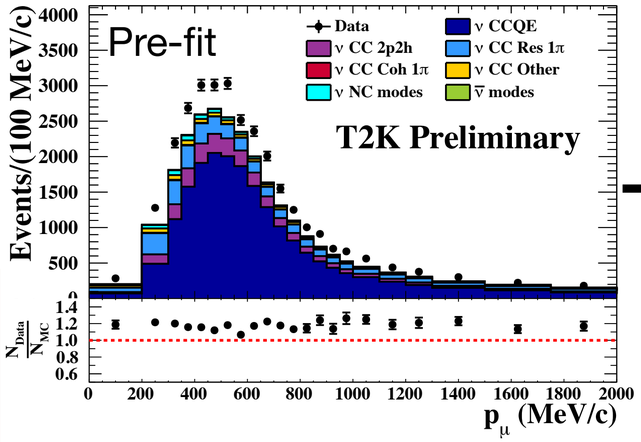

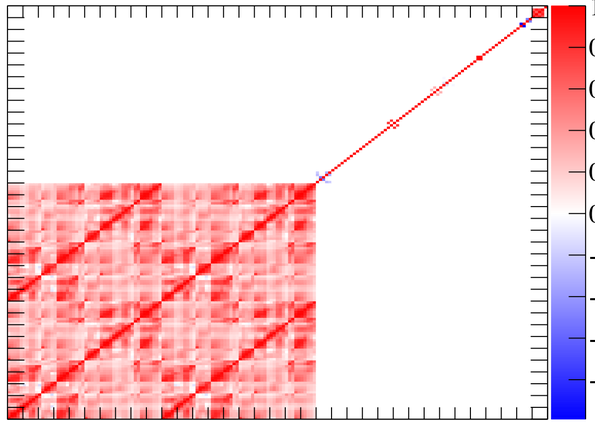

Flux Cross-section

ND280 Fit

Flux prediction:
external hadron production measurements and T2K beam monitors

ND280 measurements and model:
select CC ν_μ and $\bar{\nu}_\mu$ interactions to constrain flux and cross sections

Neutrino interactions model:
tuned using available cross-sections data

Perform an extended binned likelihood fit to the number of selected events in all the 22 sample as a function of muon kinematics. Our model is a good fit to data (p-value of 11%)

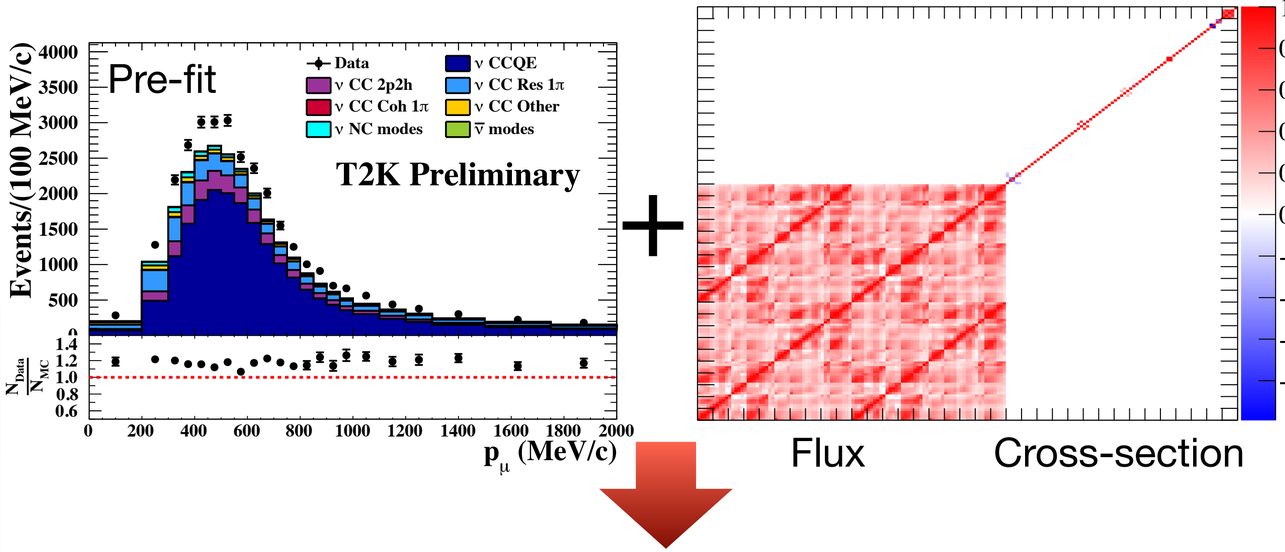

ND280 Fit

Flux prediction:
external hadron production measurements and T2K beam monitors

ND280 measurements and model:
select CC ν_μ and $\bar{\nu}_\mu$ interactions to constrain flux and cross sections

Neutrino interactions model:
tuned using available cross-sections data

Perform an extended binned likelihood fit to the number of selected events in all the 22 sample as a function of muon kinematics. Our model is a good fit to data (p-value of 11%)

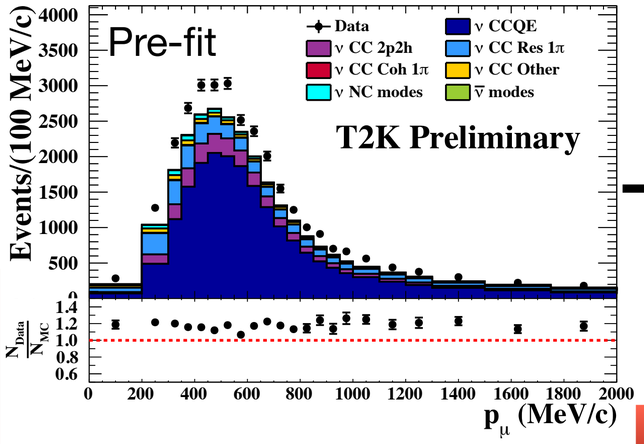

+

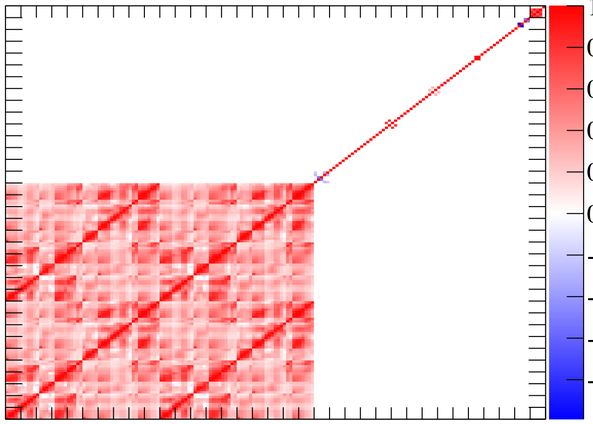

Flux Cross-section

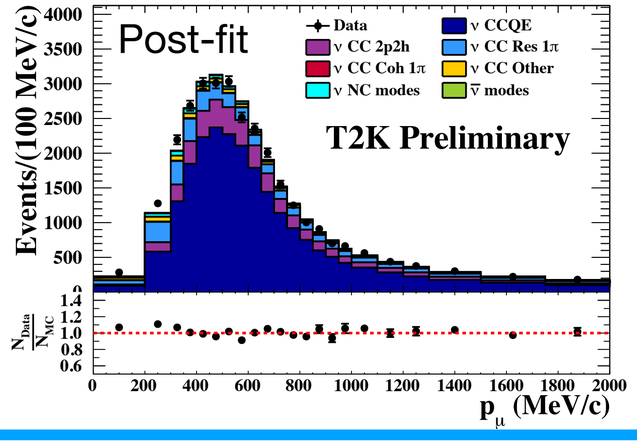

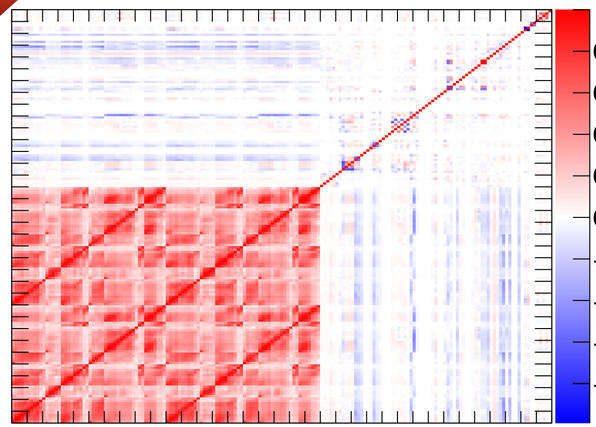

T2K oscillation analysis strategy

Hybrid-frequentist analysis

Flux prediction:
external hadron production measurements and T2K beam monitors

ND280 measurements and model:
select CC ν_μ and $\bar{\nu}_\mu$ interactions to constrain flux and cross sections

Neutrino interactions model:
tuned using available cross-sections data

Prediction at the Far Detector:
ND280 measurements predict the expected events at SK

SK measurements and model:
Select CC $\nu_\mu/\bar{\nu}_\mu$ and $\nu_e/\bar{\nu}_e$ candidates after the oscillations

Extract oscillation parameters
(θ_{13}, θ_{23}, Δm^2_{32}, δ_{CP})

T2K oscillation analysis strategy

Hybrid-frequentist analysis

Flux prediction:
external hadron production measurements and T2K beam monitors

ND280 measurements and model:
select CC ν_μ and $\bar{\nu}_\mu$ interactions to constrain flux and cross sections

Neutrino interactions model:
tuned using available cross-sections data

Prediction at the Far Detector:
ND280 measurements predict the expected events at SK

SK measurements and model:
Select CC $\nu_\mu/\bar{\nu}_\mu$ and $\nu_e/\bar{\nu}_e$ candidates after the oscillations

Extract oscillation parameters
(θ_{13}, θ_{23}, Δm^2_{32}, δ_{CP})

SK measurements

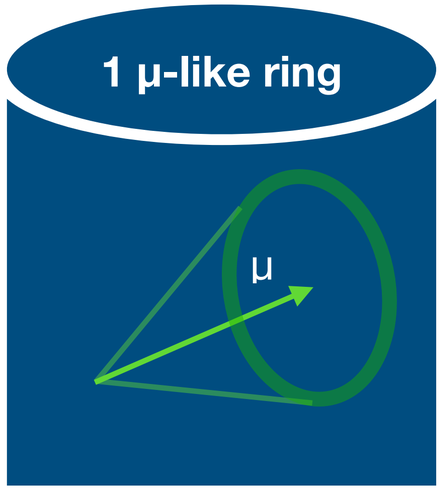

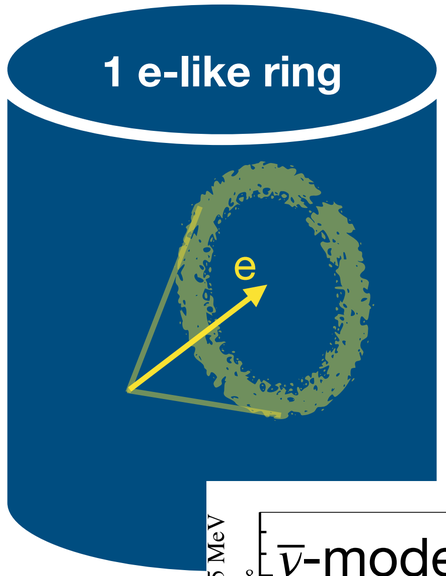

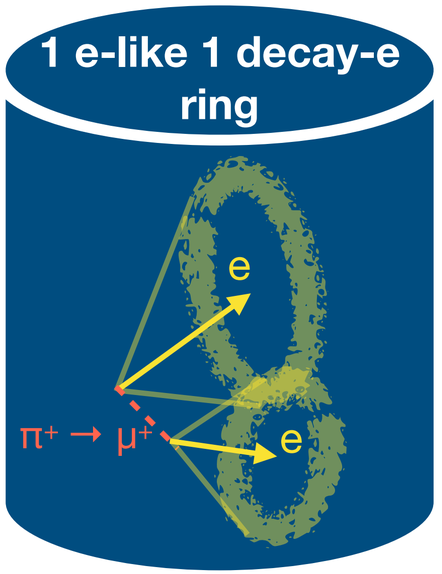

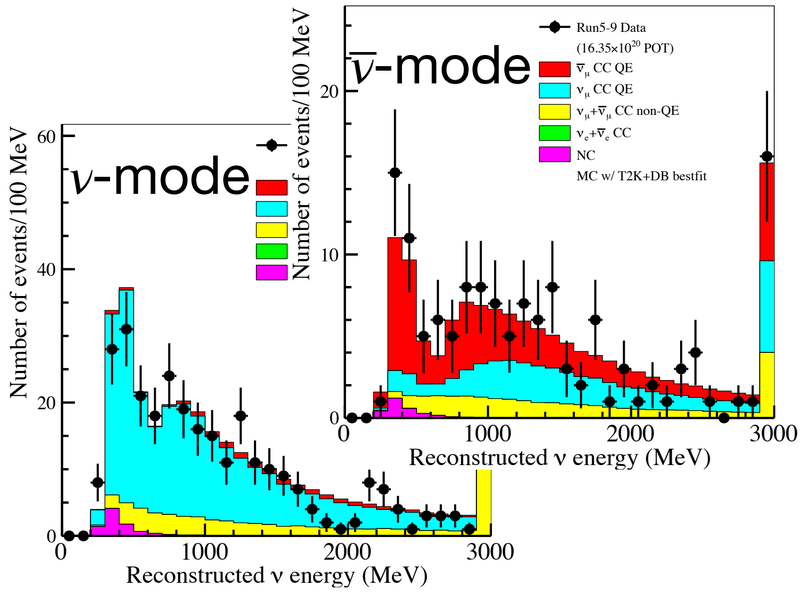

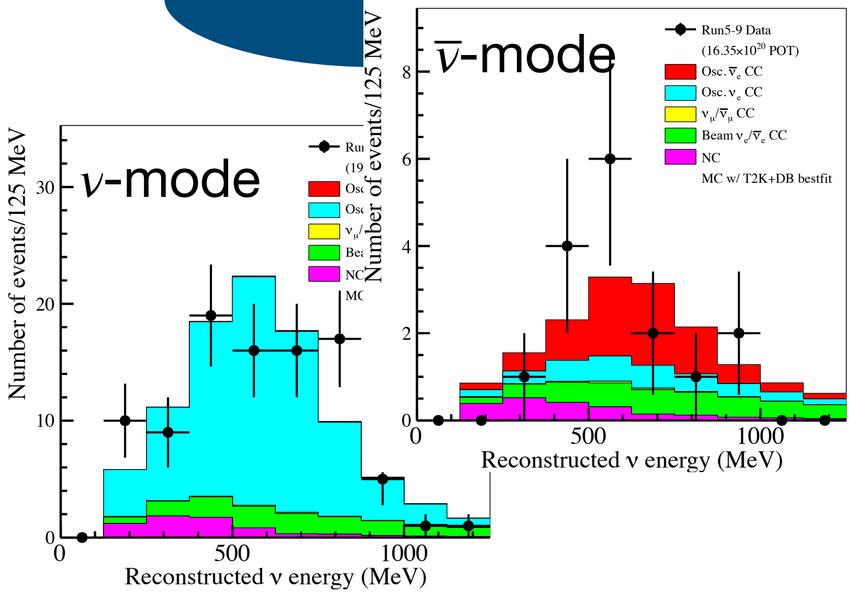

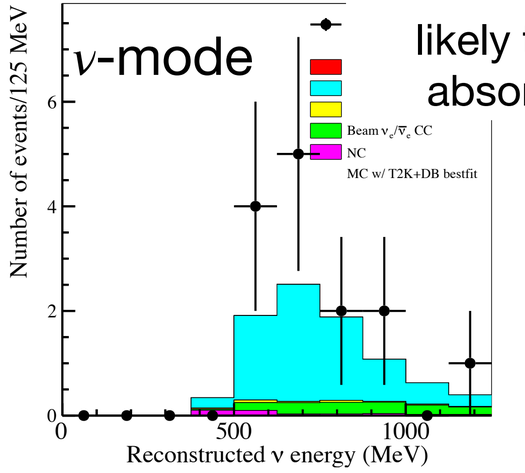

π⁻ in ν̄-mode likely to be absorbed

New SK sample

ν_μ CC Multi-Ring sample at SK: increase sensitivity atmospheric parameters

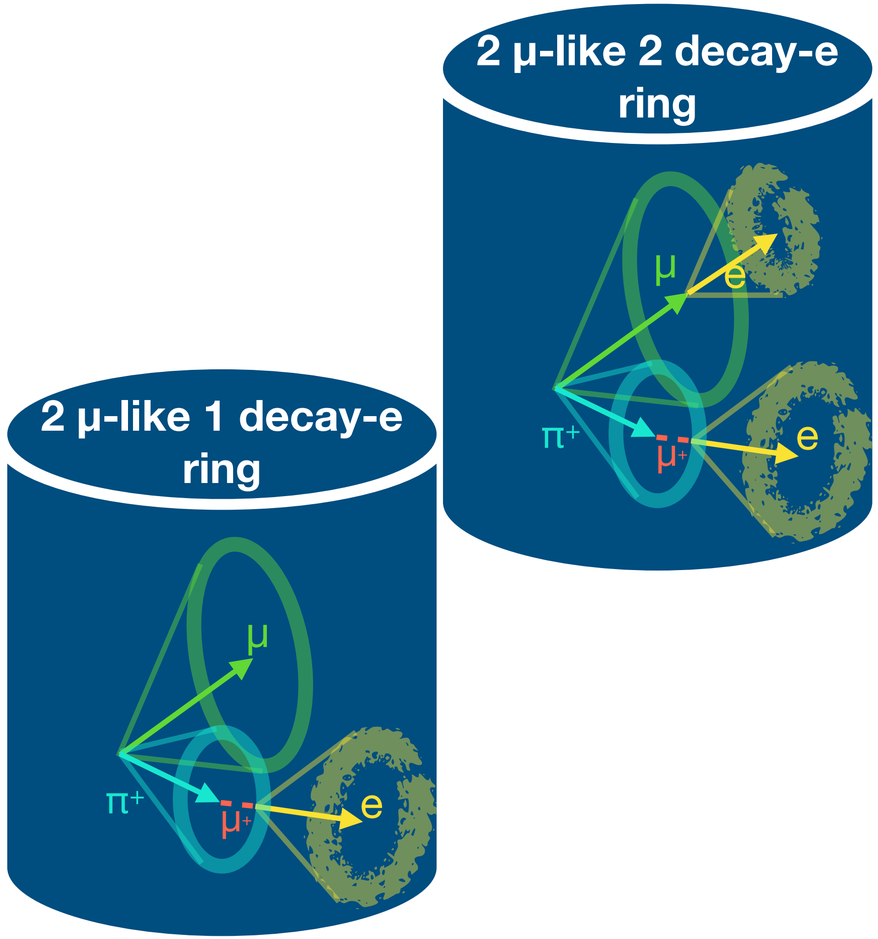

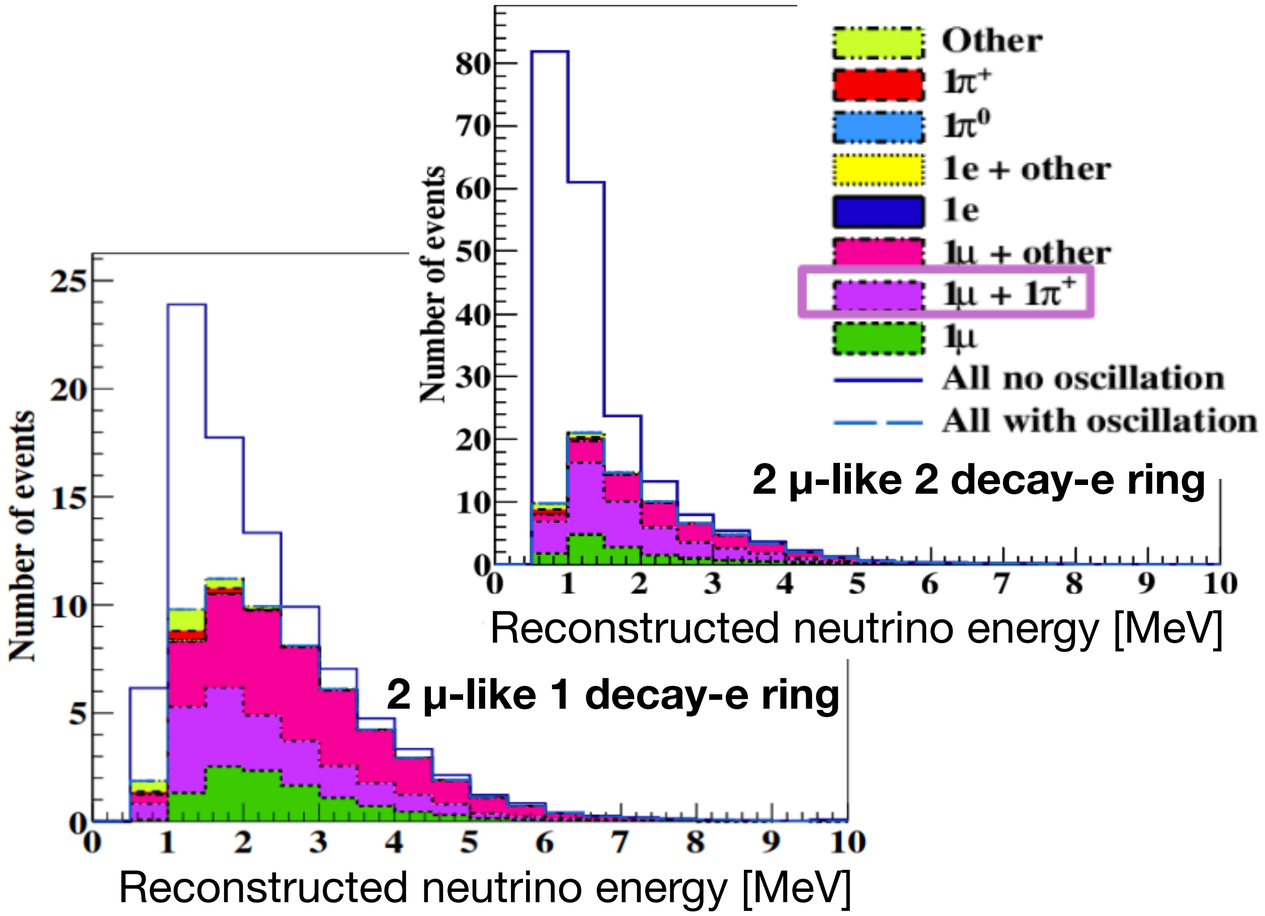

Prediction at SK: ν beam

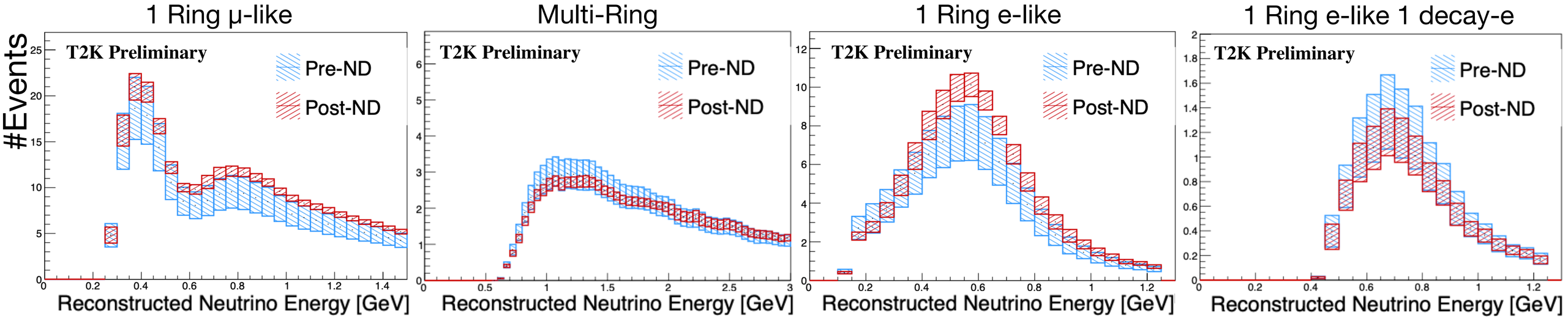

Systematics uncertainty				
SK sample	**1 Ring μ-like**	**1 Ring e-like**	**1 Ring e-like 1de**	**Multi-Ring**
Before ND280 fit	16.7	17.3	20.9	12.5
After ND280 fit	3.4	5.2	14.3	4.9

Prediction at SK: $\bar{\nu}$ beam

1 Ring μ-like

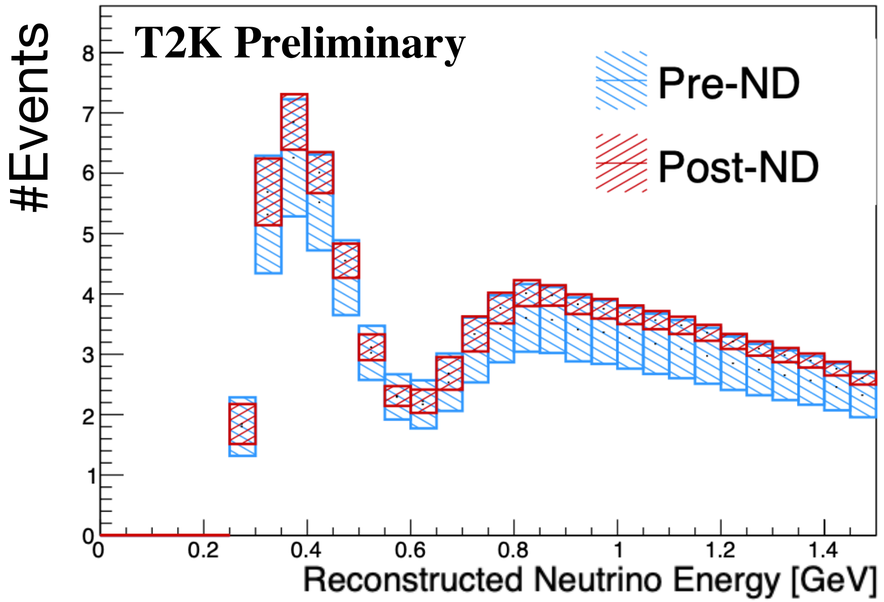

1 Ring e-like

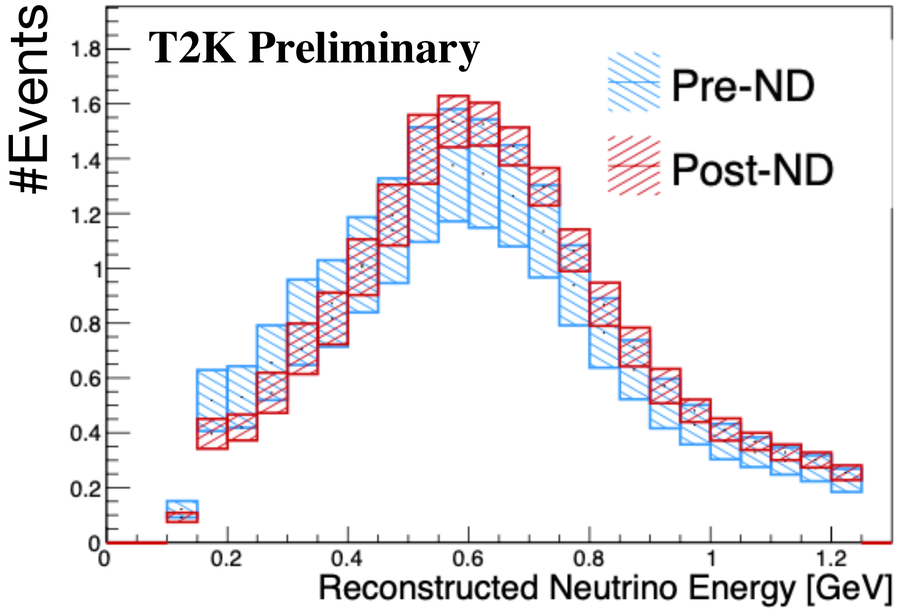

Systematic uncertainties		
SK sample	**1 Ring μ-like**	**1 Ring e-like**
Before ND280 fit	14.6	14.4
After ND280 fit	3.9	5.8

δ_{CP} vs event rates

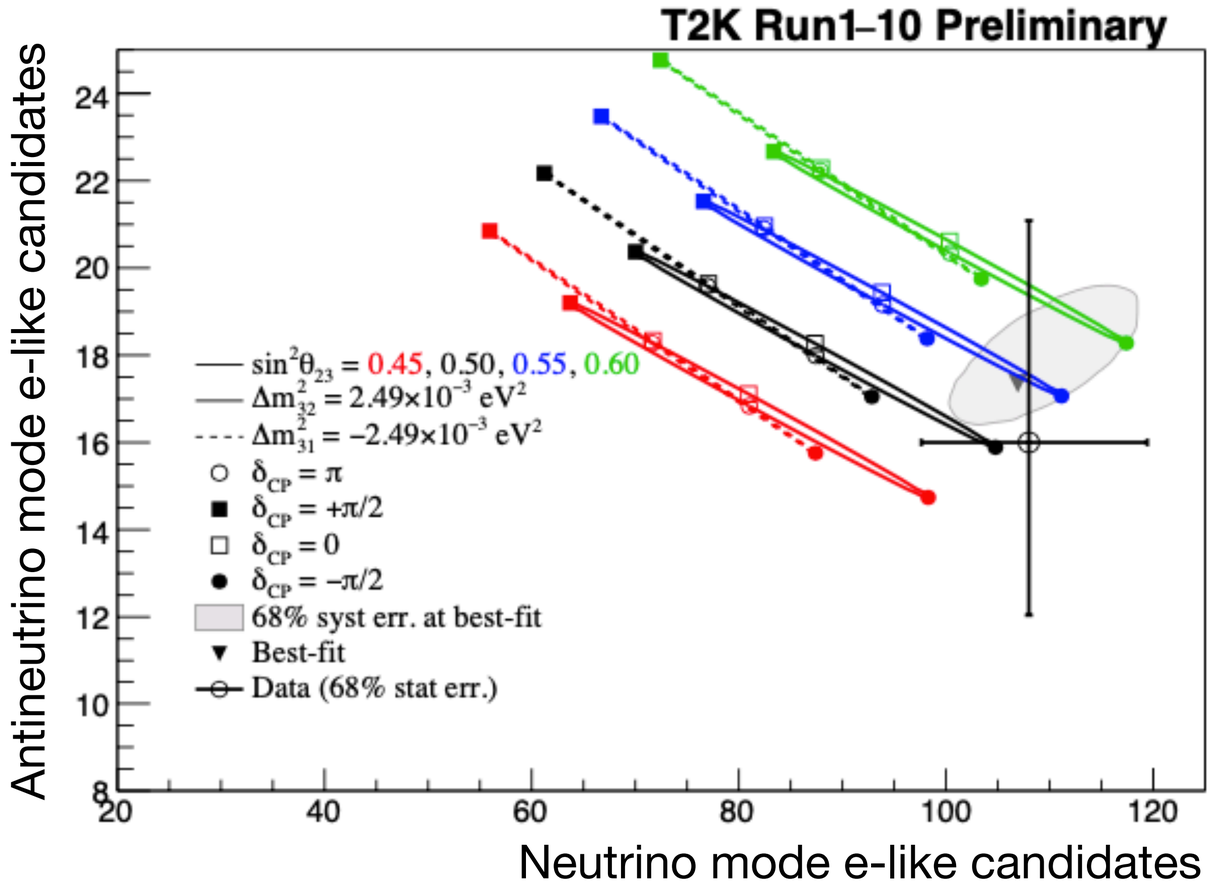

	$\sin^2\theta_{23} < 0.5$	$\sin^2\theta_{23} > 0.5$	Line total
Normal ordering	0.24	0.54	0.78
Inverted ordering	0.05	0.17	0.21
Column total	0.29	0.71	1.00

δ_{CP} vs event rates

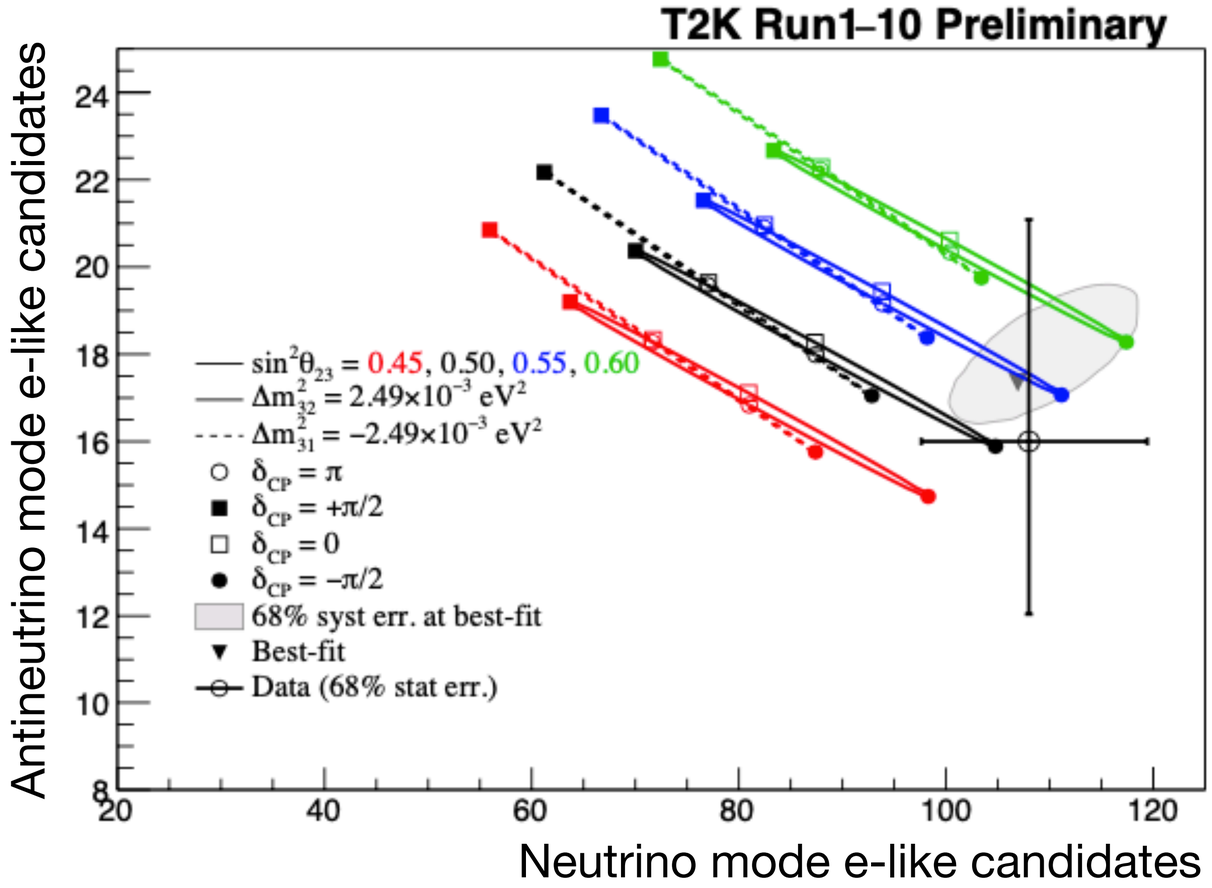

Data prefer maximal CPV

	$\sin^2\theta_{23} < 0.5$	$\sin^2\theta_{23} > 0.5$	Line total
Normal ordering	0.24	0.54	0.78
Inverted ordering	0.05	0.17	0.21
Column total	0.29	0.71	1.00

δ_{CP} vs event rates

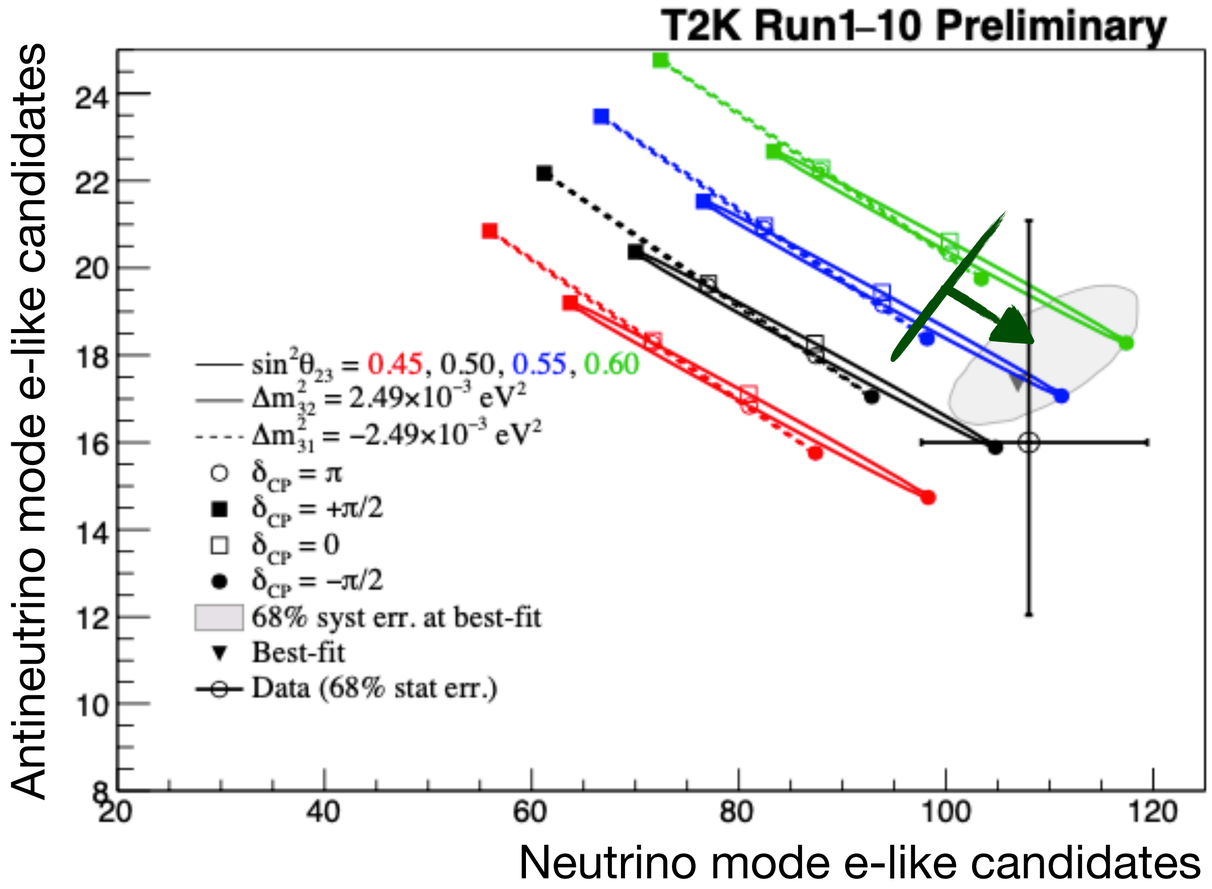

Data prefer maximal CPV

Week preference for normal ordering with Bayes factor of 3.7

	$\sin^2\theta_{23} < 0.5$	$\sin^2\theta_{23} > 0.5$	Line total
Normal ordering			0.78
Inverted ordering			0.21
Column total			1.00

δ_{CP} vs event rates

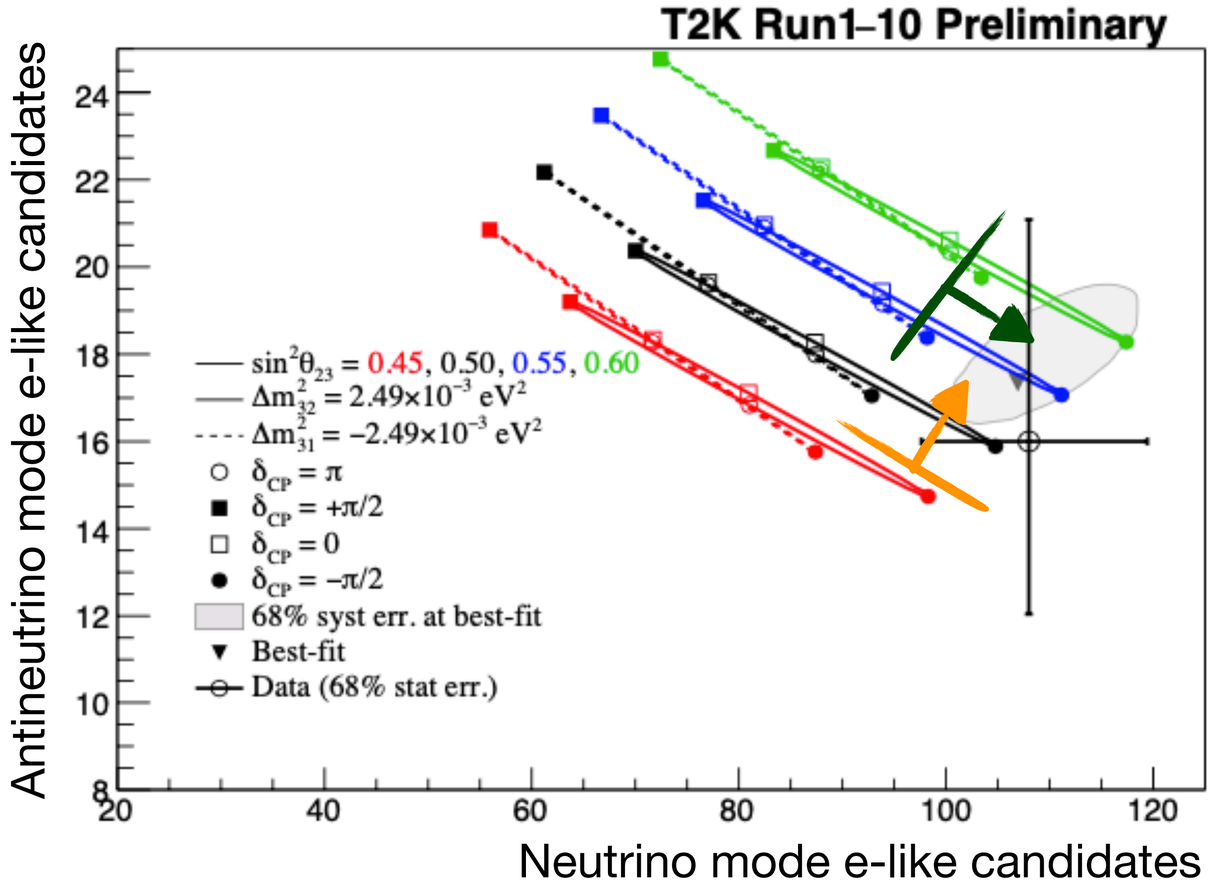

Data prefer maximal CPV

Week preference for normal ordering with Bayes factor of 3.7

Week preference for upper octant with Bayes factor of 2.4

	$\sin^2\theta_{23} < 0.5$	$\sin^2\theta_{23} > 0.5$	Line total
Normal ordering			
Inverted ordering			
Column total	0.29	0.71	1.00

δ_{CP} measurement

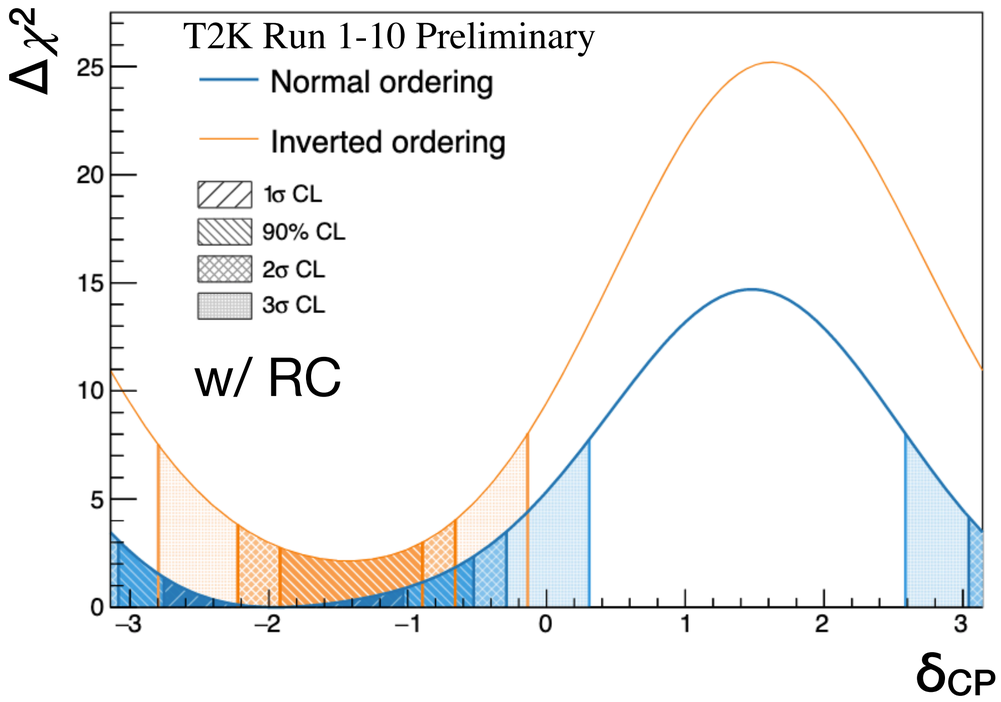

Confidence level	Interval (NH)	Interval (IH)
1σ	$[-2.76, -1.03]$	
90%	$[-3.08, -0.52]$	$[-1.92, -0.89]$
2σ	$[-\pi, -0.29] \cup [3.04, \pi]$	$[-2.22, -0.66]$
3σ	$[-\pi, 0.31] \cup [2.59, \pi]$	$[-2.80, -0.14]$

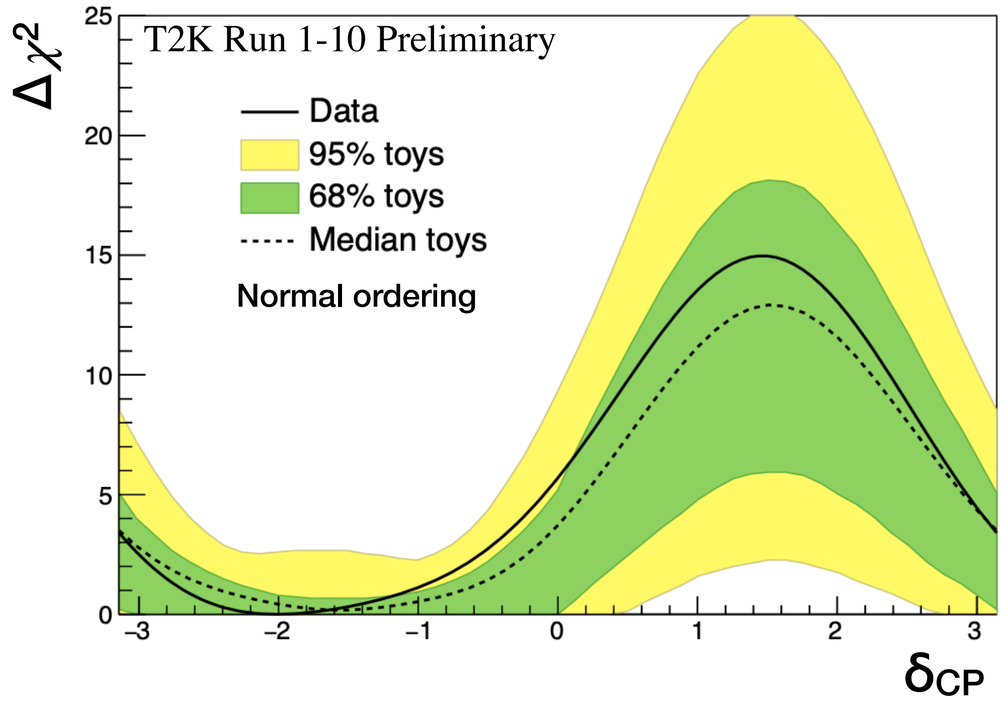

CP-conservation (0,π) excluded at 90%

Large region excluded at 3σ

Results in agreement with sensitivity

θ_{23} measurement

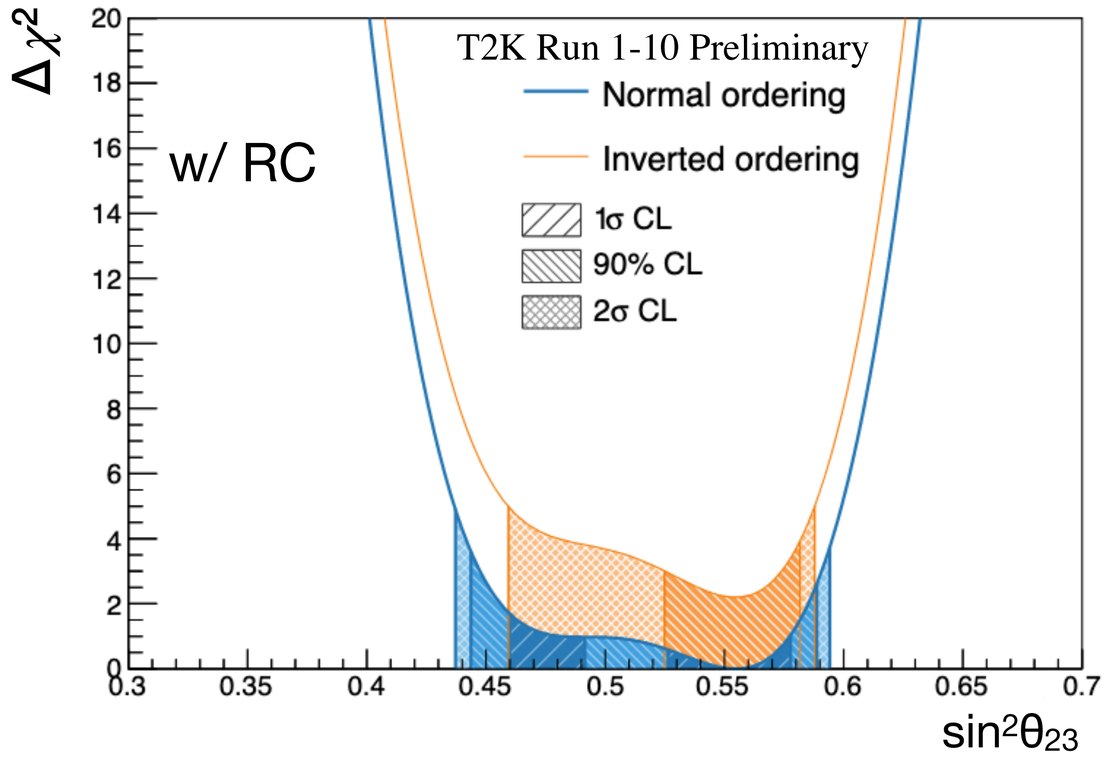

Confidence level	Interval (NH)	Interval (IH)
1σ	$[0.460, 0.491] \cup [0.526, 0.578]$	
90%	$[0.444, 0.589]$	$[0.525, 0.582]$
2σ	$[0.437, 0.594]$	$[0.459, 0.588]$

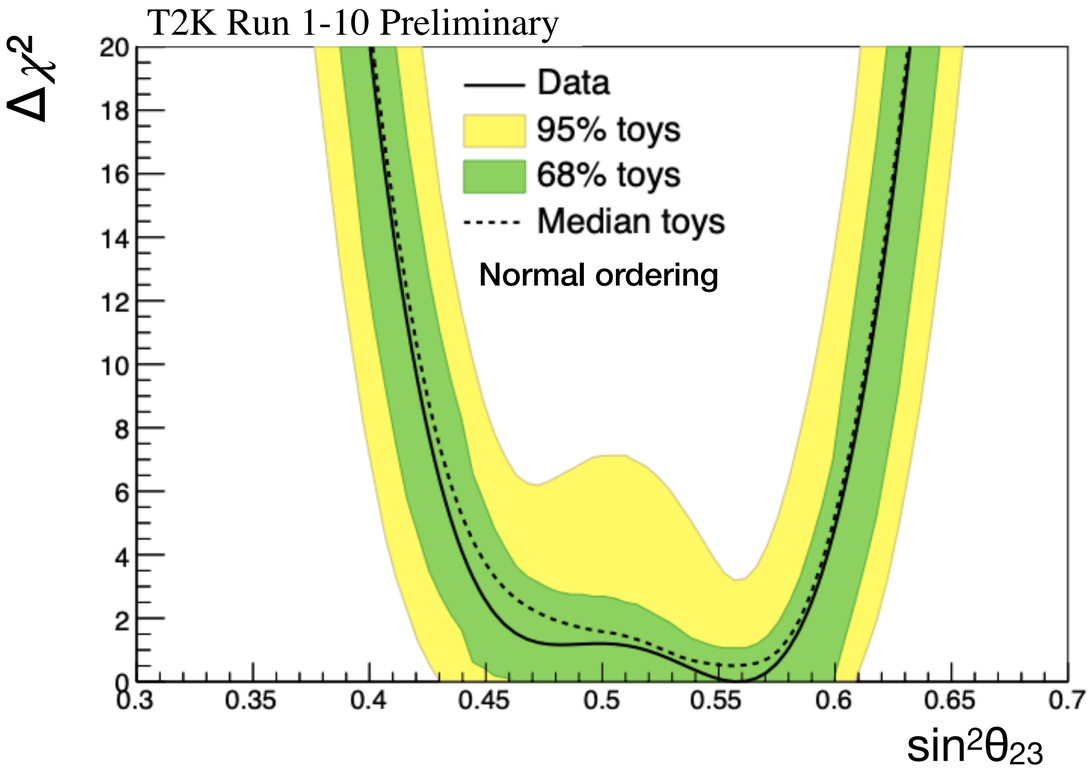

Maximum mixing excluded at 1σ CL

Octant degeneracy appears at 1σ CL

Impact of SK MR sample

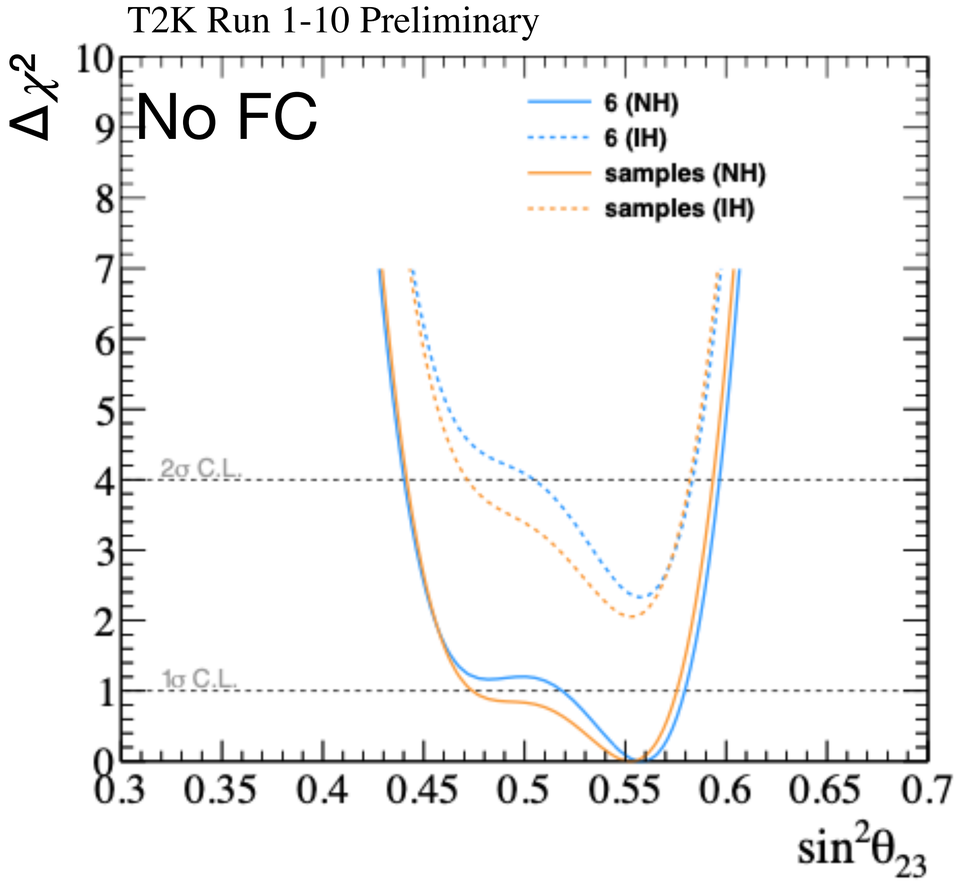

Tighter constraint on θ_{23}

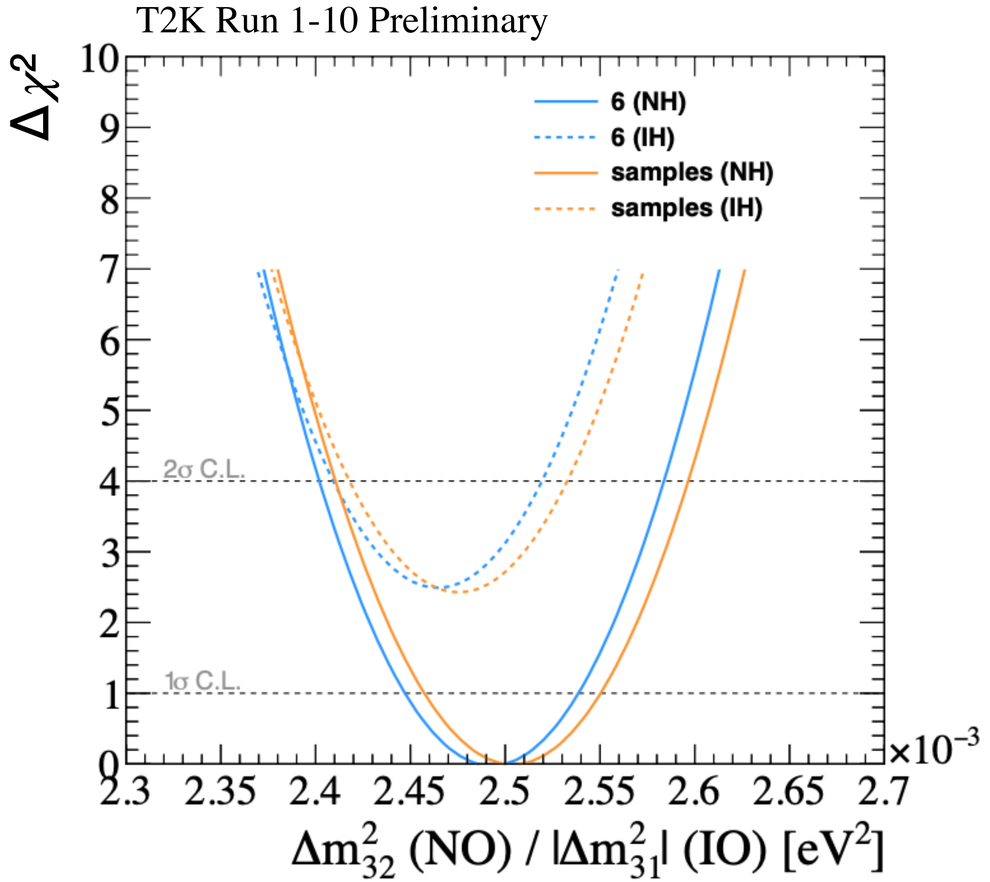

Shift toward lower values of Δm^2_{32} and slightly tighter constraint

Cross section measurements

Cross section measurements

T2K has a wide cross section measurement program: multiple targets, fluxes and detectors at different off-axis angles provide abilities to investigate neutrino-nucleus scattering in different and complementary ways

Cross section measurements

T2K has a wide cross section measurement program: multiple targets, fluxes and detectors at different off-axis angles provide abilities to investigate neutrino-nucleus scattering in different and complementary ways

Neutrino scattering understanding is crucial for the interpretation of neutrino oscillation since it affects background estimation and energy reconstruction

Cross section measurements

T2K has a wide cross section measurement program: multiple targets, fluxes and detectors at different off-axis angles provide abilities to investigate neutrino-nucleus scattering in different and complementary ways

Neutrino scattering understanding is crucial for the interpretation of neutrino oscillation since it affects background estimation and energy reconstruction

One of the **largest systematic uncertainties** in neutrino oscillation comes from neutrino interaction uncertainty and in particular from the modeling of nuclear effects

Systematic uncertainties						
Beam mode	**Neutrino**				**Antineutrino**	
SK sample	**1 Ring μ-like**	**Multi-Ring**	**1 Ring e-like**	**1 Ring e-like 1de**	**1 Ring μ-like**	**1 Ring e-like**
Flux	5.0%	5.2%	4.9%	4.6%	4.6%	4.6%
Cross-section	15.8%	10.6%	16.3%	14.7%	13.6%	13.1%
SK	2.0%	4.1%	3.1%	13.6%	1.7%	3.8%

Transverse Kinematic Imbalance

First measurements of the Transverse Kinematics Imbalance in ν_μ CC1π+Np interactions*

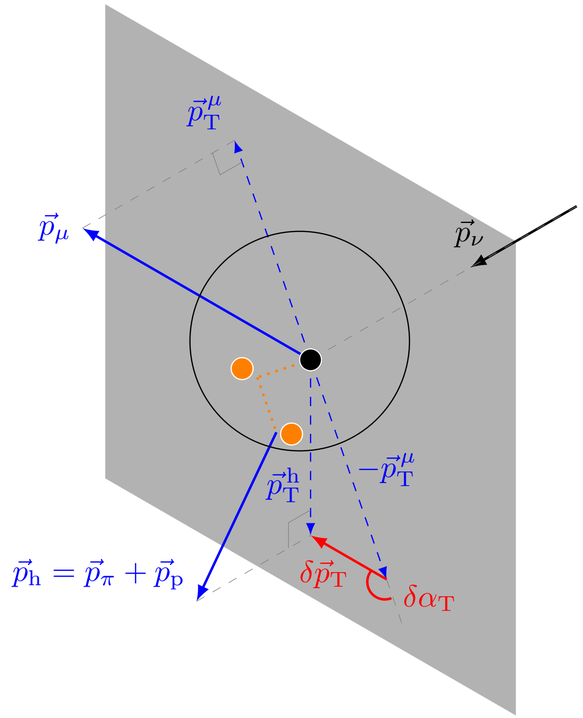

*Phys. Rev. D 103, 112009

Transverse Kinematic Imbalance

First measurements of the Transverse Kinematics Imbalance in ν_μ CC1π+Np interactions*

Initial nucleon momentum

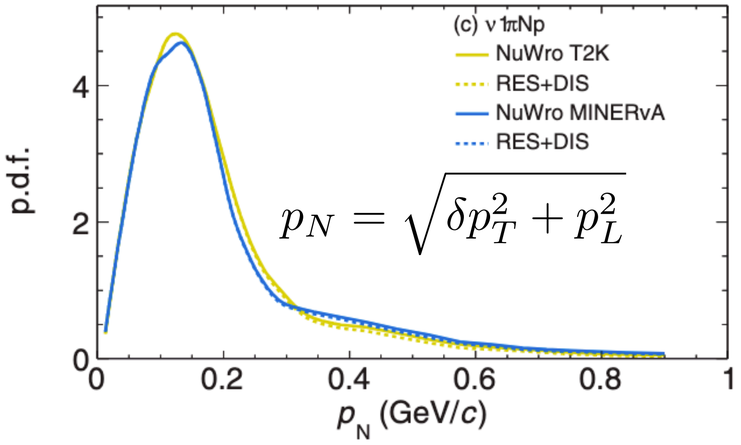

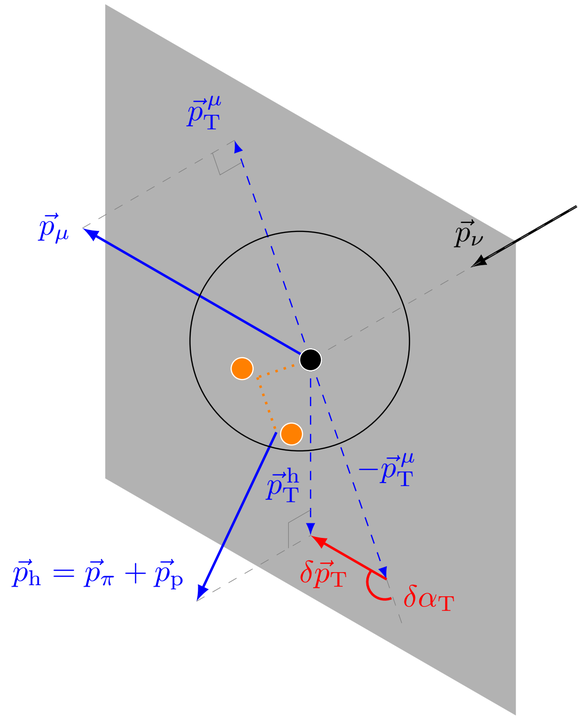

*Phys. Rev. D 103, 112009

Transverse Kinematic Imbalance

First measurements of the Transverse Kinematics Imbalance in ν_μ CC1π+Np interactions*

Initial nucleon momentum

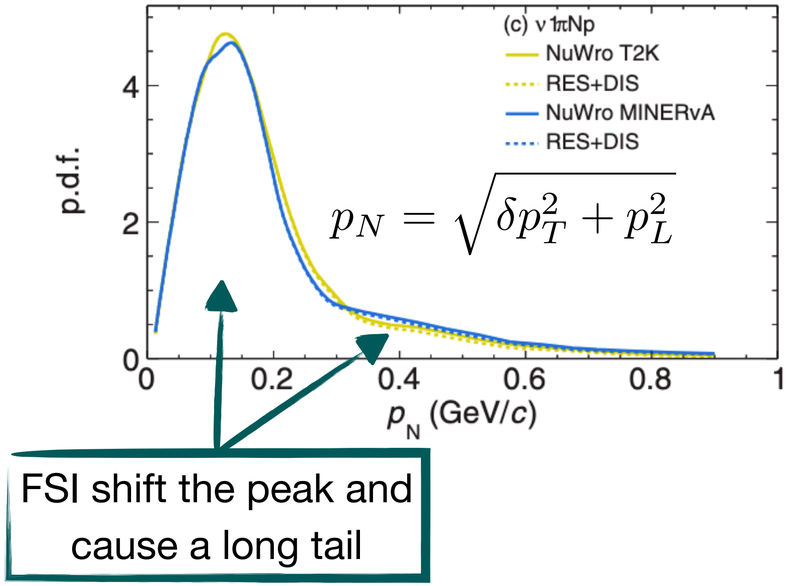

FSI shift the peak and cause a long tail

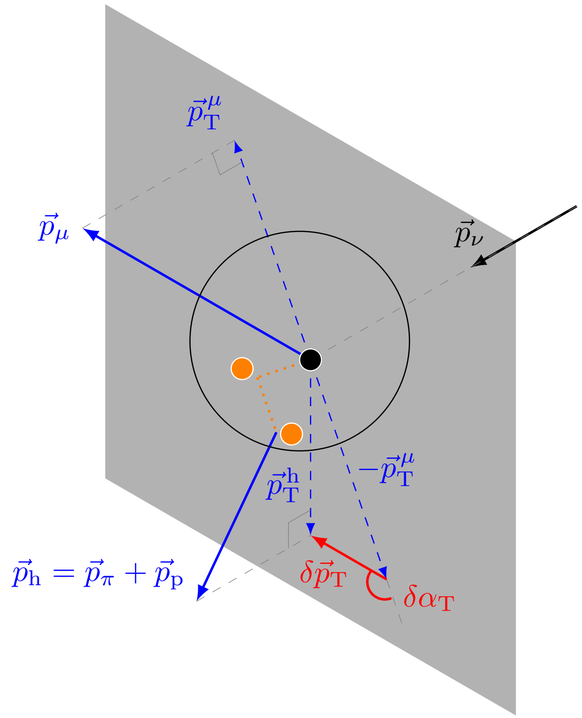

*Phys. Rev. D 103, 112009

Transverse Kinematic Imbalance

First measurements of the Transverse Kinematics Imbalance in ν_μ CC1π+Np interactions*

Initial nucleon momentum

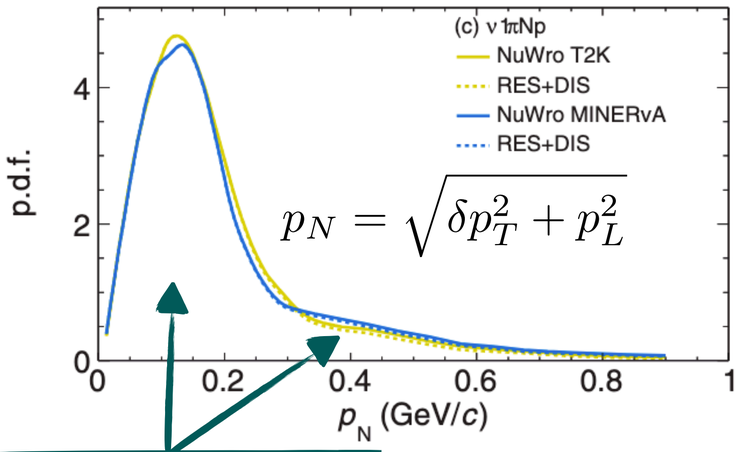

FSI shift the peak and cause a long tail

Transverse boosting angle

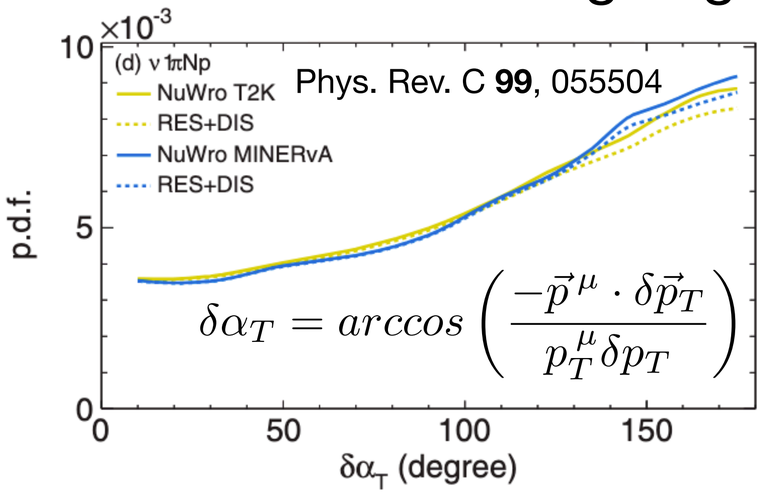

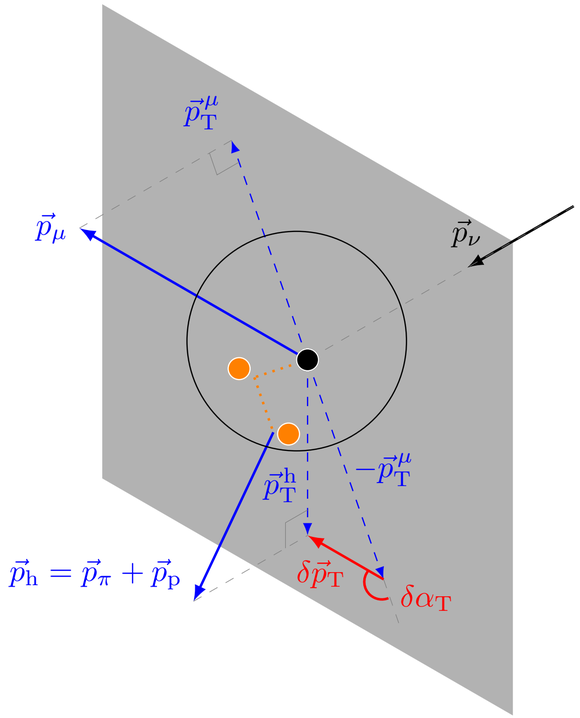

*Phys. Rev. D 103, 112009

Transverse Kinematic Imbalance

First measurements of the Transverse Kinematics Imbalance in ν_μ CC1π+Np interactions*

Initial nucleon momentum

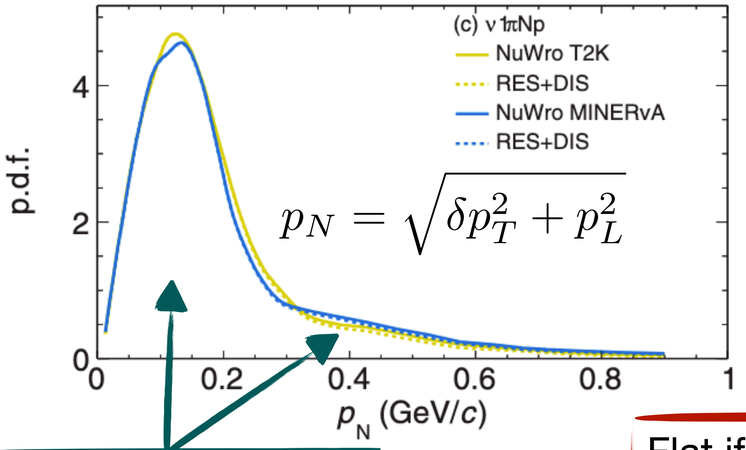

FSI shift the peak and cause a long tail

Transverse boosting angle

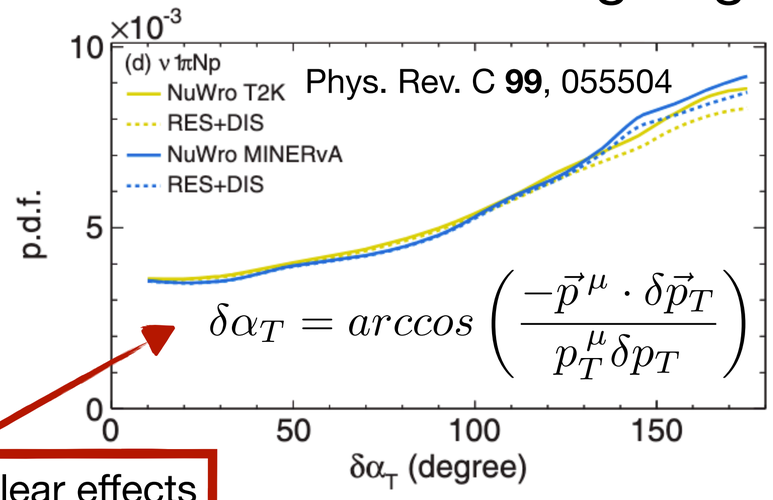

Flat if no nuclear effects

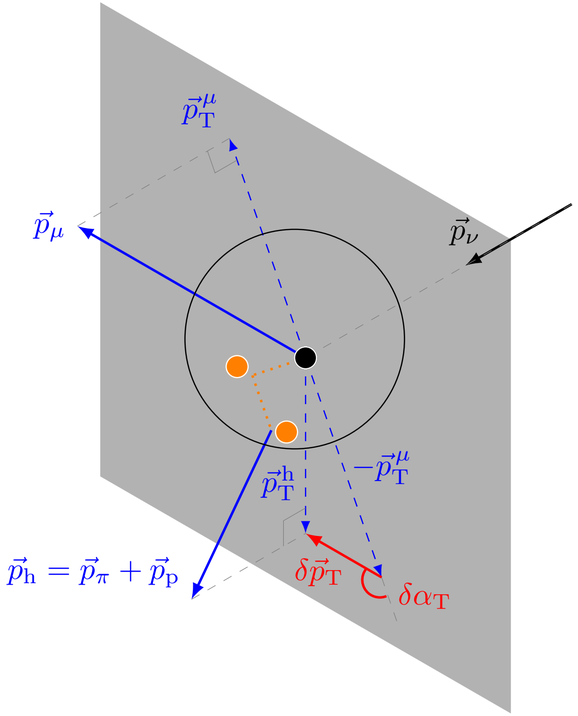

*Phys. Rev. D 103, 112009

Transverse Kinematic Imbalance

First measurements of the Transverse Kinematics Imbalance in ν_μ CC1π+Np interactions*

Initial nucleon momentum

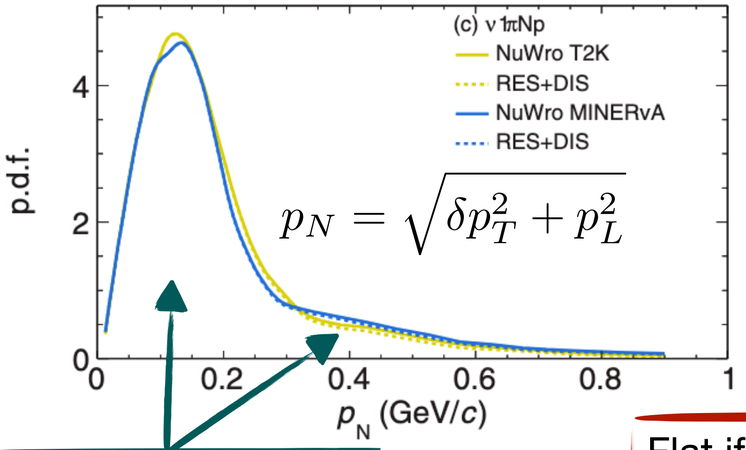

FSI shift the peak and cause a long tail

Transverse boosting angle

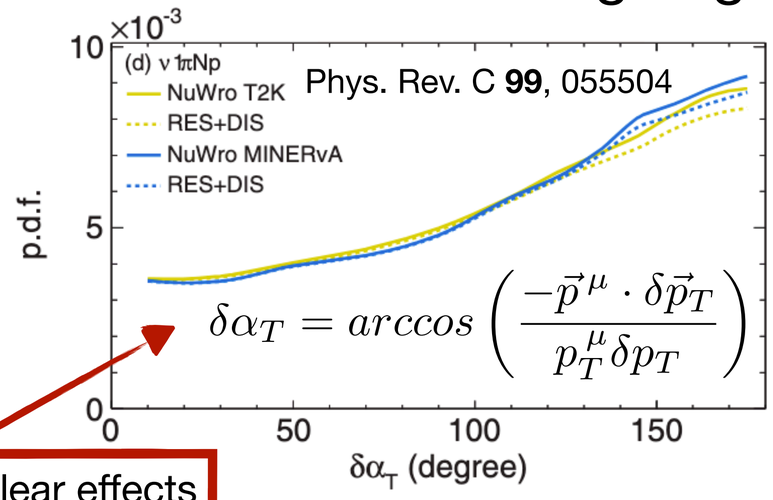

Flat if no nuclear effects

Double kinematic imbalance

$$\delta p_{TT} = p_{TT}^{p} + p_{TT}^{\pi} = \frac{\vec{p}^{\,\nu}\times\vec{p}_T^{\,\mu}}{\|\vec{p}^{\,\nu}\times\vec{p}_T^{\,\mu}\|}\cdot(\vec{p}_T^{\,\pi}+\vec{p}_T^{\,p})$$

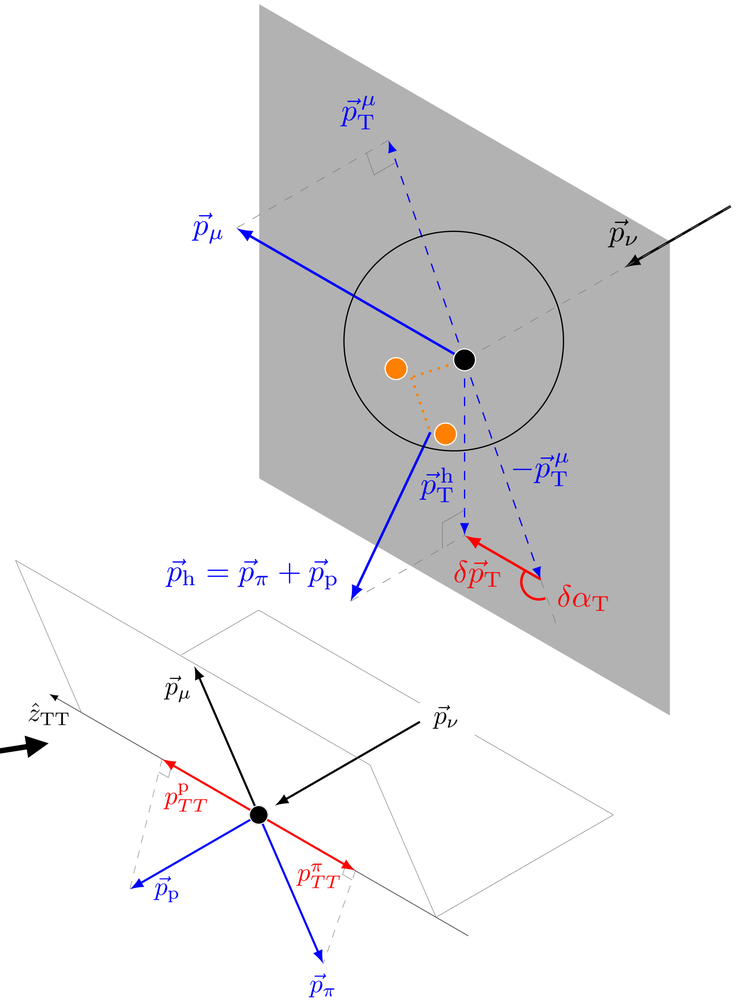

*Phys. Rev. D 103, 112009

Transverse Kinematic Imbalance

First measurements of the Transverse Kinematics Imbalance in ν_μ CC1π+Np interactions*

Initial nucleon momentum

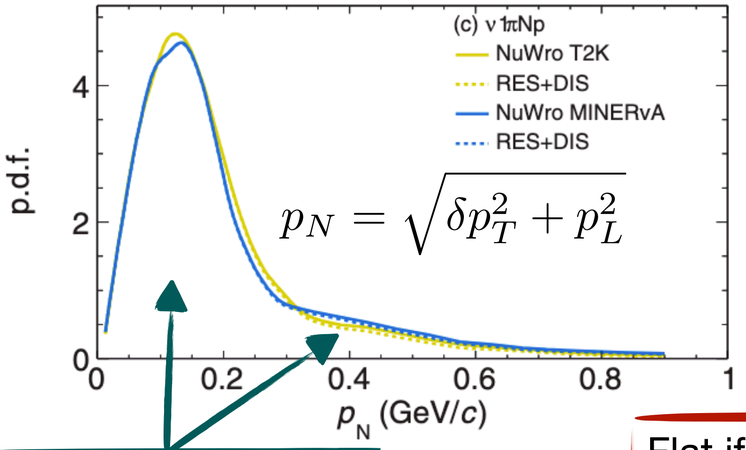

FSI shift the peak and cause a long tail

Transverse boosting angle

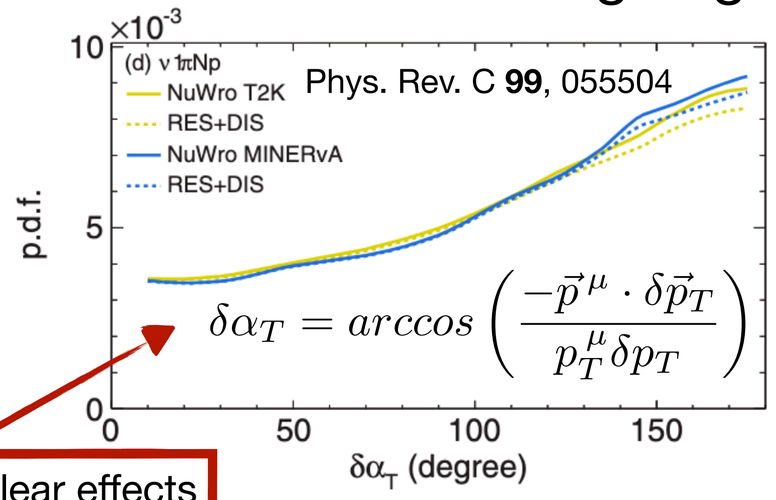

Flat if no nuclear effects

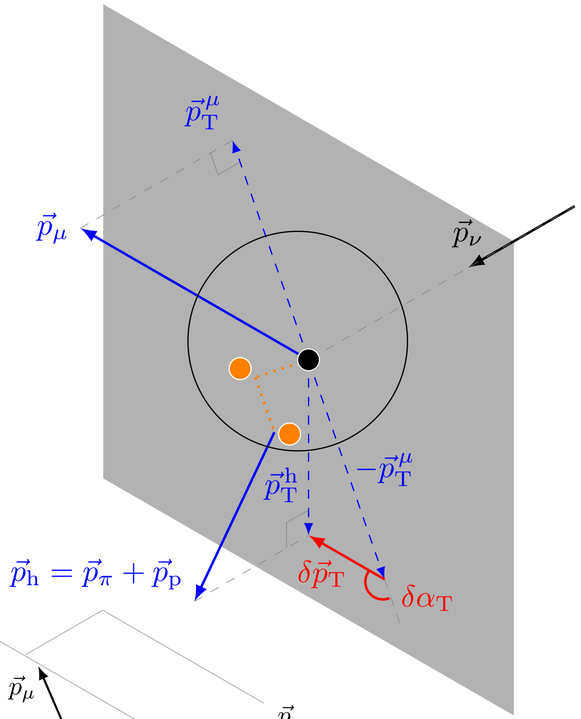

Double kinematic imbalance

$$\delta p_{TT} = p_{TT}^{p} + p_{TT}^{\pi} = \frac{\vec{p}^{\,\nu}\times\vec{p}_T^{\,\mu}}{\|\vec{p}^{\,\nu}\times\vec{p}_T^{\,\mu}\|}\cdot(\vec{p}_T^{\,\pi}+\vec{p}_T^{\,p})$$

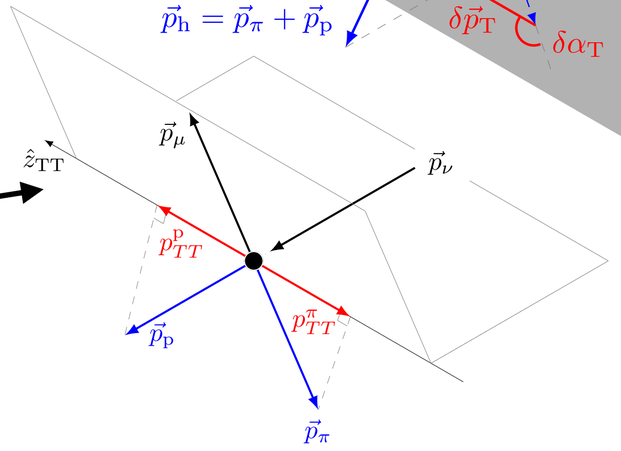

If no nuclear effects is zero

*Phys. Rev. D 103, 112009

TKI in ν_μ CC1π+Np

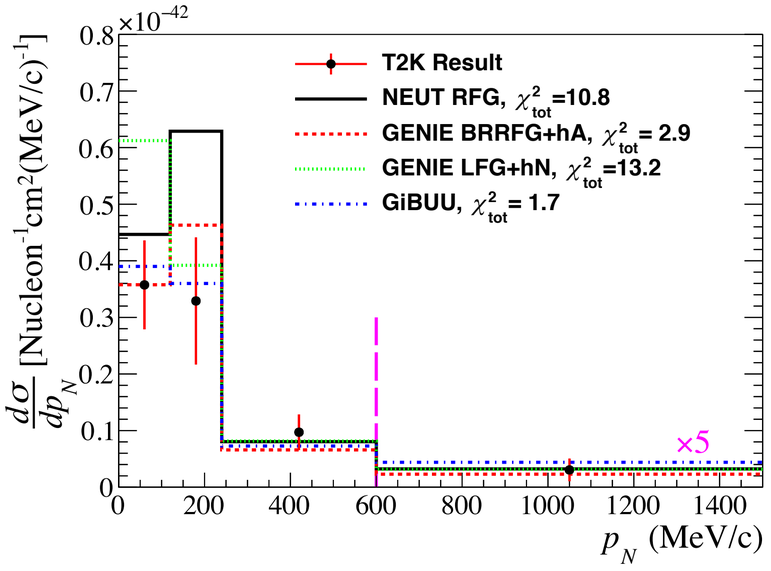

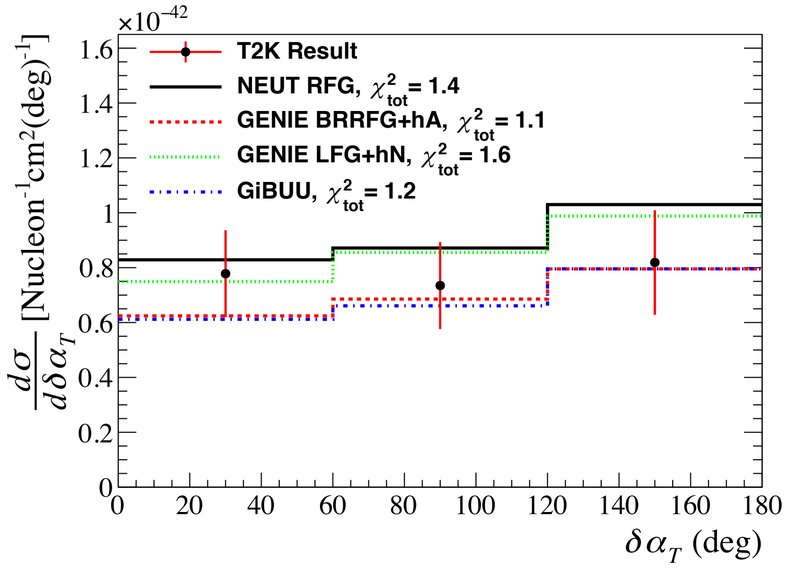

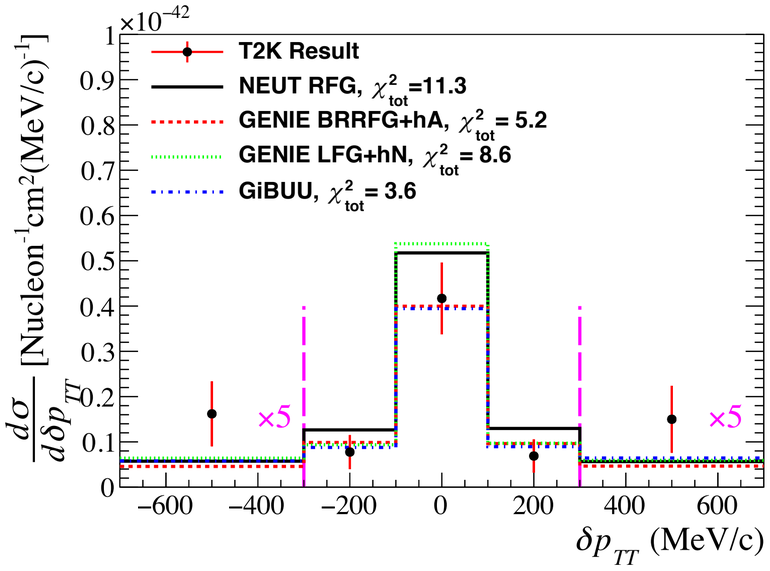

RFG and LFG nuclear models strongly disfavored at small p_N

Over-prediction in the peak region for almost all models

Curvature strongly dependent on FSI

Currently statistics and detector capabilities limit our sensitivity

Model sensitivity comes mostly from central bins

Tail mostly contributed by FSI

*Phys. Rev. D 103, 112009

On-/off-axis combined analysis

- Next generation CC0π analysis: Simultaneous fit using data from both ND280 and INGRID (central module). Paper in preparation!
- On-/off-axis positions result in different, but highly correlated, neutrino flux distributions.
- Provides an opportunity to break some of the degeneracy between flux and cross section.
- Study energy dependence of neutrino interaction processes.
- Next-to-next analysis: combined neutrino and antineutrino

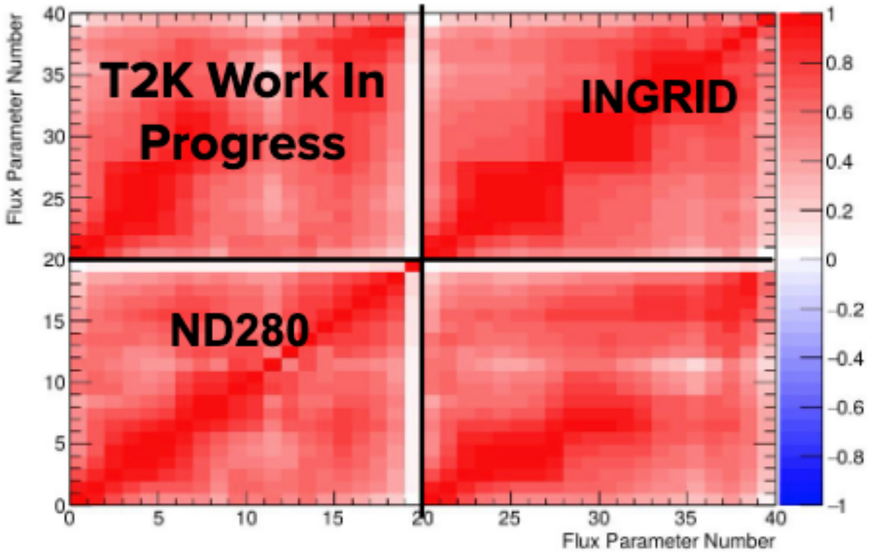

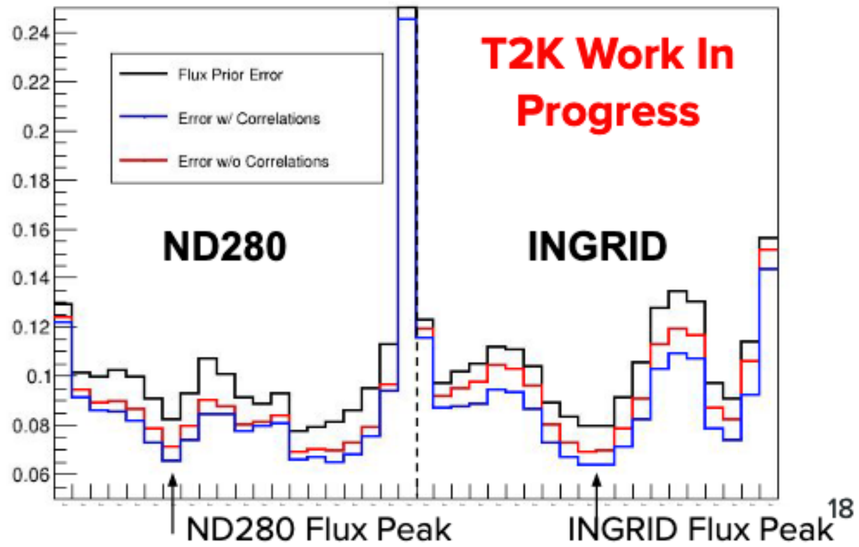

Future cross-section measurements

Planned analyses:

- Different channels: CC Coherent (paper in preparation), CC1π on different targets
- Combine interactions channels
- Explore pion kinematics

New set of detectors at 1.5 degree off-axis:

- Neutrino energy peaked around 0.86 GeV
- WAGASCI: scintillator detector with a grid structure filled with water
- BabyMIND used as spectrometer

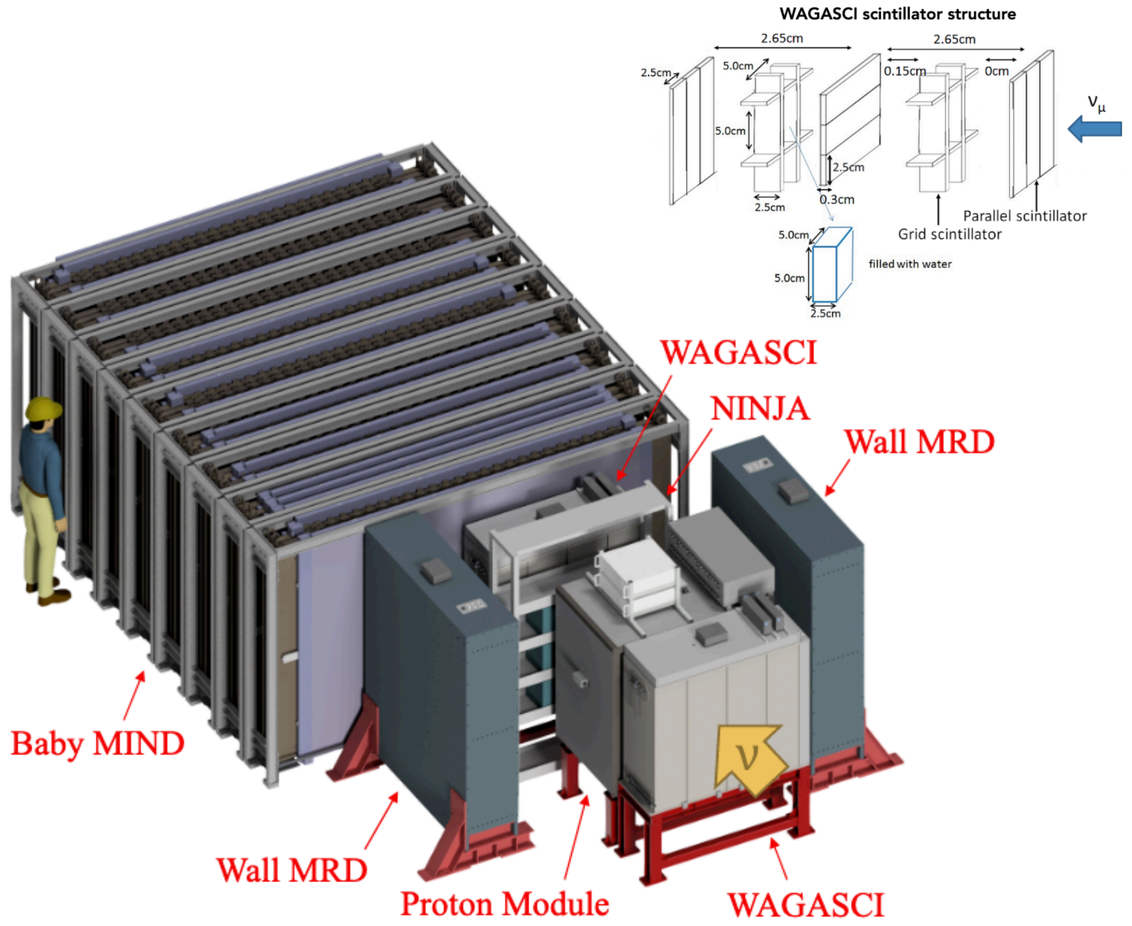

Future prospects

T2K was originally approved to collect 7.8×10^{21} POT driven by sensitivity to θ_{13}

Future prospects

T2K was originally approved to collect 7.8×10^{21} POT driven by sensitivity to θ_{13}

Proposal to extend the run until Hyper-Kamiokande starts

Future prospects

T2K was originally approved to collect 7.8x10^{21} POT driven by sensitivity to θ_{13}

Proposal to extend the run until Hyper-Kamiokande starts

3σ sensitivity to CP-violation for currently favored parameters

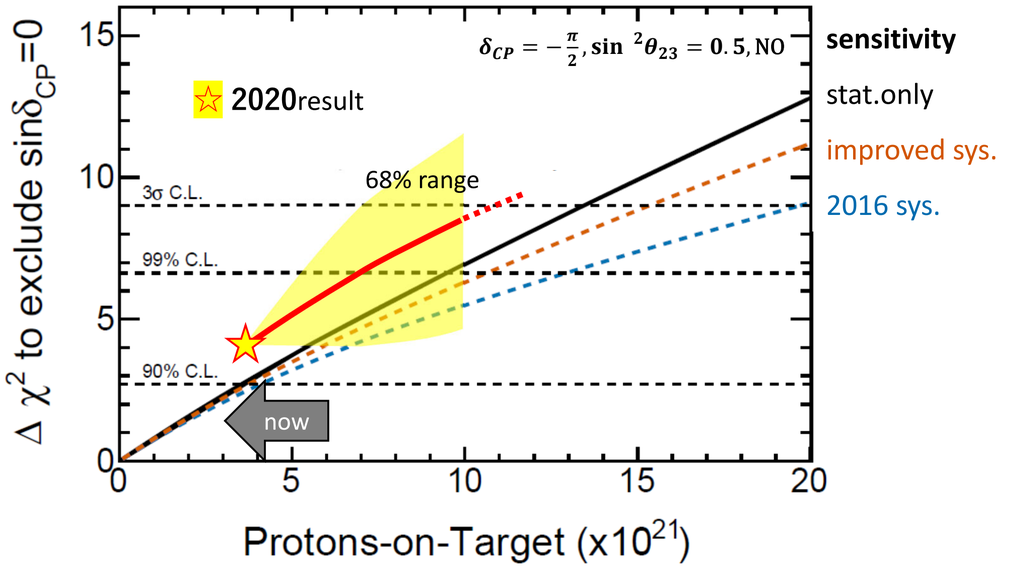

Future prospects

T2K was originally approved to collect 7.8x10^{21} POT driven by sensitivity to θ_{13}

Proposal to extend the run until Hyper-Kamiokande starts

3σ sensitivity to CP-violation for currently favored parameters

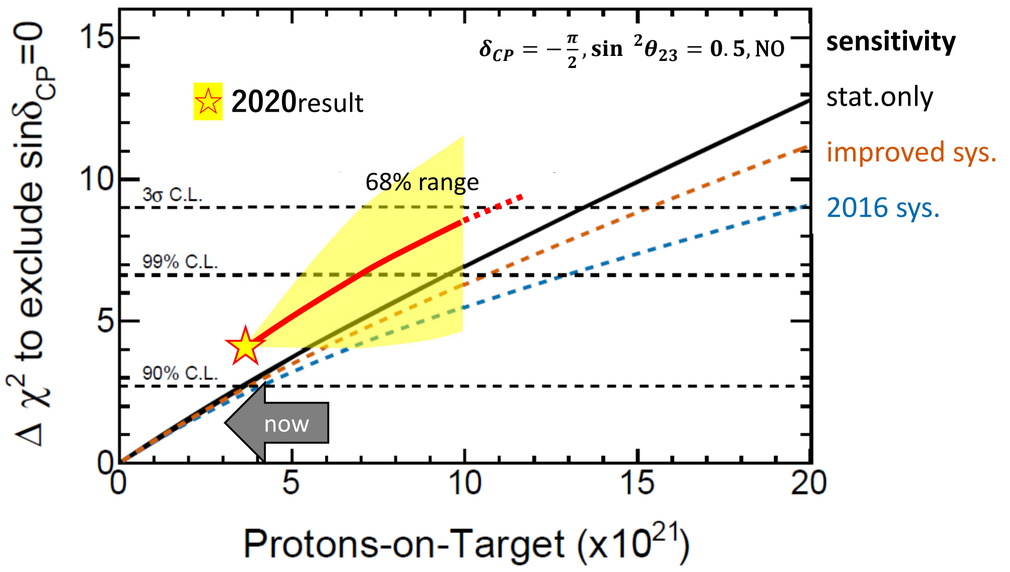

Important to reduce systematics with respect to what we have today

Future prospects

T2K was originally approved to collect 7.8×10^{21} POT driven by sensitivity to θ_{13}

Proposal to extend the run until Hyper-Kamiokande starts

3σ sensitivity to CP-violation for currently favored parameters

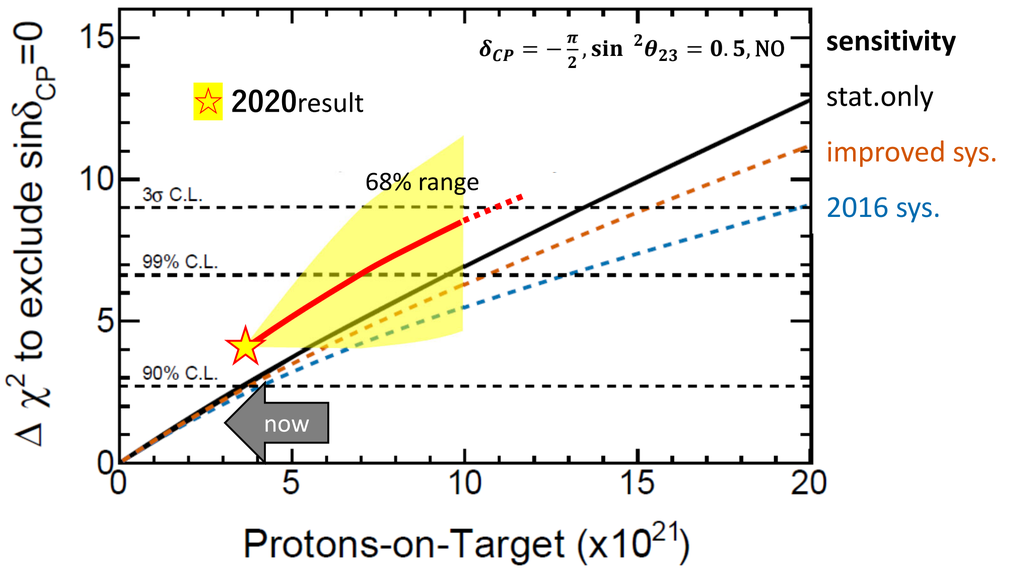

Important to reduce systematics with respect to what we have today

Future prospects

T2K was originally approved to collect 7.8x10^{21} POT driven by sensitivity to θ_{13}

Proposal to extend the run until Hyper-Kamiokande starts

3σ sensitivity to CP-violation for currently favored parameters

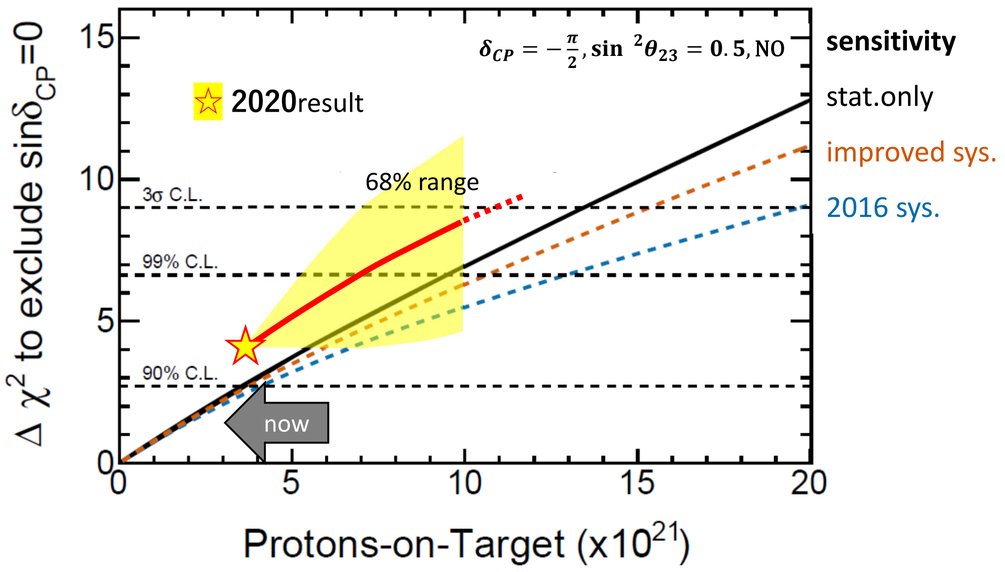

Important to reduce systematics with respect to what we have today

Increase beam power up to 1.3 MW and horn current up to ±320 kA

Future prospects

T2K was originally approved to collect 7.8x10^{21} POT driven by sensitivity to θ_{13}

Proposal to extend the run until Hyper-Kamiokande starts

3σ sensitivity to CP-violation for currently favored parameters

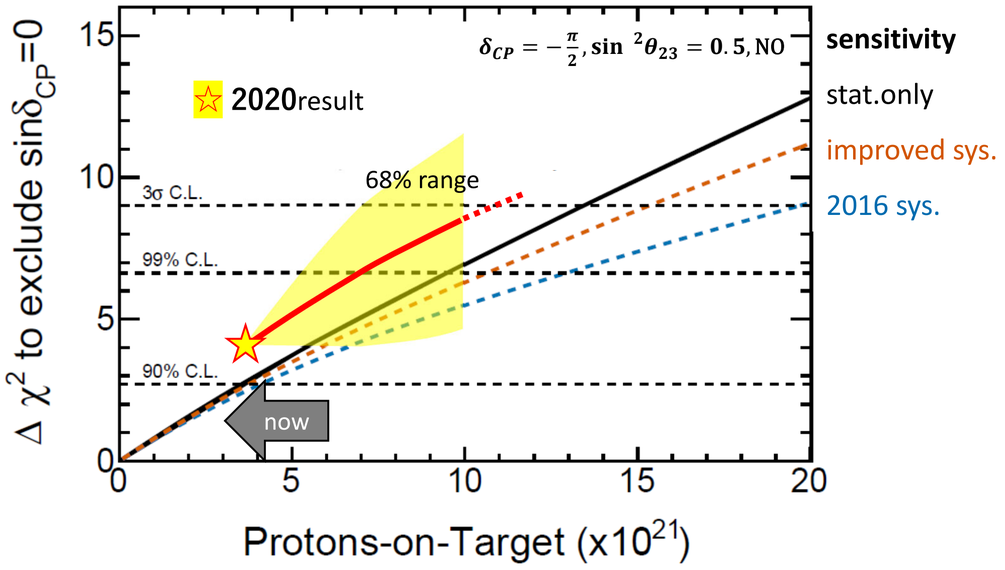

Important to reduce systematics with respect to what we have today

Increase beam power up to 1.3 MW and horn current up to ±320 kA

Upgrade ND280

J-PARC Beam upgrade

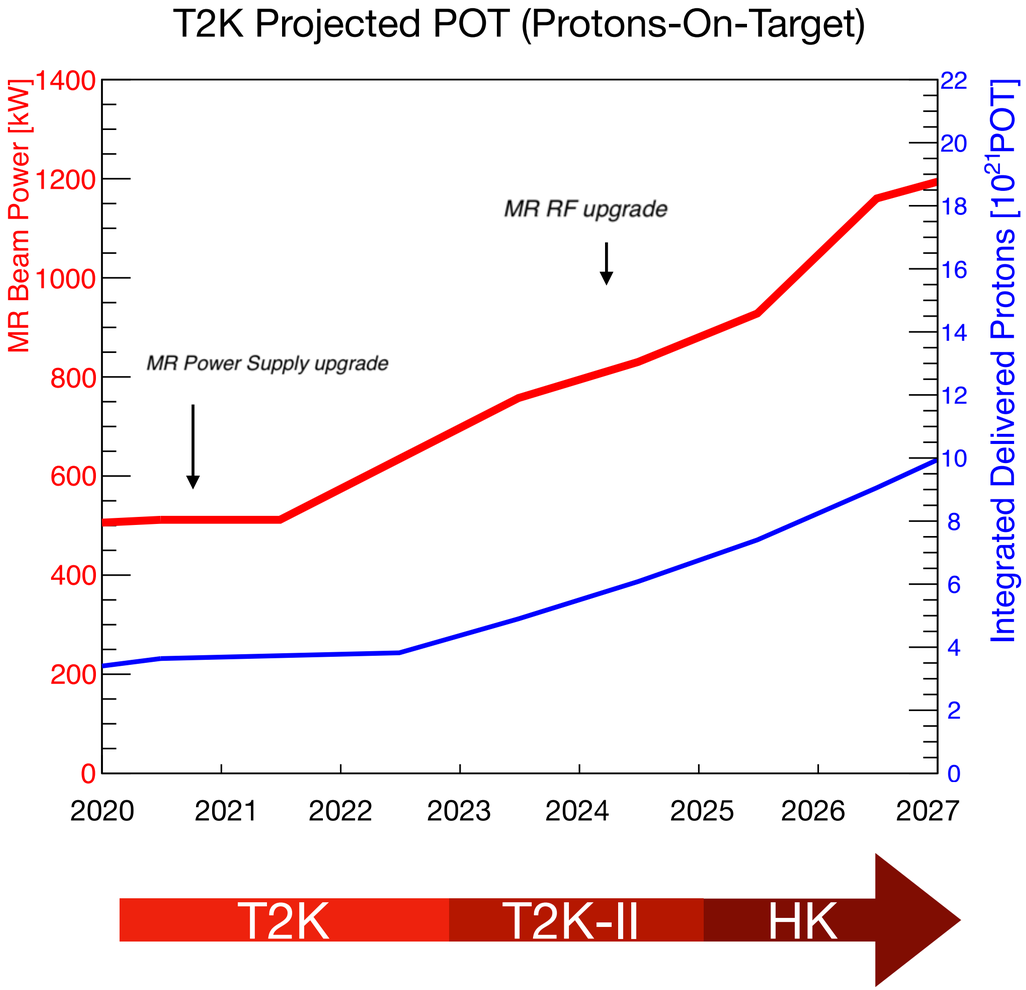

J-PARC Beam upgrade

Main ring power supply upgrade

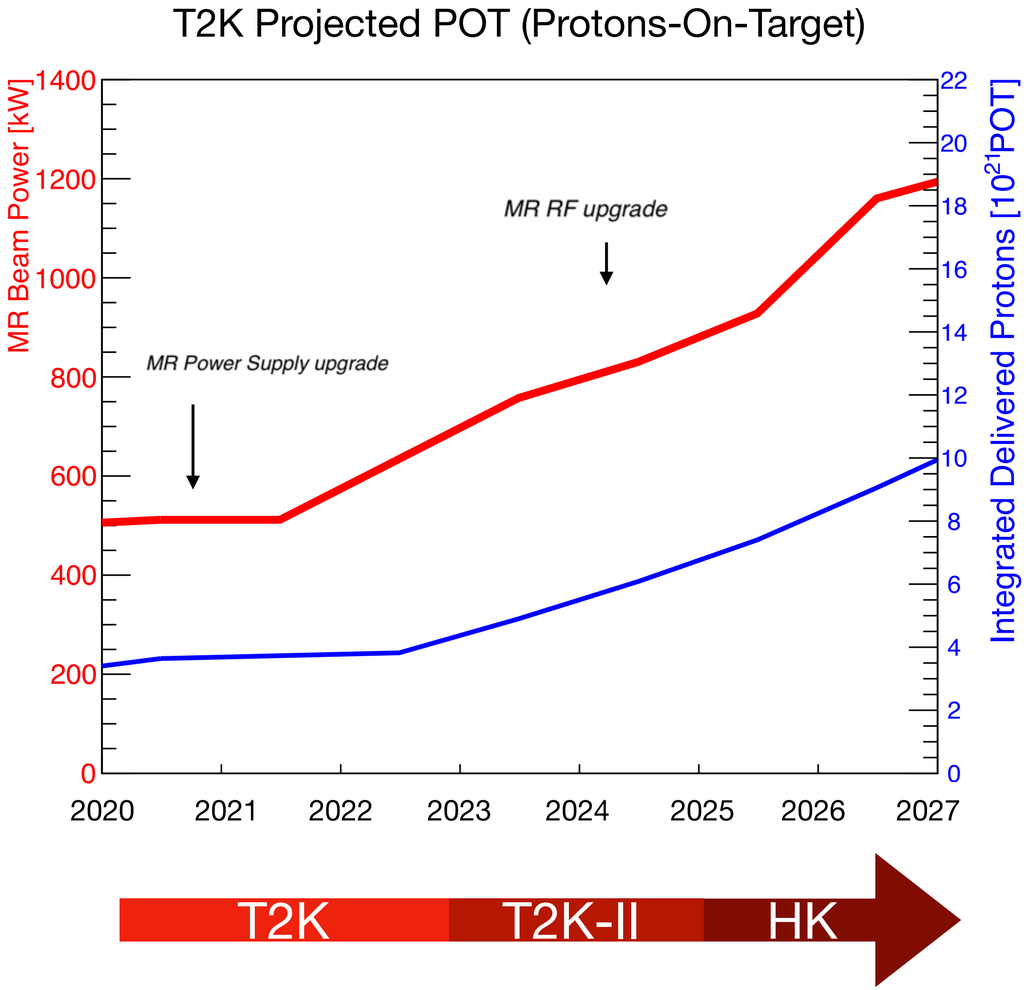

J-PARC Beam upgrade

Main ring power supply upgrade

Expect a beam power ~800 kW by 2023

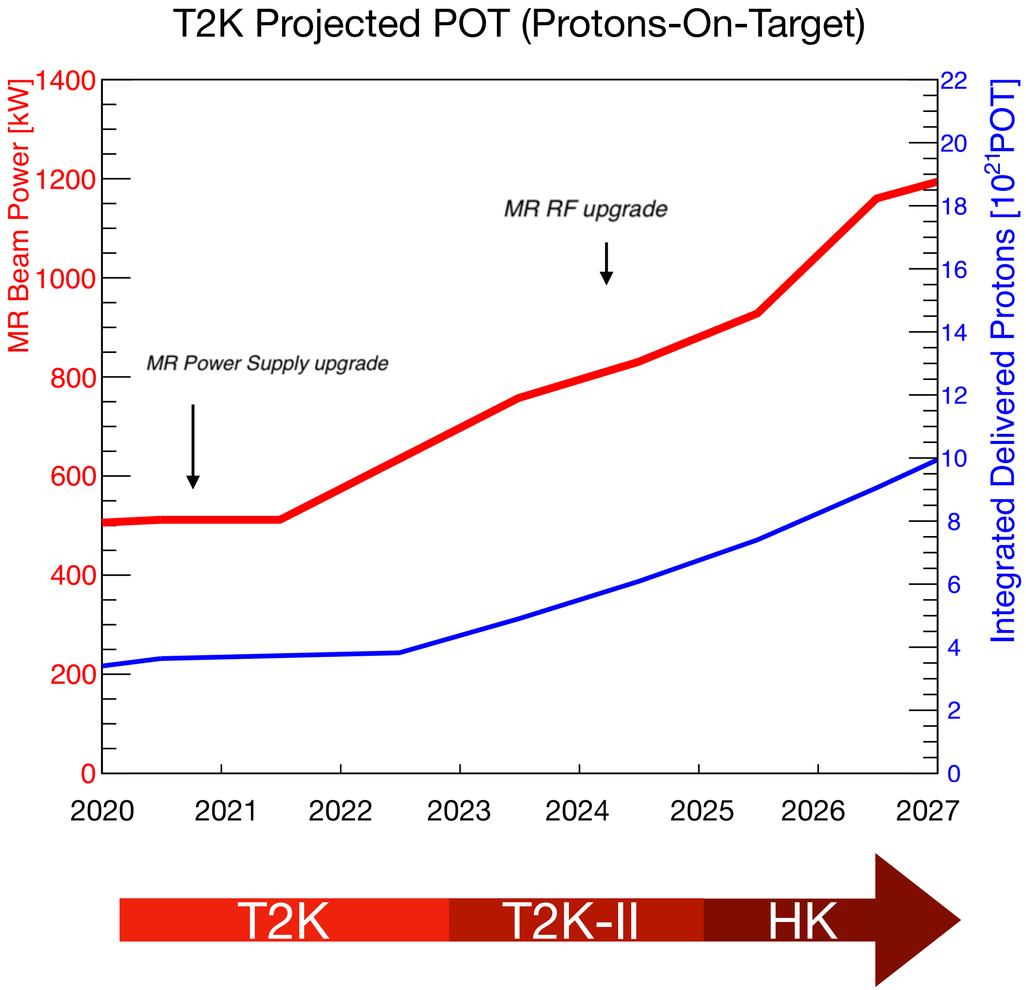

J-PARC Beam upgrade

Main ring power supply upgrade

Expect a beam power ~800 kW by 2023

Main ring RF upgrade

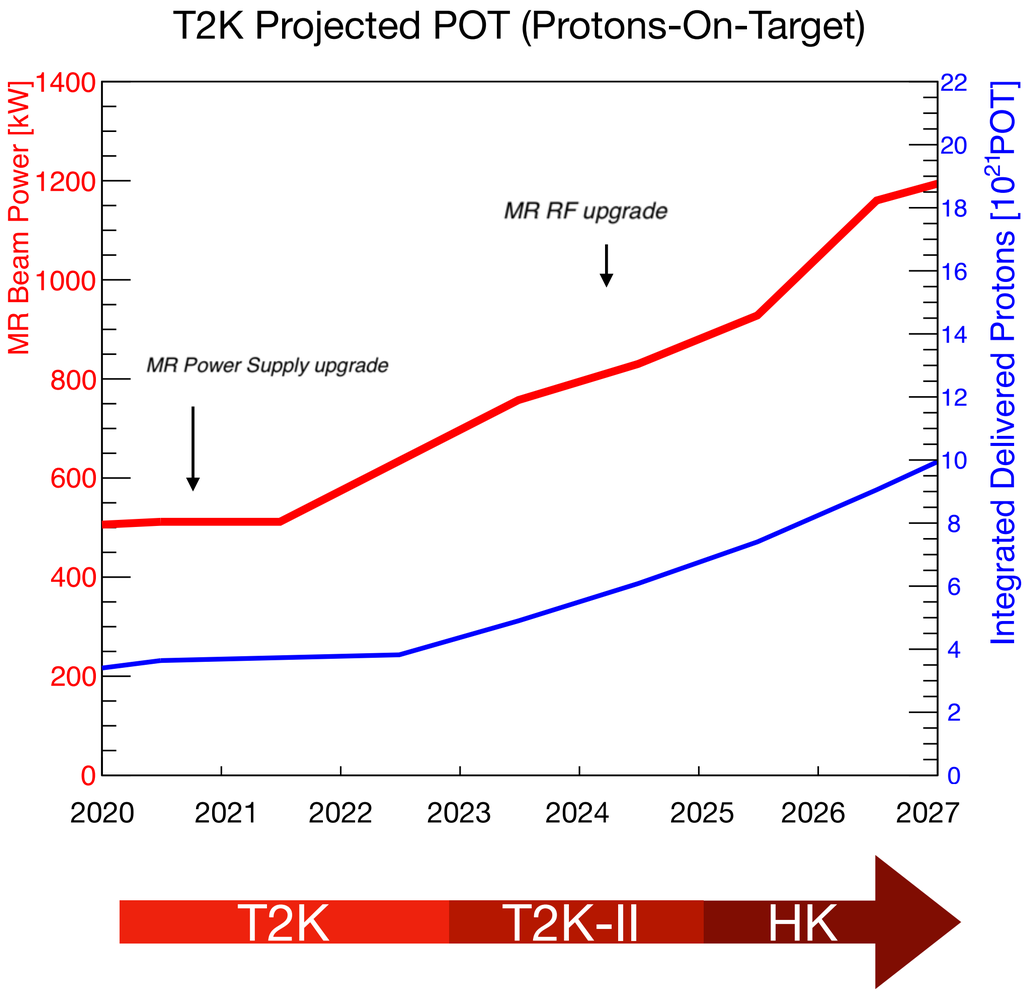

J-PARC Beam upgrade

Main ring power supply upgrade

Expect a beam power ~800 kW by 2023

Main ring RF upgrade

Expected a beam power of 1.2 MW by 2027 and a projected POT of 10^{22}

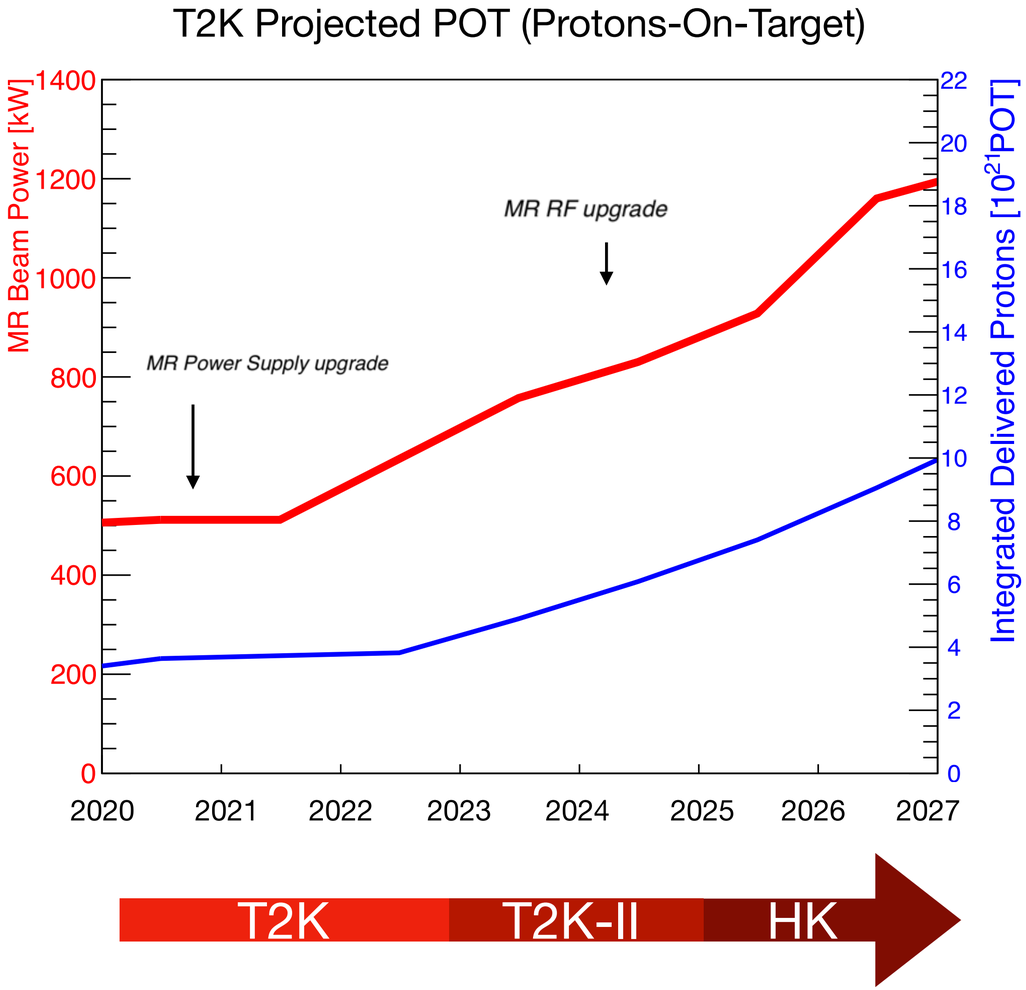

ND280 upgrade

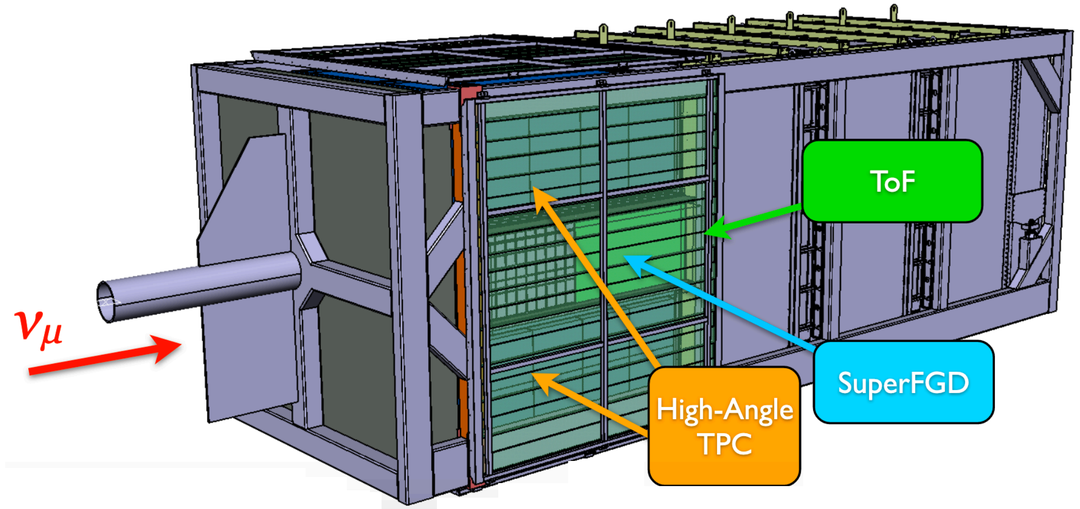

- SuperFGD: 2M 1cm-cubes
- 2 TPCs equipped with resistive MicroMegas
- 6 Time-Of-Flight detectors
- Start construction in Fall 2022 and taking data from April 2023. Then 4 months of running per year until Hyper-K starts

Main ND280 upgrade improvements beyond current ND280:

- Improved acceptance (4π as SK) and efficiency
- Lower threshold for protons
- Neutron kinematics
- Increased target mass (2 tons)

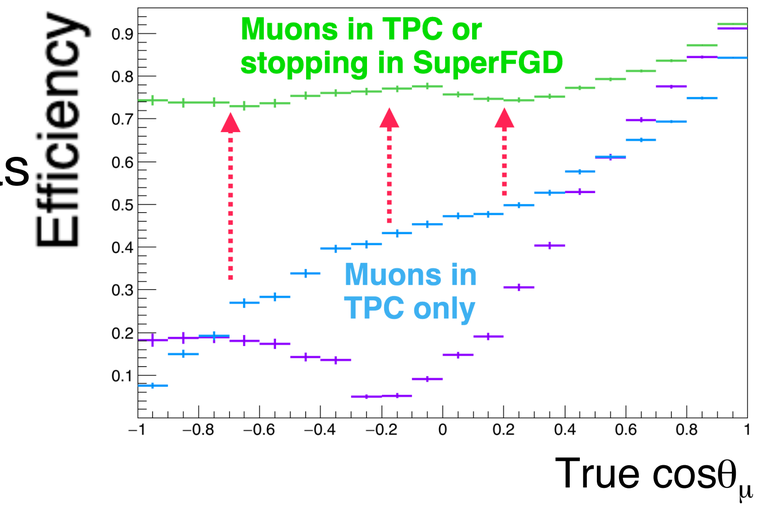

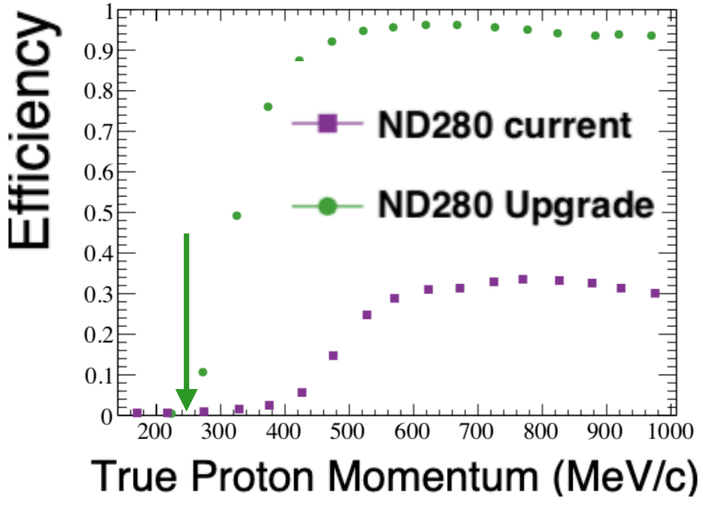

SuperFGD

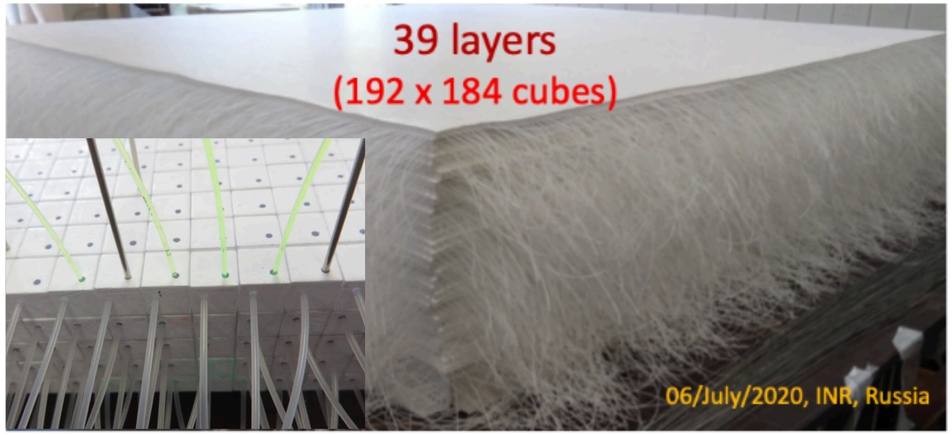

- All the cubes have been produced and assembled in x-y layers at INR and will be in Japan this summer
- Test beam activities:
  - At CERN a prototype has been exposed to a charged particle beam
  - At LANL to a neutron beam with energy 0 - 800 MeV. First goal measure total cross-section

TB have shown very good performances:

- Average LY ~58 PE per MIP
- 3% cross-talk
- Time resolution ~1 ns per channel
- Very good particle ID

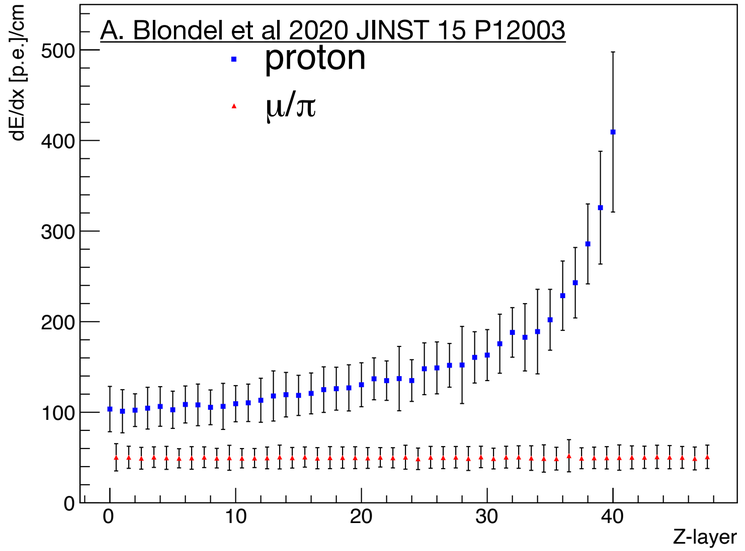

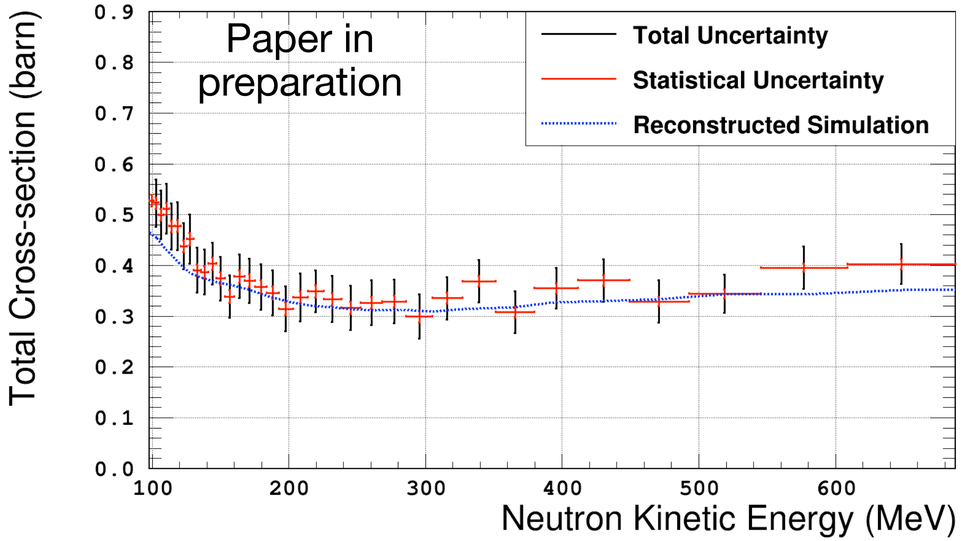

High-angle TPCs

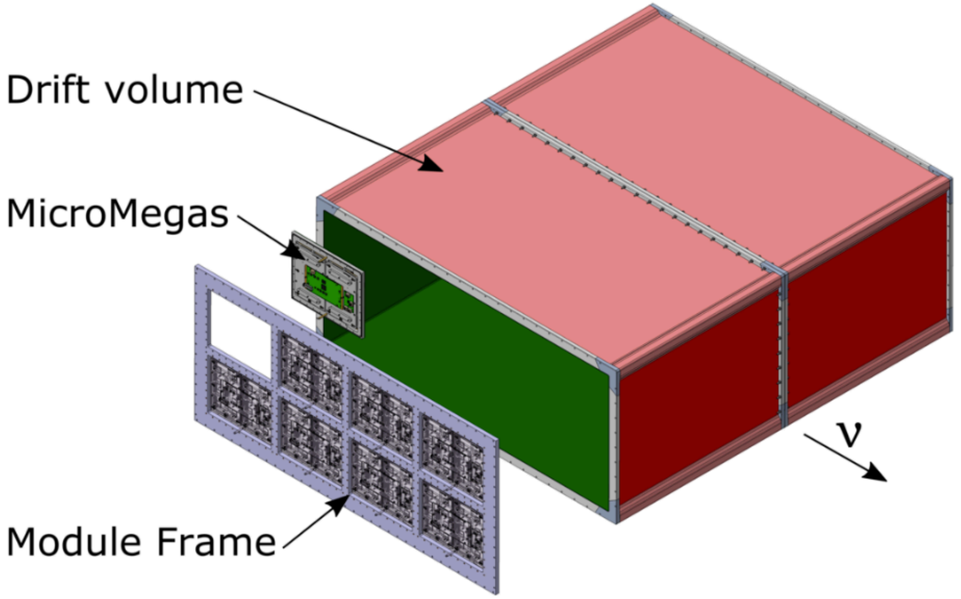

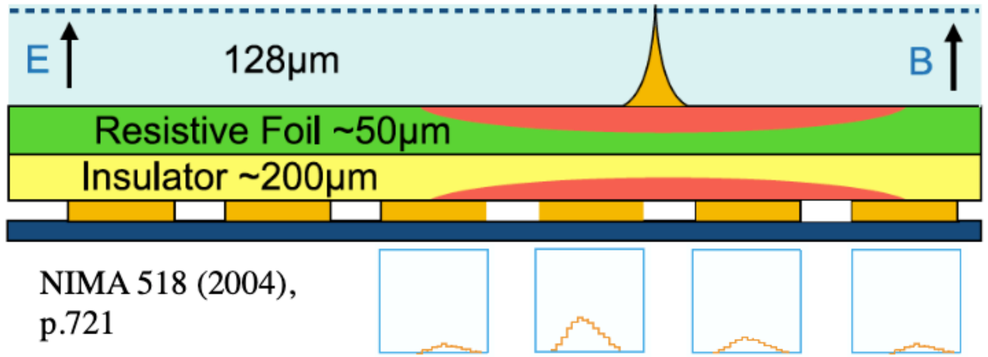

NIMA 518 (2004), p.721

- Equipped with restive MicroMegas
- Spatial resolution improved by x3 compared to current ND280 TPCs
- dE/dx resolution ~10% for MIP
- Momentum resolution 9%@1GeV
- TPC components being collected and tested at CERN
- Bottom TPC in Japan in September 2022, top TPC in February 2023

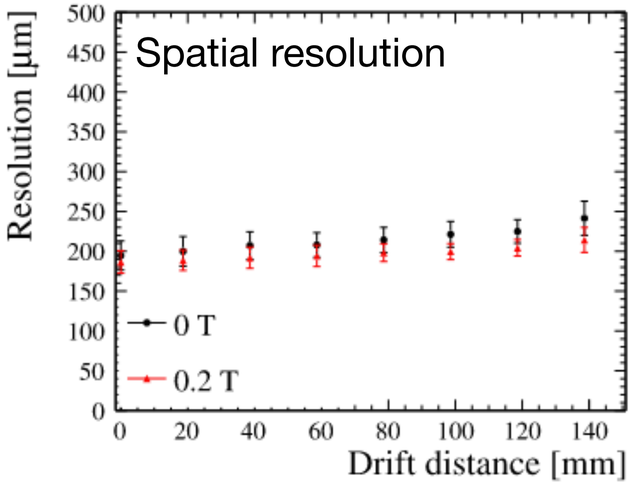

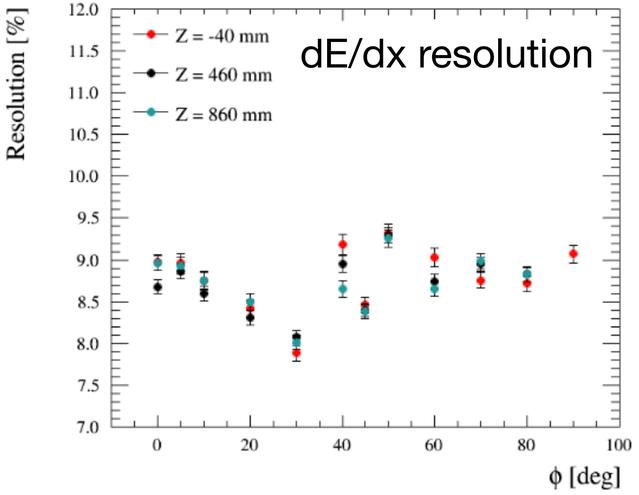

ToF detector

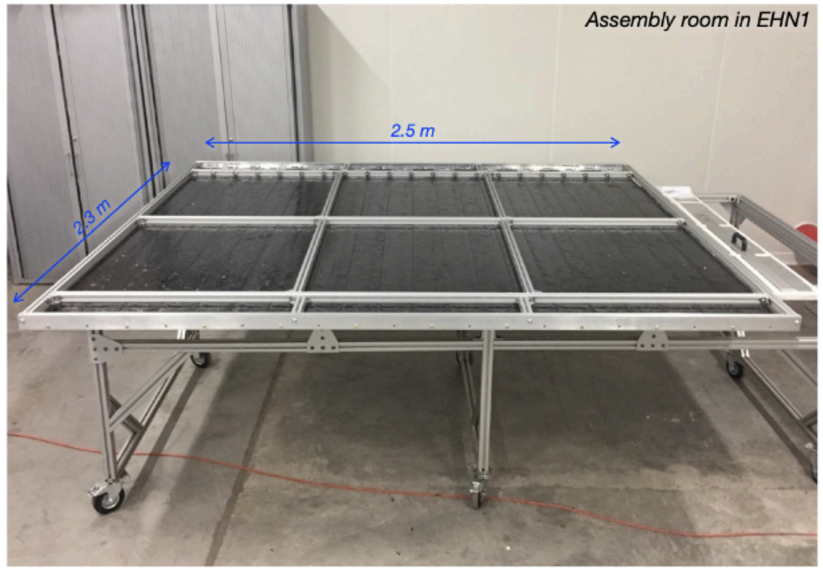

- 2.3 m x 12 cm bars of plastic scintillator read by MPPC
- Time resolution of 150 ps
- Fully tested at CERN
- Ready to be shipped in Japan

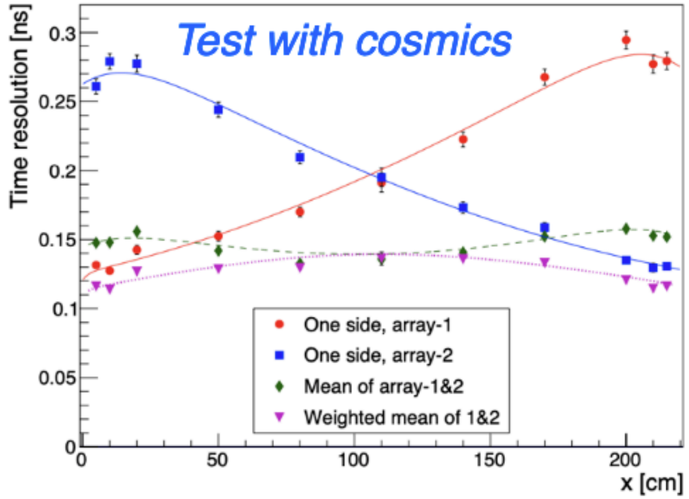

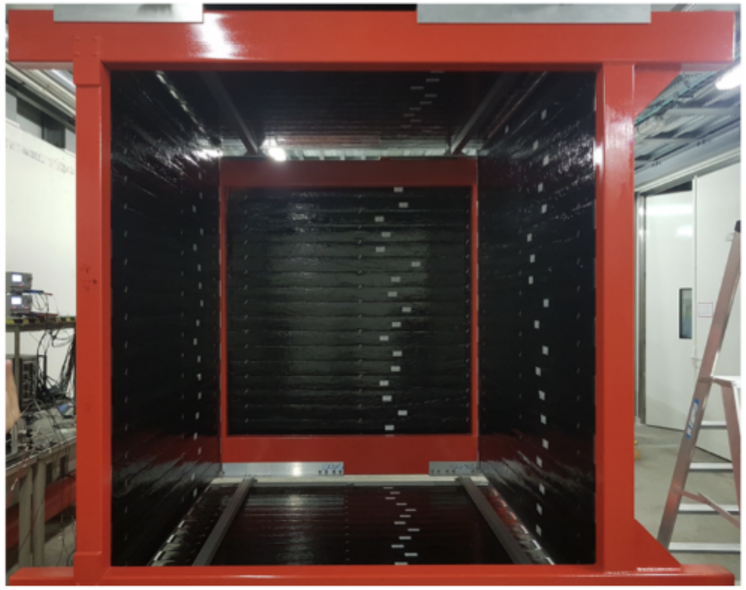

Conclusions

- Latest neutrino oscillation results use 3.6×10^{21} POT:
  - CP-conservation excluded at 90% CL
  - Weak preference for normal ordering and upper octant
- New ND280 and SK samples, improved flux predictions and cross-section modeling have been added in this iteration of the oscillation analysis
- Full program of cross-section measurements: Cross-section measurements focused on understanding nuclear effects show that more sophisticated nuclear model are favored. WAGASCI+BabyMIND took data this year and we are analyzing them
- T2K bright future:
  - Beam line upgrade to reach 1.3 MW is taking place
  - ND280 will be upgraded in Fall 2022 and data will be taken from April 2023
- Other ongoing activities:
  - SK loaded with 0.01% Gd. Start loading up to 0.03% (26 tons) from May (final goal 0.1%).
  - T2K+NOvA and T2K+SK combined analyses: different sensitivity to mass hierarchy and δ_{CP}

Backup

Oscillation results (θ_{23}, Δm^2_{32}) (θ_{13}, δ_{CP})

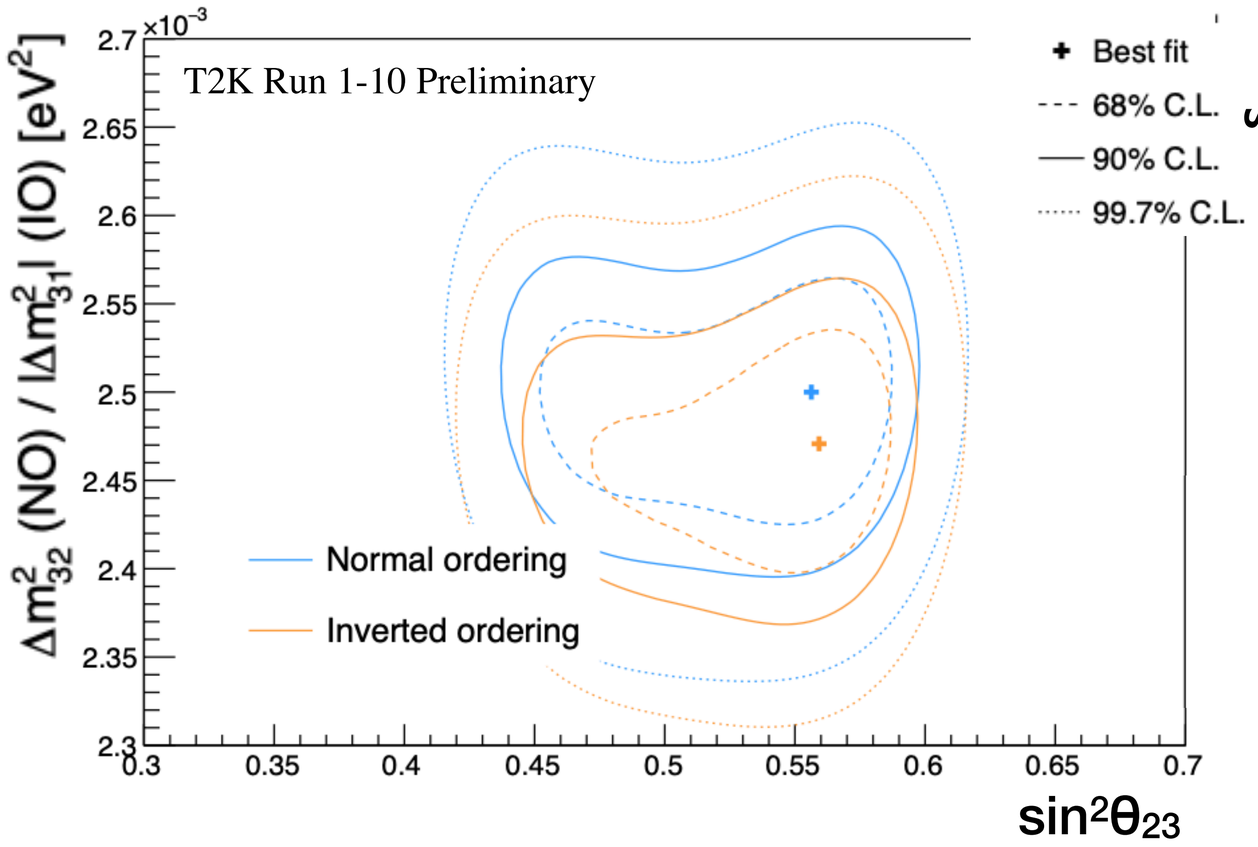

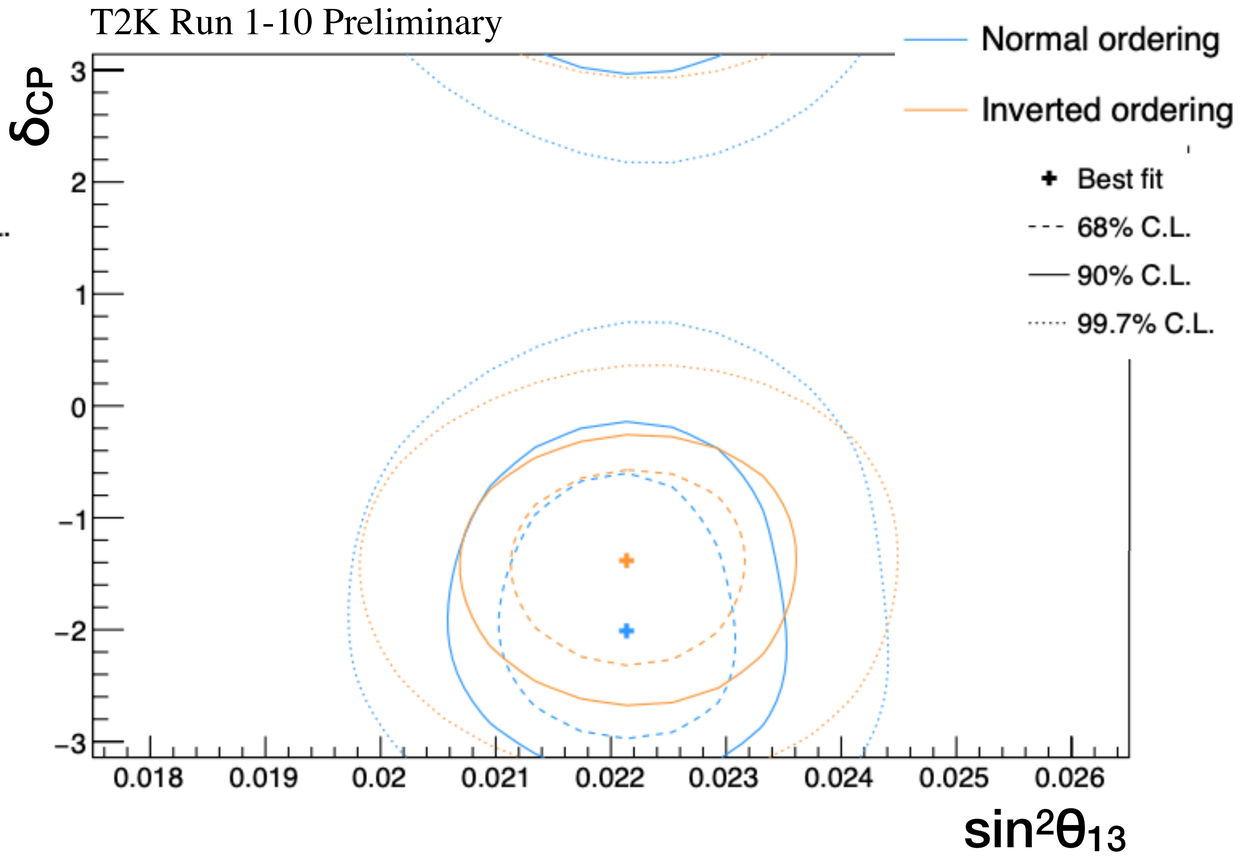

Slight preference of non-maximal $\sin^2\theta_{23}$ in upper octant

θ_{13} (w/ reactor constrain) compatible with maximal CPV

Photon tagging in FHC

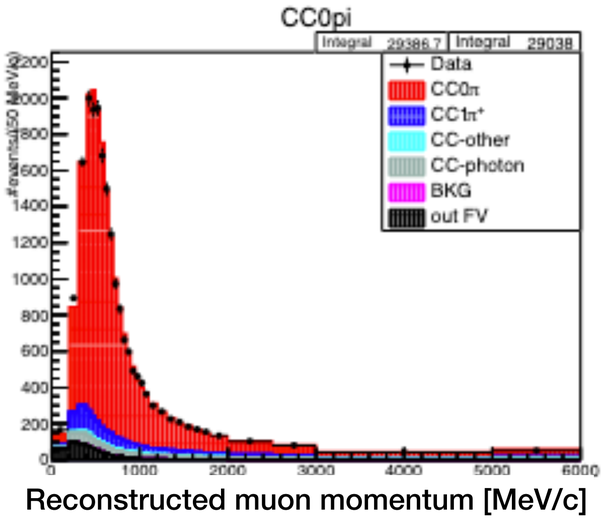

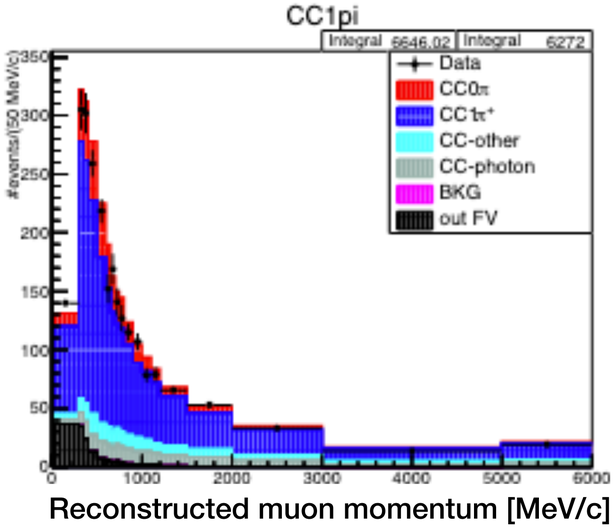

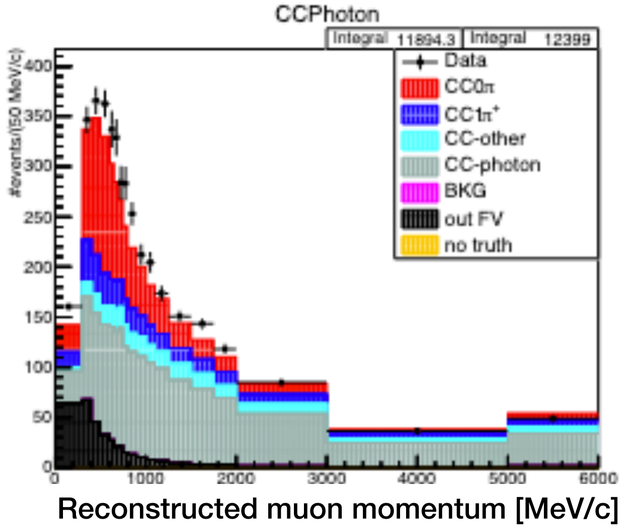

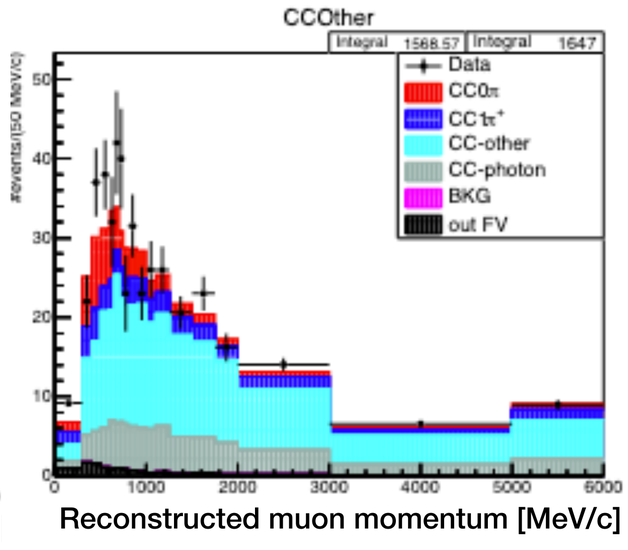

Improved selection

	Efficiency	Purity	Eff×Pur	(Eff×Pur)/(2−Pur)
CC0π	0.463	0.806	0.373	0.313
CC1π^+	0.256	0.633	0.162	0.119
CCPhoton	0.438	0.495	0.217	0.144
CCOther	0.194	0.535	0.104	0.071

Selection used for OA2020

	Efficiency	Purity	Eff×Pur	(Eff×Pur)/(2−Pur)
CC0π	0.48	0.713	0.342	0.266
CC1π^+	0.29	0.525	0.155	0.106
CCOther	0.30	0.714	0.214	0.167

Using ECal we can select a sample of events enriched with electromagnetic activity that we call CCPhoton and improve the purity of the other samples keeping similar efficiency

Proton tagging in FHC

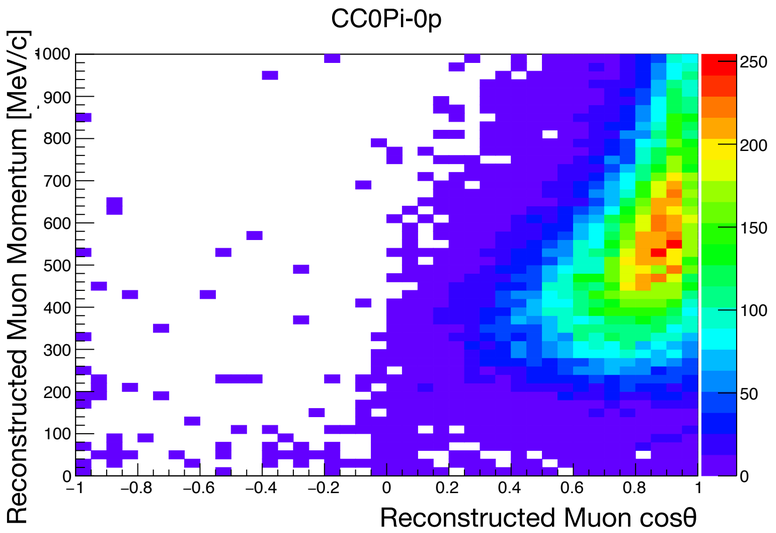

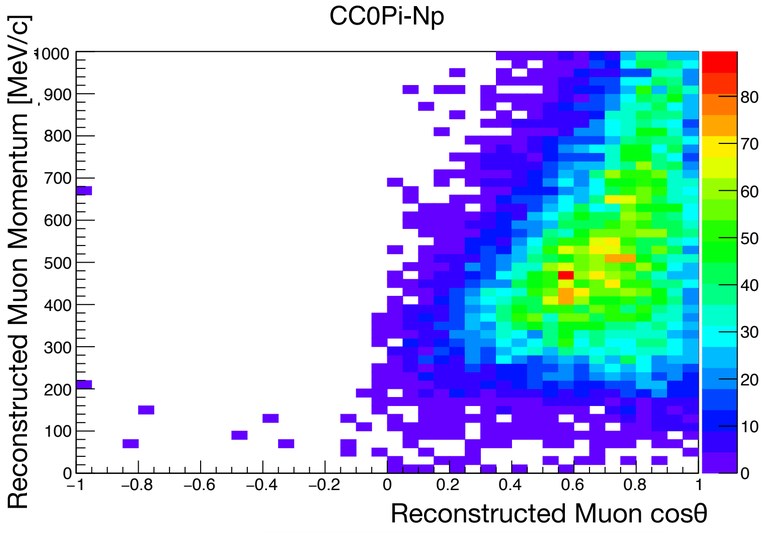

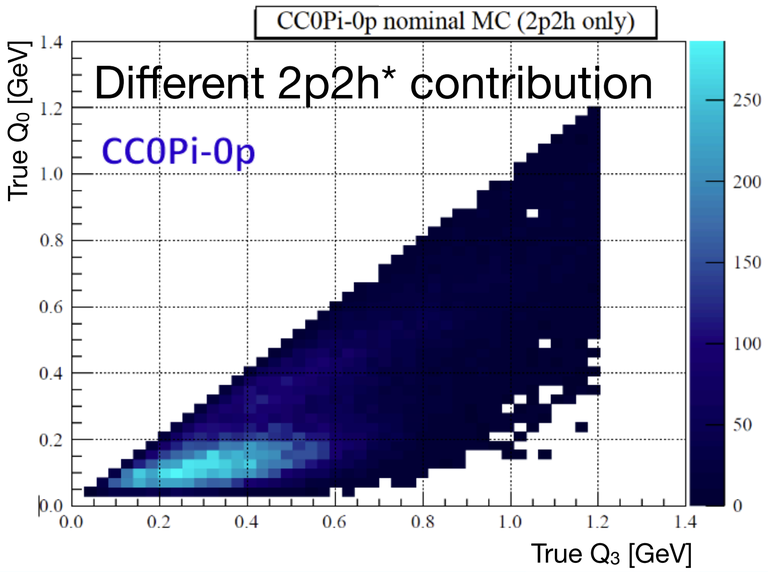

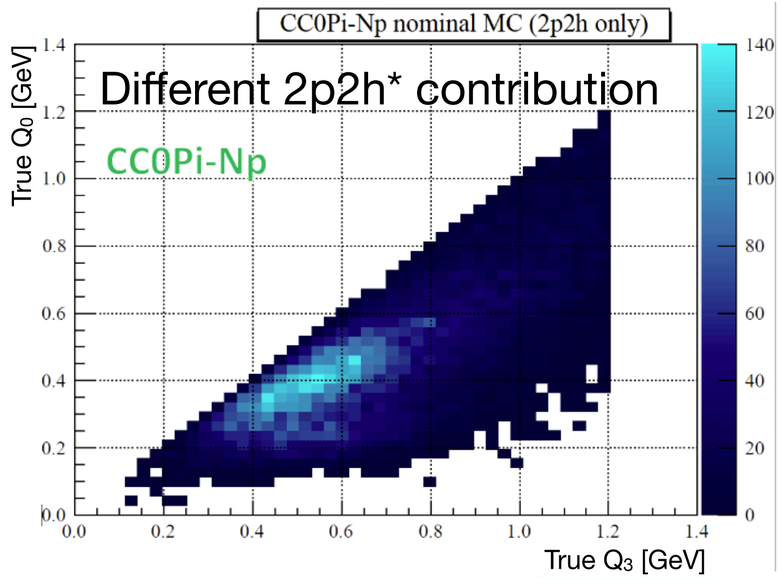

*Nieves et al.

Best fits 2022

Parameter	Best fit			
Data	T2K only		T2K + reactor	
Hierarchy	Normal	Inverted	Normal	Inverted
$\sin^2(2\theta_{13})$	0.103	0.114	0.0860	0.0865
$\sin^2(\theta_{13})/10^{-3}$	$26.5^{+3.1}_{-6.1}$	$29.3^{+0.3}_{-8.9}$	$22.0^{+0.8}_{-0.6}$	$22.1^{+0.7}_{-0.7}$
δ_{CP}	$-2.24^{+1.18}_{-0.80}$	$-1.26^{+0.20}_{-1.78}$	$-2.18^{+1.12}_{-0.50}$	$-1.37^{+0.31}_{-1.31}$
Δm^2_{32} (NH)/$\lvert\Delta m^2_{31}\rvert$ (IH) $[10^{-3}\ \mathrm{eV}^2/\mathrm{c}^4]$	$2.506^{+0.034}_{-0.059}$	$2.475^{+0.065}_{-0.028}$	$2.506^{+0.032}_{-0.059}$	$2.473^{+0.066}_{-0.026}$
$\sin^2(\theta_{23})$	$0.466^{+0.109}_{-0.019}$	$0.465^{+0.111}_{-0.017}$	$0.559^{+0.021}_{-0.040}$	$0.561^{+0.019}_{-0.042}$
$-2\ln L$	865.30	866.10	865.453	865.822

NA61/SHINE 2010

Replica tuning with 2010 data ($\pi^{\pm}, K^{\pm}, p$)

Adds K± and proton yields + increased stats.
Achieve ~4% hadron interaction uncertainty over wide energy range.

1. checked additional systematics → seems robust
2. checking consistency with thin tuning

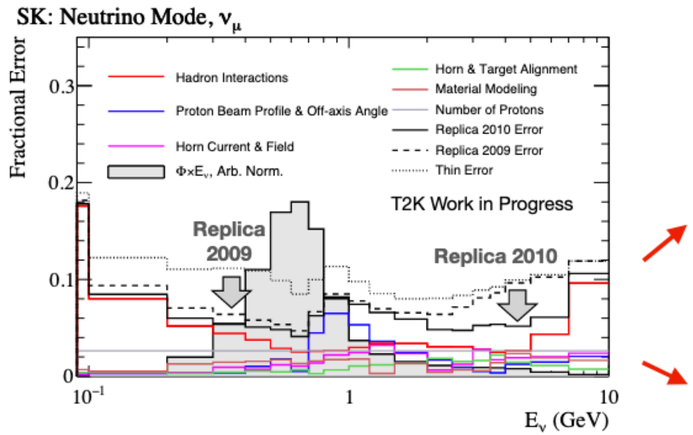

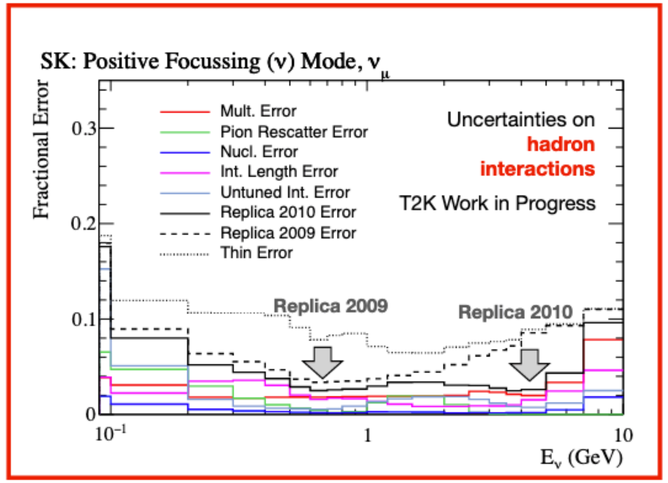

Beam	Target	Year	Stat (10^6)	Outgoing PID	Usage at T2K
protons at 31 GeV/c	Thin (2cm)	2007	0.7	$\pi^{\pm}, K^{\pm}, K^0_S, \Lambda$	past
		2009	5.4	$\pi^{\pm}, K^{\pm}, p, K^0_S, \Lambda$	in use
	T2K replica (90cm)	2007	0.2	$\pi^{\pm}$	
		2009	2.8	$\pi^{\pm}$	latest T2K results
		2010	10.	$\pi^{\pm}, K^{\pm}, p$	*this work*

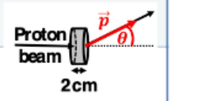

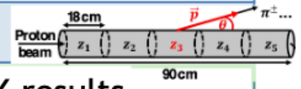

15

Beam upgrade

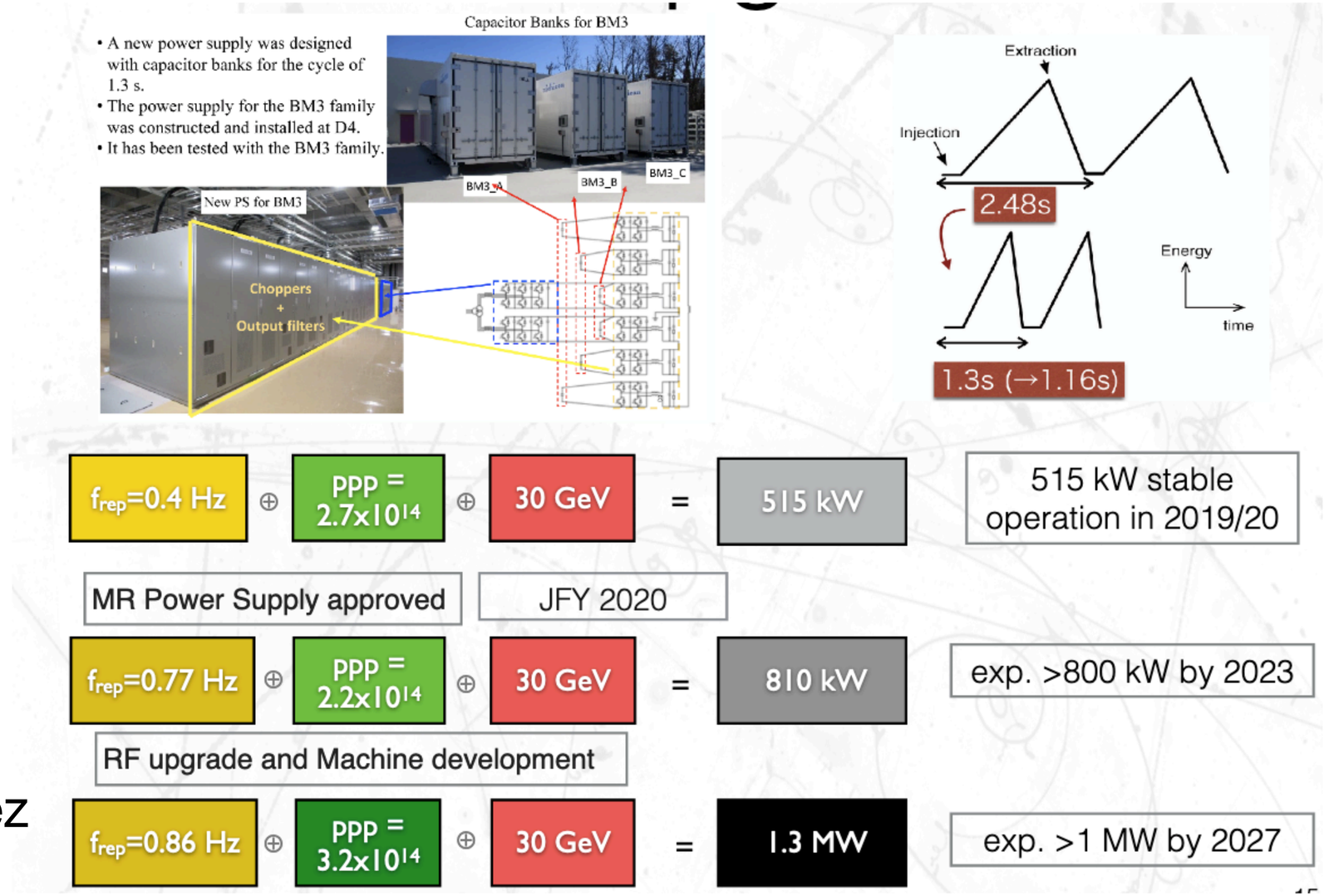

Federico Sanchez
Snowmass

SuperFGD

•Test beams at CERN with two prototypes, one made of ~10,000 cubes

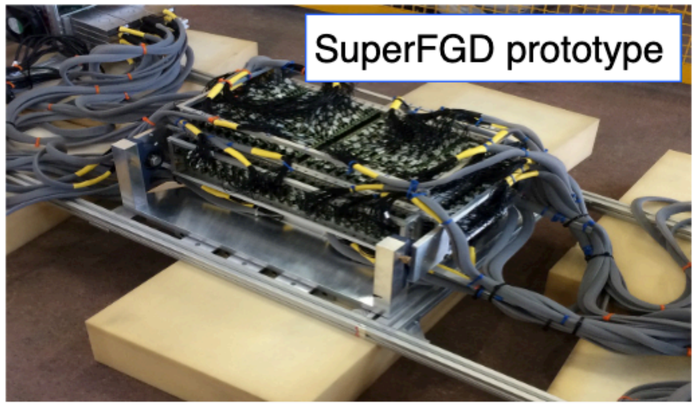

- Average L.Y. ~ 41 p.e. / fiber for MIP (@1m WLS fiber length)
- Very good intrinsic (scintillator+fiber) time resolution
  - ✦ σ_t ~ 0.95 ns (1 channel)
  - ✦ σ_t ~ 0.5 ns (1 cube)
- Cross talk ~ 3%

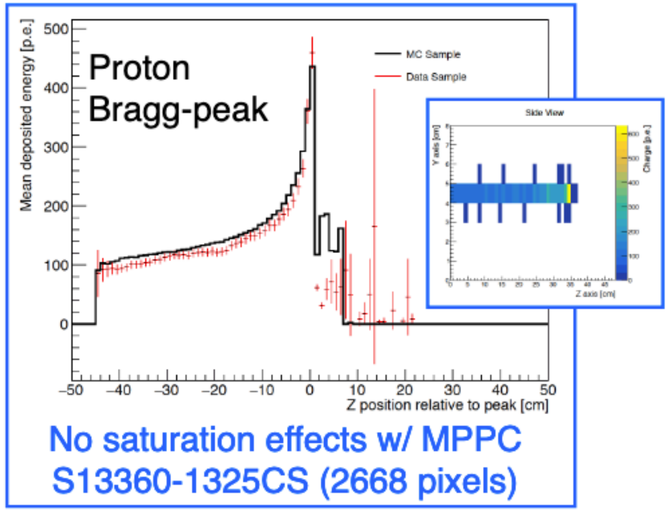

No saturation effects w/ MPPC S13360-1325CS (2668 pixels)

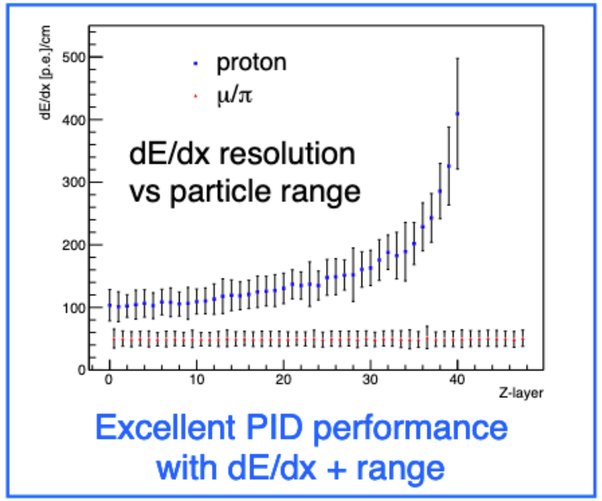

Excellent PID performance with dE/dx + range

Davide Sgalaberna
ICHEP2020

SuperFGD

- Prodution of ~2M cubes at UNIPLAST (~1.5M cubes already produced)
- Fishing lines (⌀=1.3mm) to assemble cubes ensuring proper alignment
  - ✦ Eventually replace fishing lines with WLS fibers

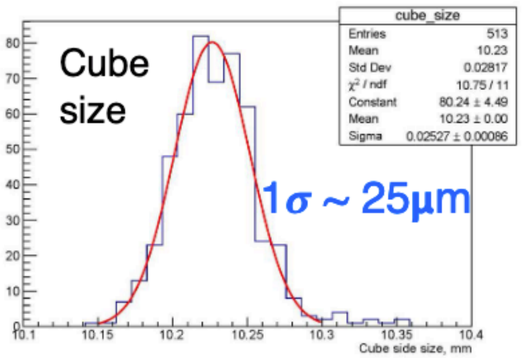

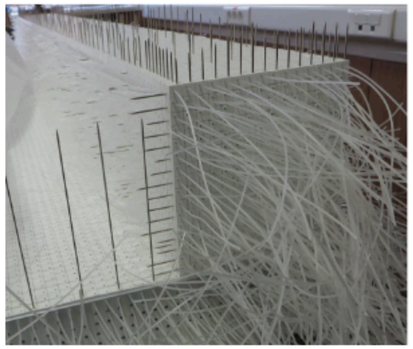

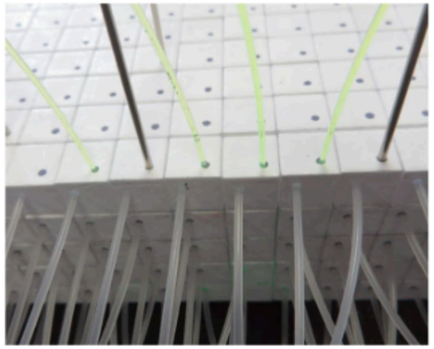

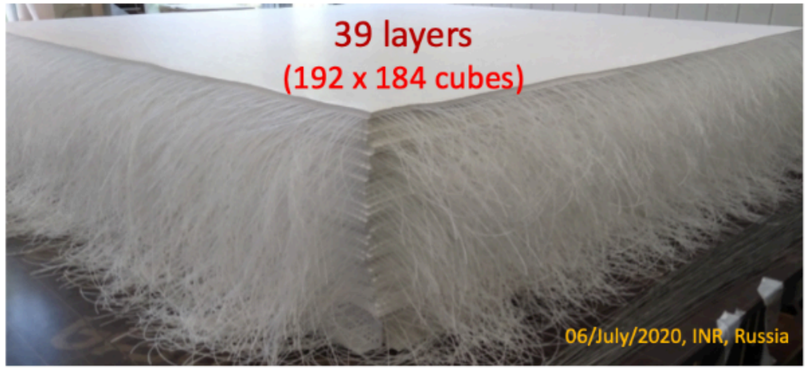

- Also developed another assembly method: ultrasonic welding to fix cubes to 0.1mm polystyrene sheet

Davide Sgalaberna
ICHEP2020

Resistive micromegas

- Goal: same or better performance of current TPCs but much more compact:
  - Momentum resolution ~ 9% @1GeV/c (~smearing from Fermi momentum)
  - For B-field of 0.2 T: space point resolution of 800 μm, 64 space points
  - dE/dx resolution of ~10% for MIPs —> e / μ and proton / μ separation

Resistive MicroMegas (RMM) to improve the spatial resolution

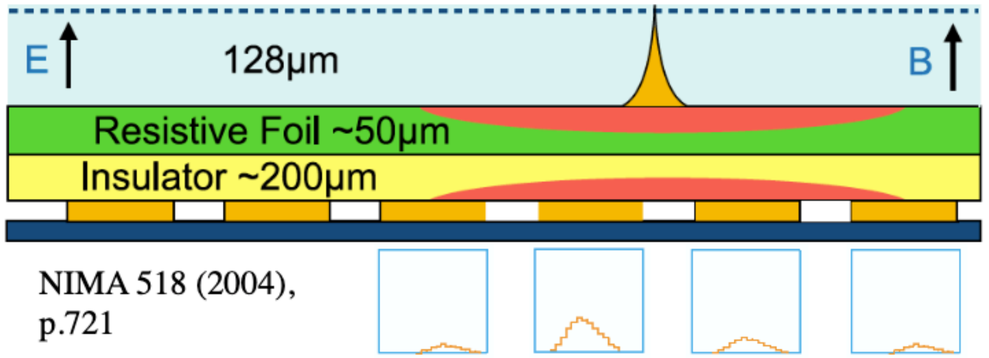

NIMA 518 (2004), p.721

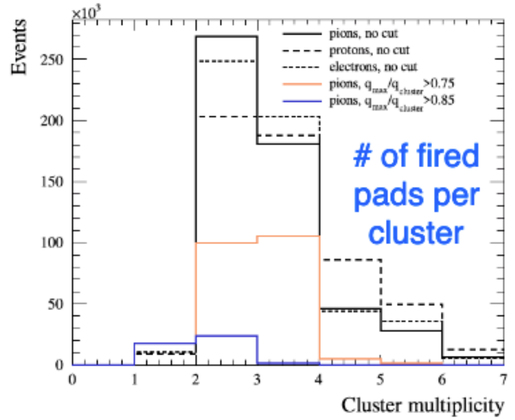

- Charge dispersion in 2-D RC network
- Gaussian spreading as a function of time

$$\rho(r,t) = \frac{RC}{2t} e^{\left[\frac{-r^2RC}{4t}\right]} \qquad \sigma_r = \sqrt{\left(\frac{2t}{RC}\right)}$$

R: surface resistivity
C: capacitance/unit area

Davide Sgalaberna
ICHEP2020

Resistive micromegas

- Beam tests at CERN (see backup - *NIM A 957 (2020) 163286*) and DESY

Prototype RMM2: new TPC pad size	
Isolation layer	75 μm glue + 50 μm APICAL
Module Sensitive area	34 x 42 cm²
Pad size	1.01 x 1.12 cm²
# of pads	1152

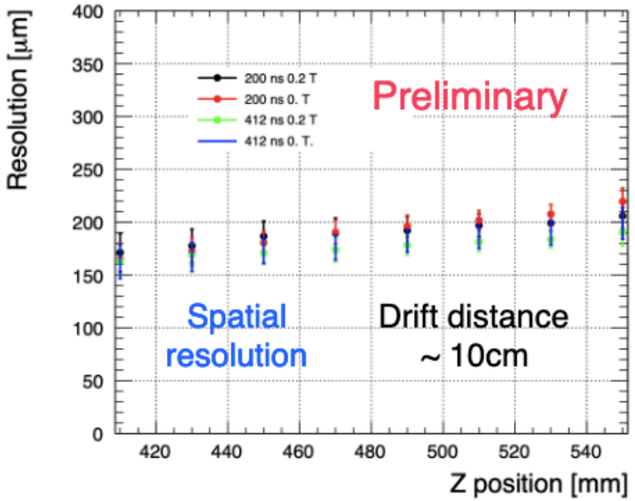

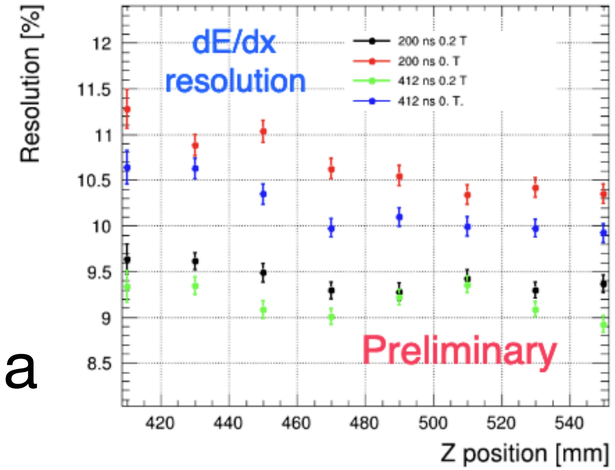

- Spatial resolution improved by x3 compared to current ND280 TPCs (<200 μm @10cm drift)
- dE/dx resolution ~ 9% for e^+ of 800 MeV/c
- Increased size of RMM pads but still excellent spatial and dE/dx resolution: # of channels can be reduced by ~33%

Davide Sgalaberna
ICHEP2020

Time-of-Flight

- Time-of-Flight detector with time resolution ~ 150 ps (arXiv:1901.07785)
  - 2.3m x 12cm bars of EJ-200 cast plastic scintillator: no WLS fibers, high light output, long attenuation length (4m), fast timing
  - Signal summed from arrays of eight 6x6 mm^2 MPPCs (S13360-6050PE). Double-end readout

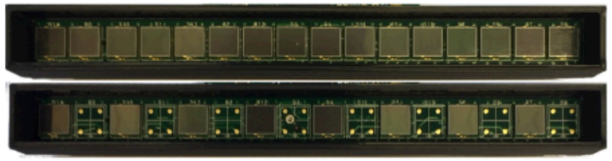

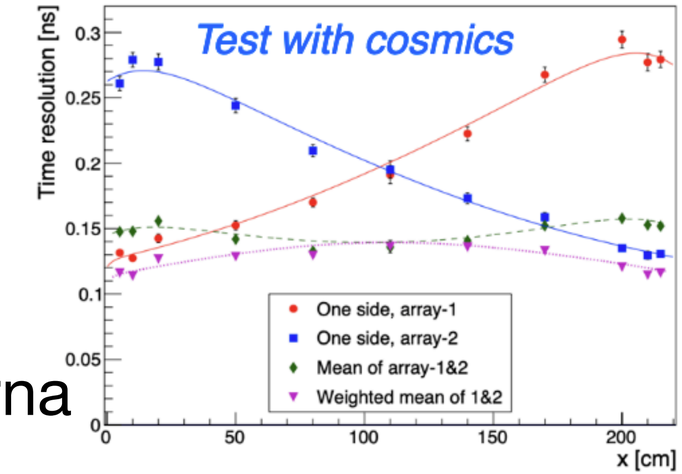

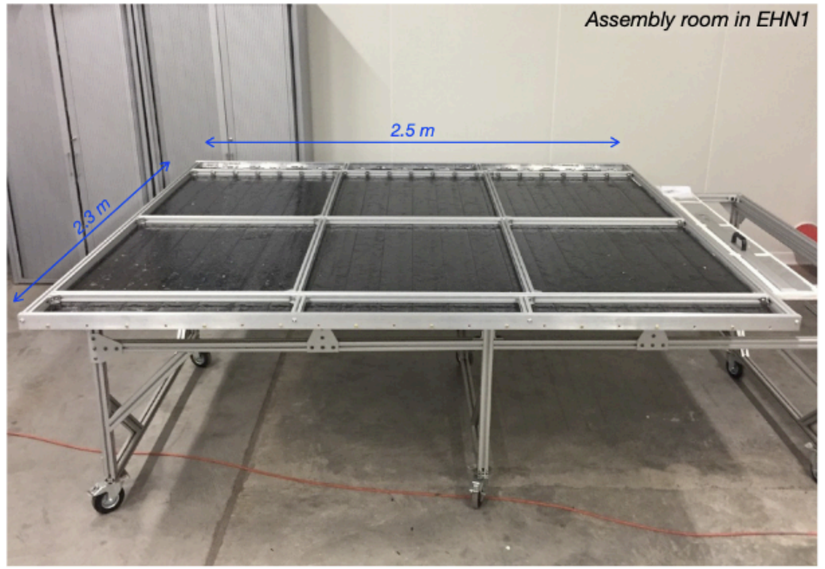

13

Davide Sgalaberna
ICHEP2020

Statistical methods

	Analysis 1	Analysis 2	Analysis 3
Kinematic variables for 1Re sample at SK	Erec-θ	p_e-θ	Erec-θ
Likelihood	Binned Poisson Likelihood Ratio	Binned Poisson Likelihood Ratio	Binned Poisson Likelihood Ratio
Likelihood Optimization	Markov Chain Monte Carlo	Gradient descent and grid scan	Gradient descent and grid scan
Contours/limits produced	Bayesian Credible Intervals	Frequentist Confidence Intervals with Feldman-Cousins (credible intervals supplemental)	Frequentist Confidence Intervals with Feldman-Cousins
Mass Hierarchy Analysis	Bayes factor from fraction of MCMC points in each hierarchy	Bayes factor from likelihood integration	Frequentist p-value from generated PDF
Near Detector Information	Simultaneous joint fit	Constraint Matrix	Constraint Matrix
Systematics Handling	Simultaneous fit then marginalization	Marginalization during fit	Marginalization during fit

Patrick Dunne
Neutrino 2020